STAT

Page Denied

# TRANSLATION

STAT

## RADIO ENGINEERING
## (RADIOTEKHNIKA)

Vol. 12, No. 1

January 1957

Pages 3 - 81

STAT

Table of Contents



STAT

# LONG-DISTANCE TROPOSPHERIC PROPAGATION OF ULTRASHORT WAVES*

by

B.A.Vvedenskiy, Honorary Member of the Society

A.G.Arenberg, Active Member of the Society

## 1. Introduction

Because of the successful development of experimental techniques and because of the multitude of new radio lines which have started operation in recent years, it has been found that in the band of ultrashort waves (meter, decimeter, and centimeter waves) transmission is possible at distances which were considered as simply inconceivable up to very recently, or if it were possible, then only under special, rare metereological conditions. This concerns directly the task assigned to the Soviet radio engineering by the historical decisions of the Twentieth Congress of the Communistic Party of the Soviet Union. These decisions open wide scientific and technical possibilities for creating new systems of long-distance broad-band communications.

However, it is not without misgivings that we accepted the proposal to write this paper. One of the reasons is that we cannot tell anything very new to the specialists; in addition, it must be admitted that there is a certain lag in the development of these problems in our country, and finally - although very recently - this problem has been discussed in an extensive and by no means always unanimous literature, which cannot be summarized, even in condensed form, without considerable difficulties.

We will begin our report with a brief reference to the history of ultrashort wave propagation. With certain reservations, the following basic stages can be dif-

* Paper read in Moscow on 12 May 1956, at the Scientific Session of the Society imeni A.S.Popov, dedicated to Radio Day.

ferentiated.

First Stage (early Twenties). The first practical steps are being made; the equipment is primitive and the distance of communications small. An interferential structure of the field becomes established in the vertical plane, and the dependence of the field on distance and altitude of the corresponding points is found. Quadratic and other interference formulas are derived. A negligent attitude toward the troposphere leads to the concept of ultrashort waves as "quasi-optical waves, spreading only to the horizon".

Second Stage ( end of Twenties-Thirties). The equipment is rapidly developed. The distance to the horizon ceases to be the limit for communications. The role of tropospheric refraction becomes known; a concept of the equivalent radius of the earth is introduced. Simultaneously, diffraction formulas are developed, and - in the form of a synthesis - refraction is introduced (by means of an equivalent radius) into the diffraction formulas. An aera of increasingly refined and exact mathematical work on these formulas has started.

Third Stage (Forties). Radar, television, etc. give a powerful impetus to the development of equipment. The study of the troposphere is intensified; radiometereology begins; the role of atmospheric humidity in the propagation of radio waves is emphasized. The number of stations operating on ultrashort waves of all types increases rapidly and continues to multiply; the volume of experimental material accumulates accordingly. Special metereological conditions make possible "ultradistant reception". To explain this fact, a theory of tropospheric wave carriers is created which in certain cases and to a certain degree corresponds to the empirical data. Theoretical mathematicians give this theory a very complicated mathematical form. The question of absorption (partially selective) in water vapor, atmospheric gases, rain, etc. is treated.

Fourth Stage. Further improvement of the equipment and a widening of the network of regularly working ultrashort wave stations in the Forties and Fifties,

STAT

especially in the last five years opens new possibilities of very distant (as far as the ultrashort wave band is concerned) and predominantly tropospheric transmissions over hundreds and even thousands of kilometers - even in absence of wave carriers in the troposphere. At present, the possibility of a regular transmission over such great distances of both speech and television has been experimentally proved, and experimental multichannel transmissions are being carried out.

Some correction must be made at this point: When speaking of "long-distance" ultrashort waves, we have in mind only the effects caused by the troposphere - not the still greater distances, chiefly in television, achieved by ultrashort waves (as, for instance, reception of Moscow television programs in Holland) and sporadically observed at wavelength not below 5 m; it can be considered as proved that this can be explained by the ionosphere. Although the mechanisms of these two types of propagation of ultrashort waves are intimately correlated, we will not speak here of ionospheric phenomena. The field of discussion is limited by the scope of the present report.

Studies by Italian scientists in 1932 and Soviet scientists in 1933 preceded the discovery mentioned before, that waves of about 60 cm (although only sporadically) reached distances of some hundred kilometers in radiotelephony. With increasing regularity, fields which in certain respects were larger than those obtained by usual diffraction computation, were observed. The number of such events during the World War II increased, and some of these did not substantiate the wave carrier theory. American authors mention 1948 as the date when a considerable number of such events became known. An important role in their accumulation is played by radar stations and radio-relay links, where unexpected mutual interference and great distances were observed.

In the beginning, super-distant fields were only considered as disturbances. However, when it became clear (about 1950) that distances of regularly stable reception can be reached on centimeter waves, detailed studies were made in the USA to determine the practical value of the newly discovered effects. In one of the American articles, the aim of the study was described as a desire "to determine the possibilities of using higher frequencies" (naturally, for tropospheric transmission). Further the article states: "Lower frequencies transmitted through the ionosphere were found less convenient because of variable conditions in the ionosphere".

Here a few words should be said on terminology. The expression "super-distant propagation of ultrashort waves", in our opinion, is unsatisfactory since, compared to the propagation of short waves, the expression "super-distant" sounds rather pretentious. The expression: "propagation of ultrashort waves beyond the horizon" is not good either, since propagation "beyond the horizon" was known before and the expression does not convey the novelty of the effect. An expression very much used at the boundary between the Forties and Fifties, namely "turbulent propagation" seems too categorical and too presumptive for the mechanics of the phenomenon. The term "scattered (or diffused) propagation" is also objectionable since scattered fields are also observed in the proximity zone.

Some authors use the expressions "extra" (or "super" or "trans") "diffractional propagation" in view of the fact that these effects have been discovered through the difference (increase by tens or even hundreds of decibels) of observed fields, as compared to those calculated according to usual diffraction formulas, containing the equivalent radius of the earth. Finally (although this enumeration might not be complete) occasionally the term "radio-crepuscular propagation" is used. This is based on the fact that, whatever the possible mechanism of long-distance propagation of ultrashort waves, the effect depends on the role of very high more or less equal atmospheric layers which, illuminated by the sun, create the crepuscular effect and the expression "radio-aurora".

We prefer to use a less compulsory and, at the same time, more adequate expression for the true status: "distant propagation of ultrashort waves through the troposphere".

STAT

The foundation for a systematic study of distant tropospheric propagation of ultrashort waves has been laid (as far as can be determined) in the USA by the Federal Bureau of Communications, the M.I.T., the US Naval Research Laboratory, and by the Bell Telephone Company. Separate papers have been published in the USSR, England, and France. USA authors call 1953 the year when technical usefulness of "distant" propagation has been proved beyond doubt. The total number of published papers by authors of these countries is more than 60-70. The problem is being studied in ten large Institutes; the number of persons mentioned by the authors, as working the projects, is over 200; the number of other participants is evidently still greater.

The studies encompass the bands from meter to centimeter waves. Studies were and are carried out on a long-range basis (months and even years). Average values of the fields (power) and characteristics of fading are indicated. Distances for which the studies were made reach 500-600 km, even 1000 km. The altitudes for the corresponding points are taken both low and high (mountains and airplanes). Most measurements were taken on land at fixed points. However, a considerable number of measurements were made with receivers moving along a certain course; for instance, approximately along a circle having the transmitter as center. This was done to evaluate the role of the obstacles (so-called "diffractional amplification by obstacles").

The results are mostly expressed as the ratio of received power to radiated power ("attenuation by propagation"*). The comparability of results is achieved by excluding such characteristics as antenna amplification (reducing to isotropic) (reduced to 1 kw), absorption in feeders, and even the influence of the earth's surface (the latter, by necessity, is only approximate).

Part of the studies is carried out with specially issued or manufactured equipment, but other results are obtained from the operation of radio, television, and

* For practical purposes, the minus sign in a logarithmic expression (when going over to decibels) is replaced by the inversed proportion.

STAT

other ultrashort wave stations, and also from radar and similar installations.

For the communication lines multistage stabilized transmitters with frequency modulation are used (for meter waves, resnatrons and for decimeter waves powerful klystrons with external circuits are used). The continuous power output reaches 10 kw. In pulse radar stations, the pulse power reaches 1 megawatt and the average power, 300-500 w.

The receivers have high sensitivity and selectivity, are free from noise, have a broad band and minimal distortions. In certain cases, the sensitivity reached 135 decibels at 1 w. Spaced reception has been used intensively and with success.

As antennas for ultrashort waves, paraboloids of rotation with diameters from a few meters to 20 meters (weighing 3 tons) are used, while the common type for meter waves are vibrating arrays. No definite advantage has been detected in using different polarizations.

## Some Experimental Data

One of the basic characteristics for the propagation of ultrashort waves always has been the dependence of the field (or power received) on the distance. In the case of interest here, this question has not been decided - chiefly on account of the considerable scattering of experimental points, although average values of fields (or power) have been collected for a considerable period of time. There is every reason to believe that this scattering is chiefly caused by changes in the tropospheric conditions including climatic; in addition, the terrain features of the earth's surface may influence the character of the field.

Since the publication of papers by Bucker and Gordon (1950) it has been tacitly agreed to accept for the field (or for the power, i.e., for its "attenuation") in the "transdiffractional tropospheric zone" which interests us, - a dependence on the distance expressed in a certain power of the original figure. With reference to the above, we analyzed a considerable amount of data in our possession and arrived at the following conclusion: In first and rough approximation, a tropospheric field in the transdiffractional zone can be considered as inversely proportional to about the $3.5^{th}$ or $4^{th}$ power of the distance, so that the attenuation is expressed by the $7\text{-}8^{th}$ power. However, not only these figures but also the "power" dependence is far from being proved.

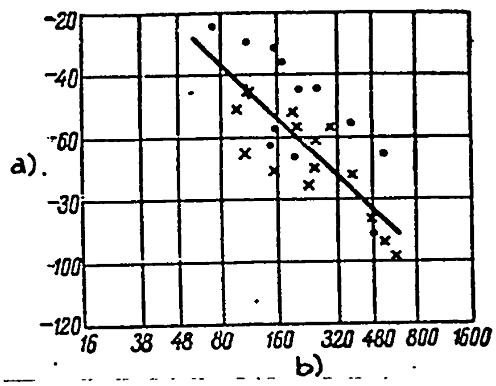


Fig.1 - Average Level of Signals for Distant Propagation of DMW and CMW in Closed Circuits (according to Bullington): • - DMW; × - CMW a) Level of signal in relation to free space, db; b) Distance km

Nonetheless the approximate dependence mentioned before is to be considered a practical figure both for observations taken at fixed points (Fig.1), and for those rather rare cases (Fig.2) when the receiver varied continuously. It is typical for distant tropospheric propagation of ultrashort waves there is no apparent difference in this approximate law. For different frequencies, however, a difference in the absolute values of the fields has been observed, notwithstanding the spacing of points already mentioned before (Fig.3).

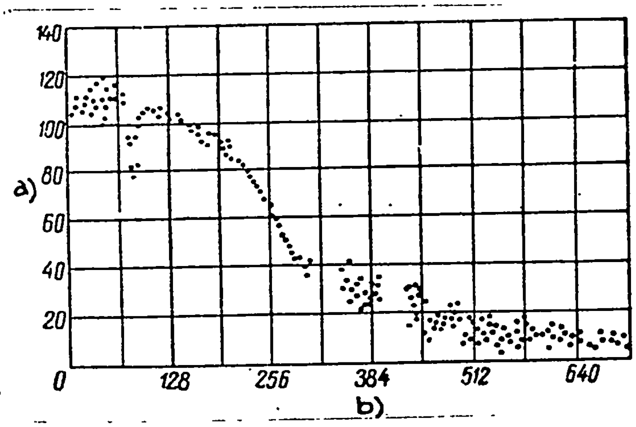


Fig.2 - Dependence of Signal Level on Distance (according to Ames, Newman, and Rogers) $\lambda$ = 13.6 cm Reception in aircraft at altitude 3000 m above sea level. a) Level of signal, db; b) Distance km

Another method of evaluating the experimental data is the prediction curve for propagation in well-mixed air, as suggested by Norton, Rice, and Vogler.

The above-mentioned authors have analyzed data for 122 radio lines, operating on waves from 4.5 m to 29 cm, at distances from 72 km to 1000 km; antenna height: lower, 2.4 - 37 m; upper, 121 - 2400 m above surroundings; time of the day 13 - $18^h$ (more quiet and free of carrier waves) and have plotted an interesting curve for the dependence of attenuation on distance (Fig.4). This curve is plotted along specially selected coordinates. Besides the usual parameter, the distance is characterized here also by the angle θ, which simultaneously represents a geocentric angle of the points on the radio horizon for both corresponding points (more correctly for their radio horizons) and also an "angle of dispersion", which constitutes an important parameter for all dispersion theories (Fig.5a). The introduction of this parameter is dictated by the theories of dispersion.

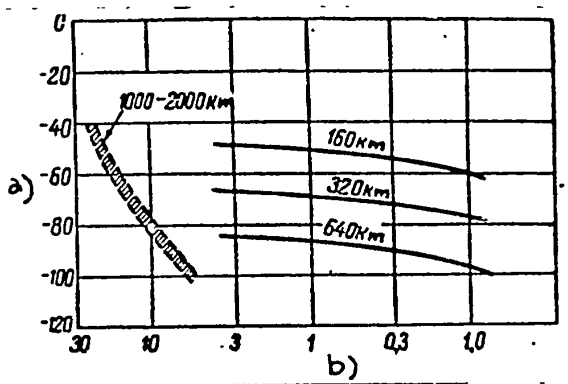


Fig.3 - Dependence of Average Signal Level on Wavelength (according to Bullington):

——— tropospheric propagation

- - - - - ionospheric propagation

a) Level of signal with reference to free space, db; b) Length of wave, meters

The possibility of such an unusual evaluation of the distance is based by the authors of the formula on complicated and not fully convincing arguments. The introduction of the angle θ is connected with a complete calculating process, developed by the same authors and aimed at an evaluation of the local relief of the terrain. We will only refer to Fig.5b and to the general indication that, in their explanations, the track is divided into four arcs of a circle lying in the plane of the great circle passing through the corresponding points. The radii of these four arcs are different and are selected by special method so that the arcs at their junction points do not form any break. As a result, this angle θ is plotted on the abscissa or, what amounts to the same, the full distance less the length of both irradiated parts of the track, i.e., $R - R_{1pg} - R_{2pg}$. On the ordinate a modified average attenuation is plotted (in decibels) which (for not very convincing reasons, since they are based on the diffraction theory) is divided by the distance. Further, to exclude the influence of the effective area of the receiving antenna, the attenu-

STAT

ation is divided by the square of the frequency. One cannot deny, however, that such a method is justified in that it permits a consolidation of extensive experi-

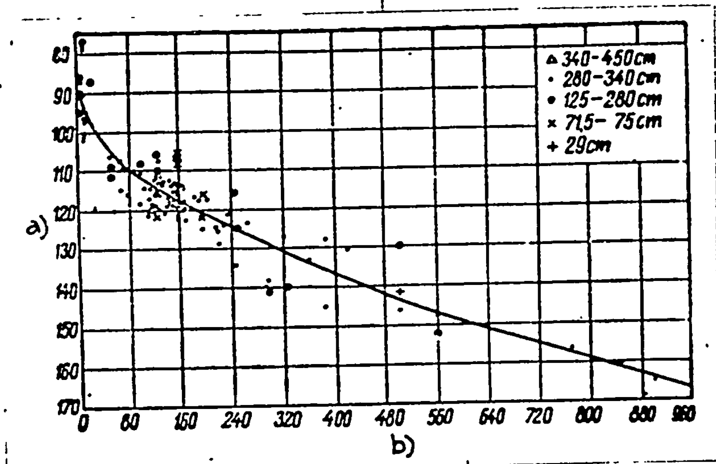


Fig.4 - Dependence of Modified Average Attenuation on the Distance, Corresponding to the Angle θ (according to Norton, Rice, and Vogler)

Daytime; Typical Atmospheric Conditions

a) Modified attenuation, db; b) Distance corresponding to angle θ, km

mental data into an acceptable empirical curve.

This curve was obtained during an attempt by the authors to create a unified theory suitable for all distances. Notwithstanding, considerable work and, at times, great intelligence as well as, at times, arbitrary methods, the work (in our opinion) did not progress beyond a very complex but purely mechanical agglomeration of - at present - heterogeneous components.

For practical purposes, however, this curve gives not less information than the theory indicated above, and gives it with a considerable saving of time and effort. This curve is preferable over different other published curves and nomograms having the same purpose.

* * *

All authors agree that a transition from the diffractional zone* into the zone

* I.e., in the zone where the "classical" (based on the concept of an equivalent earth's radius) diffraction theory is true.

STAT

which is of interest to us, namely that of distant propagation, proceeds smoothly. Depending upon the height of the corresponding points, this transition may be very far away (at great heights) or relatively near the transmitter. This is well illustrated by Trolez' experiments carried out over a closed track of 74 km (Fig.6). A practical criterion for the presence of a "transzone" can be based either on a distinct predominance of the fields over the "diffractional" zones (at equivalent earth's radius) or on an analysis of the character of fading.

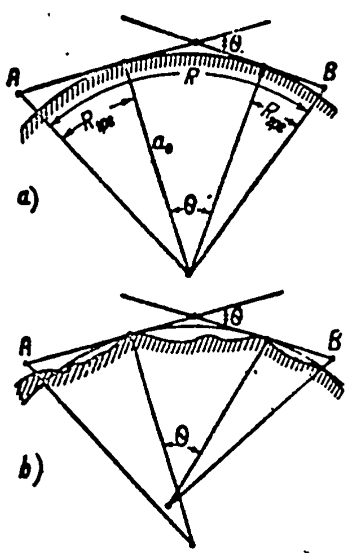


Fig.5 - For Determining the Angle θ over Flat and Hilly Terrain

Modern diffraction theories, developed to a high degree of mathematical perfection and accuracy for the case of a smooth spherical earth, are rather useless (for criticism of the methods to account for refraction, see later) for the case when the surface of the terrain relief is disregarded.

A typical example for the necessity of taking the latter point into consideration is the common case when an obstacle (not even very conspicuous) in the path of propagation leads to a considerable increase in the field values. An especially striking point is the "amplification by obstacles"*, which, when the propagation goes over an approximately wedgeshaped mountain, mountain ridge etc. is noticeable even beyond low hills.

The papers by Kerby, Dougherty, and MacKeet give data on an excessive field behind an isolated wedgeshaped mountain (Pikes Peak) in the eastern slopes of the Rockies. This excess reached a value of 20-30 db (wave range from 5 to 1.5 m). Tests with longer meter waves were made in Alaska. Bullington reports data on a

* Obviously, there are also (and even more frequently than amplification) attenuations by obstacles.

similar increase of the field by hundreds of decibels; thus the "criterion of diffraction" has to be taken with caution also from this point of view. One fact is evident: Any attempt to explain ultradistant fields by this effect is entirely unfounded.

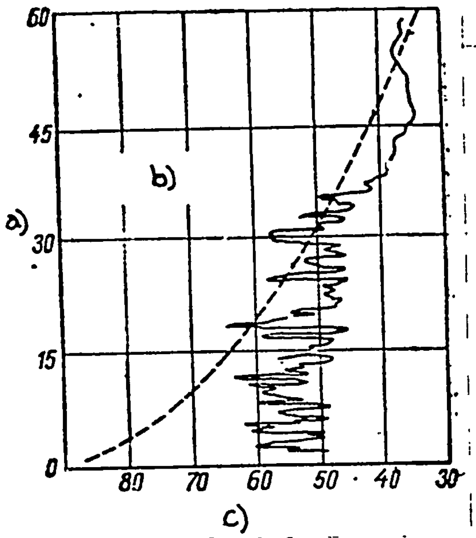


Fig.6 - Dependence of the average Signal Level on the Height of the Receiving Antenna (according to Trolez) Wave 3.2 cm; Closed track 74 km long. Height of Transmitting antenna 59 m.

a) Height of receiving antenna, m; b) Diffraction zone; c) Level of signal in relation to free space, db

It is not easy to sort the zones by analyzing the character of fading. It is generally accepted to divide fadings of ultrashort waves into "slow" and "rapid". Slow fadings are ascribed to factors changing smoothly and determining an average gradient of dielectric penetrance of the air. The variations of such fadings last for several tens of minutes, usually even for hours. They obey in a satisfactory manner the normal laws of distribution in the sense of the theory of probability. Diurnal and seasonal variations can be ascribed to the category of such fadings.

Rapid fadings, as a rule, have a periodic character measured in fractions of a minute, sometimes less. They are ascribed to mutual interference among individual elementary oscillations reaching the receiver due to secondary radiation (diffusion, reflection) of the transmitter field caused by rapid and chaotic fluctuations in the atmosphere. Different from fluctuation of a laminar type, these fluctuations are thought to be of globular structure.

A chaotic character of these fluctuations influences individual oscillations, re-radiated because of these fluctuations, and gives them phases whose value, with equal probability, may vary anywhere from 0 to $2\pi$ . As a result, the vector sum of

STAT

these oscillations (i.e., momentary values of the field) must follow a special distribution, which has been studied some time ago by Rayleigh and later by V.I.Siforov and A.N.Shchukin. This distribution, in a somewhat broadened form, forms a basis for the analysis of the character of distant fields. The studies make wide use of diagrams which directly indicate (for example) during what percentage of time the momentary values of the field - in relation to the average over a sufficiently long period of time - will exceed certain values. In addition, a special functional network is often used, for which the Rayleigh distribution can be expressed by a straight line, at a $45^{o}$ angle to the coordinate axes.

a)

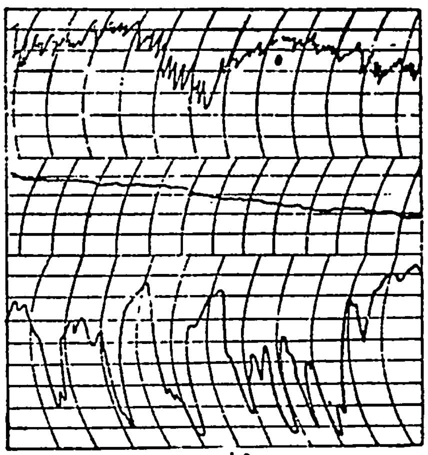

b)

Fig.7 - Samples of Aircraft Records of Signal Level (According to Ames, Newman and Rogers)

Wave 13.6 cm; one vertical section is equal to 3 db. Upper record: interferential zone (depressions correspond to intervals between lobes of the transmitting antenna); center record: zone of "classical" diffraction. Lower record: zone of distant propagation through the troposphere.

a) Signal level; b) Distance

Figure 7 shows three rather frequent types (not always distincly expressed) of recordings for the three zones: interferential (direct dependence), "classical" diffractional, and distant, as taken above the ocean by Ames, Newman, and Rogers. The rapid oscillations are so weak that they do not even conceal the field decreasing on account of distance (the records were made on an airplane flying away from the center). Conversely, rapid oscillations are very strong in the distant zone. However, the experiment shows that the transition from one case to the other is smooth. Thus, in the general case, the field represents a mixture or a superposition of both types of fields.

STAT

A study of the character of fadings is important for calculating the reliability of the given radio line. The same problem includes the possibility of considerable stabilization by using two or even three spaced antennas. This results in a stronger signal when the transmitter is aimed at a certain portion of the atmosphere and the transmitting and receiving antennas are faced in slightly different directions. Certain phenomena relative to a broadening of the directional characteristic can be explained by re-radiation in a sufficiently large air space (see Fig.8). There is also a decrease (reaching, for both antennas, a total of 10 or more decibels) in antenna amplification due to lack of a cophased front in the antenna aperture.

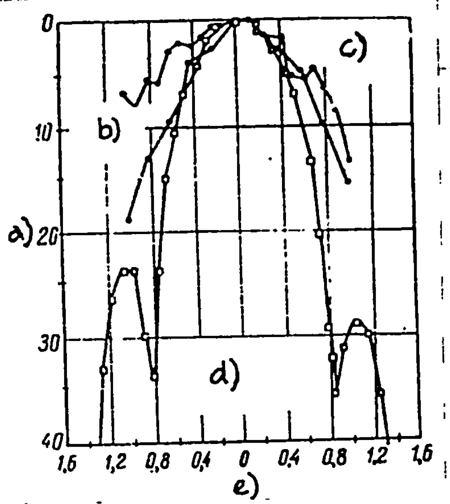


Fig.8 - Change of Received Power, with the Antennas Rotated in the Horizontal Plane (According to Chisholm, Portman, de Bettencourt, and Roch)

Wave 8.1 cm; Track 300 km long. Zero on the scale of turns corresponds to antennas facing each other.

a) Power received, db;
b) Both antennas rotate;
c) Receiving antenna rotates;
d) Measured radiation pattern; e) Angle of turn, degrees

Therefore, the number of papers dedicated - in whole or in part - to the theory of fadings and their effects, is very large. For instance, spaced reception is treated by Steres, Jerks, and Mek*; broadening of antenna characteristics is discussed by Chisholm, Portman, de Bettencourt, and Roch; the general theory of fadings is treated in papers by Rice and G.S.Hurlick. In general, these effects coincide well with the theory of dispersion.

There exists also a mathematical solution (Norton, Vogler, Mansfield, Short) for the change in the distribution diagram, if the "purely Rayleigh-type" signal is supplemented by another signal (for instance, to make it simple, with constant amplitude).

* Translator's note: Spelling of some of the Western authors unconfirmed.

However, an analysis shows that the quality of the present experiment is still insufficient to differentiate, for instance, complete absence of a constant amplitude (i.e., fields of slow fadings) from the average equality of two signals: of the Rayleigh-type and of the constant-amplitude type, superimposed and acting together. Therefore, Norton, Vogler, Mansfield, and Short arrive at a rather pessimistic conclusion, that "a full evaluation of the experimental data must wait for further development of the propagation theories, which could explain the distribution of mutually dependent phases and of amplitudes of dispersed fields".

Thus we cannot, as yet, give an answer to the question: whether or not the given field is "totally dispersed".

(To be continued)

STAT

# CERTAIN CHARACTERISTICS OF RADIO EMISSION FROM COSMIC OBJECTS

by

A.D.Kuz'min

A brief review of the characteristics of radio noise from cosmic bodies, of interest to radiotechnical use, is given.

## 1. Introduction

Many cosmic bodies (Sun, Moon, Galaxy and certain extragalactic conglomerates) are sources of radiation in the range of radio waves. Only a part of this radiation reaches the earth, i.e., frequencies within the "transmission band" of the earth's atmosphere. This "transmission band" extends from waves around 1 cm to waves near 15-30 m. The limit of the "transmission band" for short waves can be explained by molecular absorption in the atmosphere. Radiation, exceeding a wavelength of 15-30 m, is reflected from the ionosphere.

Radio noise from the cosmic bodies is of great interest for radiotechnique. The coordinates of cosmic bodies, representing sources of radio radiation, are accurately known. These sources are located at very great distances from the receiving equipment and are therefore always within the wave zone of this equipment. Further, the intensity of radio noise from a series of cosmic objects (for instance, moon, extragalactic bodies, galactic stars) is constant with a practically sufficient accuracy and its value is known.

The above-mentioned features permit the use of cosmic sources of radio radiation for a number of radiotechnical measurements (Bibl.1,15) such as measuring the directive gain and the efficiency of antennas, recording their radiation patterns and their adjustment. Sources whose radio radiation is constant in time can be utilized for control of sensitivity of radio receivers.

In certain cases, cosmic sources of radio noise may interfere with radio recep-

STAT

tion.

2. Parameters of Radio Radiation from Cosmic Bodies

One of the basic characteristics of radio radiation by cosmic bodies, which determines its usefulness for radio-technical purposes, is its intensity. For a quantitative characteristic of radio radiation the following parameters are normally used:

Radio Radiation Flux. The radio radiation flux p characterizes the total energy radiated by the body in a single frequency band, during unit time through unit surface in a direction normal to this surface.

Brightness. The brightness I characterizes the distribution of radio noise intensity over the body. It is determined by the relation

$$I = \lim_{\Delta\Omega \to 0} \frac{\Delta p}{\Delta\Omega}, \qquad (1)$$

where $\Delta\Omega$ is the solid angle of the area of the cosmic body for which the brightness is determined.

The radio noise flux p is correlated with the brightness I by the following obvious relation

$$p = \int_{(4\pi)} I \, d\Omega. \qquad (2)$$

Practically speaking, the integration should be made only within the limits of the solid angle of the source since, without these limits, the integral is equal to zero.

Temperature. The spectral density of radio radiation by cosmic bodies depends on the wavelength. However, within the limits of the transmission band of the receiving set the temperature can be considered as constant. This permits application of the theory of heat radiation and characterization of the radiation intensity by temperature.

STAT

The radio radiation brightness is usually expressed by the brightness temperature. The brightness temperature T is determined as the temperature of a black body which, at a given frequency in a given direction, has the same brightness as the source under study.

In the radio-frequency band, the radiation of a black body is determined by the Rayleigh-Jeans formula, according to which the brightness I is related to the brightness temperature T by following ratio

$$I = \frac{2kT}{\lambda^2}, \qquad (3)$$

where $k = 1.38 \times 10^{-23}$ joule degrees is the Boltzman constant; $\lambda$ is the wavelength of observed radiation.

The brightness temperature T, in the general case, just as the brightness I, depends on the coordinates of the emission area

$$T = T(\varphi, \theta)$$

and characterizes the distribution of radiation over the source.

The radio radiation flux is usually expressed by the effective temperature $T_e$. The effective temperature of radio radiation by the source is determined as the temperature of a black body having angular dimensions of the source and emitting at a given frequency the same flux of energy, as the described source. According to definition, we have

$$p = \frac{2kT_e\Omega_e}{\lambda^2}, \qquad (4)$$

where $\Omega_e$ is the solid angle of the source. A comparison of eqs.(2), (3), and (4) readily permits establishing a connection between the effective and the brightness temperatures

$$T_e = \frac{1}{\Omega_e}\int\limits_{(4\pi)} T(\varphi, \theta)\, d\Omega. \qquad (5)$$

STAT



Declassified in Part - Sanitized Copy Approved for Release @ 50-Yr 2013/11/13 : CIA-RDP81-01043R002700130004-0

## 3. Determination of Power at the Input of a Radio Receiver, Caused by Cosmic Radio Radiation

The power received by an antenna in the interval df between frequencies within the solid angle $d\Omega$ and emitted to the balanced antenna load is equal to

$$dP = \frac{1}{2} I A df d\Omega = \frac{\kappa T(\varphi, \theta)}{\lambda^2} A df d\Omega, \tag{6}$$

where A is the effective area of the antenna*.

The factor $\frac{1}{2}$ is due to the fact that an antenna receives the energy corresponding to only one polarization**.

The effective area of a receiving antenna A depends on its type, size, and direction of reception. The area is correlated with the factor of directional action G $(\varphi \theta)$ of the antenna by the following relation:

$$A(\varphi, \theta) = \frac{\lambda^2}{4\pi} G(\varphi, \theta). \tag{7}$$

The total power P (in the frequency band df), emitted by the antenna under coordinated load, is equal to

$$P = \frac{\kappa df}{4\pi} \int_{(4\pi)} T(\varphi, \theta) G(\varphi, \theta) d\Omega \tag{8}$$

To compare the power of cosmic radio radiation arriving at the input of the receiver with the power of its inherent noise, it is convenient to use the concept of equivalent temperature of the source $T_a$, as delivered to the antenna. In radioas-

---

* In deriving eq.(6), losses in the antenna were not taken into consideration. In the band of radioastronomic observations, such an omission is permissible.

** It should be mentioned that this property is not due to the type of antenna used, but to the mechanics of antenna reception. Therefore, the use of a nonpolarized receiving antenna for reception of a nonpolarized signal, does not yield a greater power than with a polarized antenna, receiving only a signal of one polarization.

tronomy this value is simply denoted as antenna temperature.

The equivalent temperature of the source delivered to the antenna is a resistance temperature equal to the output resistance of the antenna; when coupled to the input of the receiver instead of the antenna, this yields at the load of the receiver the same volume of noise as the source under observation. On the basis of this determination and on the determination of the noise factor F of the receiving device, it is not difficult to show that the power ratio of the cosmic signal to the inherent noise of the receiver is equal to

$$\eta = \frac{T_a}{FT_0}, \qquad (9)$$

where $T_o$ = 290°K is the standard temperature of the surroundings. The noise power emitted from a coordinated load by a resistance at the temperature $T_a$ is known to be

$$P_R = \kappa T_a df. \qquad (10)$$

A comparison of eqs.(8) and (10) will yield the following relation for the equivalent temperature of the source, as delivered at the antenna:

$$T_a = \frac{1\pi}{4} \int_{(4\pi)} T(\varphi, \theta) G(\varphi, \theta) d\Omega. \qquad (11)$$

Considering that $\int_{(4\pi)} G(\varphi, \theta) d\Omega = 4\pi,$ the latter expression can be reduced to the following form

$$T_a = \frac{\int_{(4\pi)} T(\varphi, \theta) G(\varphi, \theta) d\Omega}{\int_{(4\pi)} G(\varphi, \theta) d\Omega}. \qquad (12)$$

The formulas obtained permit calculating the equivalent temperature of the source delivered at the antenna, if the radiation pattern of the antenna $G(\varphi, \theta)$ and the distribution of the brightness temperature $T(\varphi, \theta)$ of the emitting body are known.

For a further analysis, let us introduce the concept of the effective solid

STAT

angle for the radiation pattern of the antenna

$$\Omega_a = \int_{(4\pi)} F(\varphi, \theta)\, d\Omega, \tag{13}$$

where $F(\varphi, \theta) = \dfrac{G(\varphi\theta)}{G_{max}}$ is a function describing the radiation pattern of the antenna.

Let us review two particular cases of considerable practical interest, where the recorded ratios can be greatly simplified.

1. Case of reception from emitting areas whose brightness temperature changes negligibly within the limits of the radiation pattern of the antenna. Then, in eq.(12) the term T can be removed from under the integration sign, which gives

$$T_a = T. \tag{14}$$

Thus, the equivalent temperature of the source as delivered at the antenna is equal to the brightness temperature of the observed section in the emitting area. This happens usually when receiving the radio radiation of galactic background by narrow-beam directional antennas.

2. Case of radio reception from sources whose angular sizes are small in comparison with the width of the radiation pattern of the antenna ($\Omega_e \ll \Omega_a$). Here, it can be expected that, within the limits of the solid angle, $G(\varphi, \theta) = G_{max} = \text{const.}$ Then eq.(12) is reduced to the form

$$T_a = T_e \frac{\Omega_e}{\Omega_a} \tag{15}$$

The equivalent temperature of the source as delivered at the antenna can be also expressed in this case as a flux of radio radiation. Substituting into eq.(15) the expressions (4) and (5) and making simple transformations, we obtain

$$T_a = \frac{pA}{2k} \tag{16}$$

Equation (16) is more convenient for practical purposes. It differs from eq.(15) where, in order to determine $T_a$, two parameters of the source must be known (effective temperature of the source $T_e$ and angular dimensions $\Omega_e$). Here it is sufficient to know only one parameter of the source (the radio-radiation flux p). This fact is particularly important when calculating $T_a$ of discrete sources, whose angular dimensions have not yet been accurately determined.

## 4. Basic Intensity Characteristics of Radio Radiation from Cosmic Objects

a) Solar Radio Emission (Bibl.2-6). Differentiation must be made between the radio radiation of a so-called "quiescent" sun, observed during periods when the solar surface has no spots or other active formations that would create disturbances in the solar atmosphere, and the radio radiation of the so-called "disturbed" sun when such formations are present.

The intensity of radio radiation from a quiescent sun is fairly constant from day to day in the meter and millimeter bands and is the same for years of maximum and minimum solar activity. In the band of centimeter and especially decimeter waves, the intensity of radio radiation from a "quiet" varies according to the cycle of solar activity (11 years) and increases in the years of maximum solar activity. Average data on the intensity of solar radio radiation in the 8 mm to 10 m band are given in Table 1.

For convenience, the intensity is expressed both by the flux p in units of $10^{-21} \frac{W}{M^2 cycles}$ and by the effective temperature of solar radio radiation $T_e$, reduced to the visible solid angle of the sun $\Omega_e = 6.8 \times 10^{-5}$ sterad = 0.22 square degrees. The figures in the numerator corresponds to the years of maximum, while those in the denominator denote the years of minimum of solar activity.

The radio noise of a "disturbed" sun are characterized by a general increase in radiation intensity and by its considerable fluctuations. This increase depends on the wavelength and constitutes, on the average, a few percent in the millimeter wave band (MMW), a few tens of percent in the centimeter wave band (CMW) and 1.5-3 times more in the decimeter wave band (DMW), but tens and hundreds of times in the meter wave band (MW). The duration of the disturbance is from a few minutes in the MMW

STAT

band to a few days in the MW band.

Besides the above-mentioned increase in intensity, occasional (a few times a year) especially powerful radio radiation bursts occur during which the intensity in-

Table 1

| $\lambda$ | $p \cdot 10^{21}\ \frac{W}{m^2\,cycles}$ | $T_e$, K° |
|---|---|---|
| 8 mm | 200 | $6{,}7 \cdot 10^3$ |
| 3 cm | $\frac{32}{27}$ | $\frac{17{,}5 \cdot 10^3}{15 \cdot 10^3}$ |
| 10 cm | $\frac{13}{6{,}5}$ | $\frac{80 \cdot 10^3}{40 \cdot 10^3}$ |
| 25 cm | $\frac{7}{3{,}5}$ | $\frac{2 \cdot 10^5}{1 \cdot 10^5}$ |
| 50 cm | $\frac{5}{2{,}5}$ | $\frac{6 \cdot 10^5}{3 \cdot 10^5}$ |
| 1,5 m | 0,85 | $1 \cdot 10^6$ |
| 3 m | 0,3 | $1{,}5 \cdot 10^6$ |
| 10 m | 0,035 | $2 \cdot 10^6$ |

creases by 20-30% in the MMW band; by tens of times in the CMW band; by hundreds of times in the DMW band; by tens and hundred thousands of times in the band of MW.

The duration of such bursts is from a few minutes to an hour.

The proportion of periods during which solar radio noise has a "quiet" or "disturbed" character depends on the phase of the eleven-year cycles of solar activity. In the years of maximum solar activity, up to 30-50% of the time, the solar radio radiation has a "disturbed" character. In the years of minimum solar activity, the

STAT

number of days when the solar radio radiation has a "disturbed" character is only 10%. The last minimum of solar activity was in 1953. In the next few years an increase in solar activity, with a maximum in 1958, will be observed.

b) Galactic Radio Radiation. In 1932, in studying atmospheric radio disturbances (Bibl.7) a source of radio radiation was discovered which periodically changed its location during 24 hours. Further studies showed that the source of observed radio radiation is the general galactic background (Milky Way).

The intensity of galactic radio radiation depends on the coordinates and on the wavelength. The greatest amount of radio radiation comes from the galactic center (right ascension $\alpha = 17^h\ 50^m$, inclination $\delta = -28^o$) which is in the direction of the Sagittarius constellation; the minimum comes from the galactic poles.

Table 2

| *f*, mc | 18,3 | 100 | 160 | 200 | 480 | 1200 | 3000 |
|---|---|---|---|---|---|---|---|
| *T*, °K | 140 000 | 3860 | 1370 | 447 | 107 | 17 | 2,6 |

In Table 2, taken from a literature review (Bibl.8-9) values for intensity of radio radiation from the galactic center are given, expressed in units of brightness temperature.

The distribution of radio brightness over the galaxy also depends on the wavelength. In the centimeter and decimeter wave bands, a pronounced concentration of radio radiation occurs at the galactic equator, with a direction toward the galactic center. For instance, for a wave of $\lambda = 25$ cm the zone at whose border the intensity of radio radiation decreases to half (as compared with the intensity of radio radiation toward the galactic center) extends to $10^o$ in the direction of the galactic plane (along the Milky Way) and about $4^o$ in the direction perpendicular to this plane. With an increase in wavelength, the maximum of galactic radio radiation broadens. Thus, for the wave $\lambda = 60$ cm the area of the mentioned zone is included

STAT

between about $40^{\circ}$ along the galactic plane and about $8^{\circ}$ in a direction perpendicular to this plane.

For waves of the meter band, the maximum of radio radiation spreads even more. For instance, for the 3-meter wave the zone at whose borders the intensity of radio radiation drops to half, has an area of about $80^{\circ} \times 20^{\circ}$. For this wave, the radio brightness in the direction of the galactic poles is 10-12 times less than toward their center. For longer waves, this difference decreases still more. Thus, for the 16.4 m wave (Bibl.9) radio brightness in the direction of the galactic poles is only 4-5 times lower than in the direction of the center.

c) Radio Radiation from Discrete Sources. In 1946 (Bibl.10), when studying the fine structure of radio radiation from the galactic background a powerful source of radio radiation was discovered in the constellation of Cygnus, having a compartively small angular size. Later, research on other areas of the sky discovered a great quantity of radio radiation sources of similar type. These sources were called "radio stars".

Further studies have shown, however, that the concept of "radio stars" as a special type of cosmic bodies cannot be identified with any optical bodies of a size similar to those of normal stars. The extraordinarily powerful radiation on radio frequencies leads to a series of conclusions which are unacceptable from the physical point of view.

Measurements taken during recent years have shown that the angular magnitudes of a series of "radio stars" are of the order of a few angular minutes. Moreover, a considerable part of discrete sources of radio radiation could be identified with optically observed nebulae. Therefore, at present the expression "radio star" is being changed to a more adequate expression conveying the essence of the effect, i.e. that of a "radio nebula".

At present a large number (about 2000) of discrete sources of radio radiation is known. The radiation flux from these sources depends on the frequency, usually increasing with an increase in wavelength.

In Table 3 gives the coordinates and the intensity of radio radiation of the most intense discrete sources observed over the territory of the USSR (Bibl.11-14).

Table 3

| a) | b) | | c) | | | | | | |
|---|---|---|---|---|---|---|---|---|---|
| | d) | e) | 3,2 cm | 10 cm | 20 cm | 50 cm | 1 m | 3 m | 10 m |
| Cassiopeia | $23^h\ 21^m$ | $+58°\ 30'$ | 5,9 | 15 | 25 | 40 | 60 | 150 | 600 |
| Cygnus A | $19^h\ 57^m$ | $+40°\ 35'$ | — | 8 | 12 | 20 | 35 | 110 | 400 |
| Taurus | $05^h\ 31^m$ | $+22°\ 04'$ | 7,3 | 8 | 10 | 13 | 16 | 18 | 13 |
| Virgo | $12^h\ 28^m$ | $+12°\ 44'$ | — | 1,8 | 2,3 | 3 | 5 | 12 | — |
| Centaurus A | $13^h\ 22^m$ | $-42°\ 46'$ | — | 2,2 | 2,8 | 4,5 | 7 | 18 | — |
| Orion M-42 Nebula | $5^h\ 33^m$ | $-5°\ 37'$ | 2,7 | 4,5 | 4,5 | — | — | — | — |
| Omega M-17 | $18^h\ 17^m$ | $-16°$ | 7,5 | 7 | 8 | — | — | — | — |
| Nebula M-20 | $17^h\ 59^m$ | $-23°$ | — | 1 | 4 | — | — | — | — |

a) Source; b) Coordinates; c) Radio radiation flux $\times\ 10^{-24}$ w/m$^2$ cycles on waves of; d) Direct ascension; e) Inclination

The radiation flux is expressed in units $10^{-24}\ \frac{w}{m^2 cycles}$. The coordinates of the sources are given in an equatorial system of coordinates. Conversion of the equatorial system of coordinates into a horizontal system is shown in another paper (Bibl.16).

Besides discrete sources of small angular magnitude (in the range of a few angular minutes) there are also comparatively spread discrete sources of radio radiation with angular magnitudes in the range of a few degrees. Data covering two more intensive sources of the above type are found in Table 4. The intensity of radio radiation is expressed in units of effective temperature of the source $T_e$.

As indicated in these Tables, the constellation of Cygnus contains two neighboring sources of radio noise. Considerable difficulties in separating them and a possible error in determining the antenna parameters makes the use of these two sources undesirable for radiotechnical purposes.

d) Radio Radiation of the Moon and Planets. Radio radiation from the moon has a thermal character. In the wave band $\lambda = 3$ cm, the effective moon temperature, characterizing the intensity of its radiation, is equal on the average to $T_e \approx 200$ K

Table 4

| a) | b) | | e) | f) | | | |
|---|---|---|---|---|---|---|---|
| | c) | d) | | 10 cm | 20 cm | 50 cm | 1 m |
| g) | $20^h 20^m$ | 40° 00' | i) | 5° | 16° | 50° | 160° |
| h) | $17^h 43^m$ | −29° | j) | 20° | 70° | 300° | — |

a) Sources; b) Coordinates of center; c) Direct ascension; d) Inclination; e) Spread; f) Effective temperature $T_e$ °K for waves of; g) Cygnus-X; h) Sagittarius; i) $10° \times 2°$ spread along galactic equator; j) $12° \times 2°$ spread along galactic equator.

and apparently depends only insignificantly on the phase of the moon. The radio radiation flux from planets is very small because of their small angular dimensions.

The author expresses his gratitude to N.A.Logova and U.V.Khangil'din, who participated in composing the review on the sun.

Article received by the Editors on 30 January 1956.

BIBLIOGRAPHY

1. Aarons,J. - Measuring Characteristics by Means of Solar and Cosmic Radio Radiation. Proc. IRE, Vol.42, No.5 (1954), pp.810 - 815

2. - Quarterly Bull. on Solar Activity, Nos.87 - 106 (1947 - 54)

3. Hagen,J.P. - Temperature Gradient in the Solar Atmosphere for Measuring of Radi-

Waves. Astrophys. J. Vol.113, No.3 (1951), pp.547 - 566

4. Minett,H.C. and Labrum,N.R. - Radio Radiation of the Sun on the 3.18 cm Wave, Austral. J. Scient. Res., Vol.3, No.1 (1950), pp.60 - 71

5. Christiansen,W.H., Hindman,J.V., Little,A.G., Payne, Scott,R., Vabsley,D.E., and Allen,C.W. - Radio Observations During Two Solar Flares. Austral. J. Scient. Res., Vol.4, No.1 (1951), pp.51 - 61

6. Christiansen,W.H. and Hindman,J.V. - Slow Variations in the Intensity of Radio Radiation of a "Quiet" Sun in the Decimeter Wave Range. Nature, Vol.167, No.4251 (1951), pp.635 - 636

7. Jansky,K.G. - Radiation in the Direction of Arrival of Atmosphere Noise at High Frequency. Proc. IRE, Vol.20, No.12 (1932), pp.1920 - 1932

8. Brown,R.H. and Hazard,C. - Model of Galactic Radio Radiation. Philos. Magazine, Vol.44, No.356 (1953), pp.939 - 963

9. Shain,C.A. and Higgins, C.S. - Observation of General Background and Discrete Sources of Radio Radiation at 18.3 mc Frequency. Austral. J. Phys., Vol.7, No.1 (1954), pp.130 - 149

10. Hey,J.S., Phillips,J.W. and Parsons, S.J. - Cosmic Radio Radiation on 5-m Wave. Nature, Vol.157, No.3984 (1946), pp.296 - 297

11. Haddock,F.T., Mayer,C.H. and Slonnaker,R.M. - Radio Observations on Accumulation of Ionized Hydrogen in Various Discrete Sources on the 9.4 cm Wave. Nature, Vol.174, No.4421 (1954), pp.176 - 177

12. Hagen,J.P. and McClain,E.F. - Discrete Sources of Radio Radiation on the 21-cm Wave. Proc. IRE, Vol.42, No.12 (1954), pp.1811

13. Mills,B.V. - Distribution of Discrete Sources of Cosmic Radio Radiation. Austral. J. Scient. Res., Vol.5, No.2 (1952), pp.266 - 287

14. Kaidanovskyi,H.L., Kardashev,N.S. and Shlovsky,I.S. - Dokl. Ak. Nauk Vol.104, No.4 (1955), pp.517 - 519

15. Troitsky,V.S. - Radioastronomy Methods for Measuring Antenna Losses.





Declassified in Part - Sanitized Copy Approved for Release @ 50-Yr 2013/11/13 : CIA-RDP81-01043R002700130004-0

Zh. Tekh. Fiz. Vol.26, No.2 (1956), pp.485 - 486

16. Blazhko, - Course in Spherical Astronomy. Gostekhmizdat (1954)

STAT



Declassified in Part - Sanitized Copy Approved for Release @ 50-Yr 2013/11/13 : CIA-RDP81-01043R002700130004-0

# CALCULATION OF COMPLEX RESONATORS

by

A.I.Zhivotovskiy

Active Member of the Society

The article reviews complex resonators, composed of several sections of homogeneous concentrical lines with different wave resistances. Deductions of expressions for the technical calculation of such resonators are made.

## 1. Introduction

In the technique of decimeter waves resonators having the shape of concentric lines are frequently used as oscillatory circuits. If the length of such lines does not exceed one quarter wavelength, they usually permit the transfer of a very broad frequency band and permit operation with a high efficiency factor.

If the working frequency is raised, the line is made longer using resonance on longitudinal overtones. This leads, however, to a decrease in the active input resistance of the unloaded resonator, to a lower efficiency, and to a narrowing of the transmitted frequency band.

These deficiencies can be eliminated or lessened either by using complex lines, in which transformed resistances, both distributed along the circuit or concentrated, are used. These include important contact resistances whose value frequently exceeds the total of all other resistances.

Such transformation of resistances is usually much more effective if the resistance is greater in the vicinity of current antinodes (for instance, contact resistances) in the total balance of circuit resistances.

Before reviewing complex circuits, let us discuss the simple circuits.

## 2. Simple (Uniform) Circuits

When a capacitance is connected into the beginning of a uniform circuit (Fig.1), its geometric length at resonance is determined by the expression

$$\boxed{L = l + (n-1)\frac{\lambda}{4},} \tag{1}$$

where $l$ is the geometric length from the beginning of the circuit to the first voltage node;

$n$ is a whole positive number;

$\lambda$ is the wavelength, corresponding to the resonance frequency.

The value n can be odd or even. With an even value of n, the end of the circuit must be loaded with a very considerable resistance, while with an odd n the load must have a very small resistance, for instance, it can be shorted; such circuits are frequently used as oscillatory circuits. In the present work only circuits with an odd n are considered.

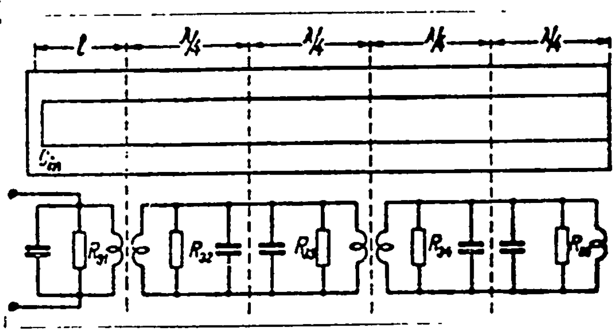

Fig.1

It is known (Bibl.1-4) that a line shorted at the end with distributed parameters and having a capacitance at the beginning, can be exchanged for an equivalent one with concentrated parameters - if the frequencies are near resonance - and having the same resonance frequency, quality factor, and active input resistance.

Transforming known formulas, the parameters of such a circuit can be expressed in the following manner:

$$R_{exx} = \frac{2w^2 \sin^2\theta}{R_1 l\left(1 + \frac{\sin 2\theta}{2\theta}\right) + R_1(n-1)\frac{\lambda}{4} + 2r}, \tag{2}$$

$$Q_{xx} = \frac{2\pi w}{R_1\lambda + \frac{8\pi r}{2\theta + \sin 2\theta + (n-1)\pi}}, \tag{3}$$





Declassified in Part - Sanitized Copy Approved for Release @ 50-Yr 2013/11/13 : CIA-RDP81-01043R002700130004-0

$$C_e = \frac{1}{2} C_{in}\left(1 + \frac{2\theta + (n-1)\pi}{\sin 2\theta}\right), \qquad (4)$$

$$\rho_e = \frac{1}{\omega C_e} = \omega L_e = \frac{4w \sin^2\theta}{2\theta + \sin 2\theta + (n-1)\pi}. \qquad (5)$$

Here $R_{exx}$ and $Q_{xx}$ are the active input resistance and the quality factor of an unloaded circuit; $C_e$ and $\rho_e$ are the capacitance and characteristic of the equivalent circuit;

$R_1$ is the resistance of unit length of the circuit;

r is the resistance at the current antinode together with other added resistances (except $R_1$);

$\theta = 2\pi \frac{l}{\lambda}$ is the electric length of the circuit section $l$.

At $n > 1$, a uniform line can be exchanged not only for an equivalent circuit, but for a system n of connected circuits, as shown in Fig.1 for $n = 5$.

All other resistances, besides $R_1$, can be attributed to any circuit. For a more definite and easy calculation, a part of other resistances (for instance, contact resistances between circuit and capacitances, etc.) can be attributed to the first current antinode and called $r_1$, while the other resistances (for instance, the resistance between the circuit contacts and the shorting device, etc.) can be attributed to the last current antinode and called $r_n$.

Then the circuits will have as parameters

$$R_{e1} = \frac{2w^2 \sin^2\theta}{R_1 l\left(1 + \frac{\sin 2\theta}{2\theta}\right) + 2r_1}. \qquad (6)$$

All other equivalent resistances, except the last one, are identical

$$R_{e2} = R_{e3} = \ldots = R_{e\,n-1} = \frac{8w^2}{R_1 \lambda}. \qquad (7)$$

The equivalent resistance of the last circuit is determined by the expression

$$R_{en} = \frac{8w^2}{R_1\lambda + 8r_n}. \tag{8}$$

In accordance with the above, the quality factor of these circuits will be equal to

$$Q_{x1} = \frac{2\pi w}{R_1\lambda + \frac{8\pi r_1}{2\theta + \sin 2\theta}}, \tag{9}$$

to the quality factor of the other circuits except the last one

$$Q_{x2} = Q_{x3} = \ldots = Q_{xn-1} = \frac{2\pi w}{R_1\lambda}. \tag{10}$$

while the quality factor of the last one will be

$$Q_{xn} = \frac{2\pi w}{R_1\lambda + 8r_n}. \tag{11}$$

The characteristics of the circuits are determined by the expressions

$$\rho_{e1} = \frac{4w\sin^2\theta}{2\theta + \sin 2\theta}, \tag{12}$$

$$\rho_{e2} = \rho_{e3} = \ldots = \rho_{en} = \frac{4w}{\pi}. \tag{13}$$

The voltage in the first circuit will be

$$U_1 = U_{p1}\sin\theta = I_{p1}w\sin\theta.$$

The voltages in the other circuits are equal to $U_{p1}$, where $I_{p1}$ and $U_{p1}$, respectively, are the current and the voltage in the antinode.

## 3. Complex Lines

Here lines will be reviewed whose feature consists in following: to the first uniform section of length $l$ are added uniform sections of a length equal to $\frac{\lambda}{4}$ having different characteristic impedances. The influence of discontinuity is disregarded since, in many cases, it has no practical significance.

Such a complex line with resonance can also be visualized as a system of connected circuits, as shown in Fig.2.

The voltages of the circuits are determined according to the formulas

$$U_1 = I_{p1} w_1 \sin\theta, \tag{14}$$

$$U_{2,3} = I_{p1} w_2. \tag{15}$$

$$U_{4,5} = I_{p3} w_4. \tag{16}$$

. . . . . . . . . . . . . . .

$$U_{n-1,n} = I_{p(n-2)} w_{n-1}. \tag{17}$$

Here $I_p$ indicates the current in the antinode of the corresponding circuit. The equivalent resistances of the circuits are, respectively, equal to

$$R_{e1} = \frac{2w_1^2 \sin^2\theta}{R_{11} l\left(1 + \frac{\sin 2\theta}{2\theta}\right) + 2r_1} = \frac{8w_1^2 \sin^2\theta}{\lambda\left[\left(\frac{2\theta + \sin 2\theta}{\pi}\right) R_{11} + \frac{8r_1}{\lambda}\right]}, \tag{18}$$

$$\left.\begin{aligned} R_{e2} &= \frac{8w_2^2}{R_{12}\lambda} \\ R_{e3} &= \frac{8w_3^2}{R_{13}\lambda} \end{aligned}\right\} \tag{19}$$

. . . . . . . . . . . .

$$R_{en} = \frac{8w_n^2}{R_{1n}\lambda + 8r_n}, \tag{20}$$

while the quality factor is

$$Q_{x1} = \frac{2\pi w_1}{R_{11}\lambda + \frac{8\pi r_1}{2\theta + \sin 2\theta}}, \tag{21}$$

$$Q_{x2} = \frac{2\pi w_2}{R_{12}\lambda}, \tag{22}$$

. . . . . . . . . . . . . . .

$$Q_{xn} = \frac{2\pi w_n}{R_{1n}\lambda + 8r_n}. \tag{23}$$

STAT

The characteristics of the circuits will be

$$\rho_{e1} = \frac{4w_1 \sin^2\theta}{2\theta + \sin 2\theta}, \tag{24}$$

$$\rho_{e2} = \frac{4w_2}{\pi}, \tag{25}$$

$$\cdots\cdots\cdots$$

$$\rho_{en} = \frac{4w_n}{\pi}. \tag{26}$$

Taking into account the above relations, the system of these connected circuits can be replaced by one equivalent circuit, with the parameters:

$$R_{exx} = \frac{8w_1^2 \sin^2\theta}{\lambda A}, \tag{27}$$

$$Q_{xx} = \frac{2\pi}{\lambda} \cdot \frac{B}{A}, \tag{28}$$

$$\rho_e = \frac{4w_1^2 \sin^2\theta}{\pi B}. \tag{29}$$

where

$$A = \frac{2\theta + \sin 2\theta}{\pi} R_{11} + \frac{8r_1}{\lambda} + R_{12} + \left(\frac{w_2}{w_3}\right)^2 R_{13} + \left(\frac{w_2}{w_3}\right)^2 R_{14} + \\ + \left(\frac{w_2 w_4}{w_3 w_5}\right)^2 R_{15} + \ldots + \frac{8}{\lambda}\left(\frac{w_2 w_4 \ldots w_{n-1}}{w_3 w_5 \ldots w_n}\right)^2 r_n,$$

$$B = \frac{2\theta + \sin 2\theta}{\pi} w_1 + w_2 + \left(\frac{w_2}{w_3}\right)^2 w_3 + \left(\frac{w_2}{w_3}\right)^2 w_4 + \\ + \left(\frac{w_2 w_4}{w_3 w_5}\right)^2 w_5 + \ldots + \left(\frac{w_2 w_4 \ldots w_{n-1}}{w_3 w_5 \ldots w_n}\right)^2 w_n.$$

It is convenient to use eqs.(27), (28), (29) for calculating such complex resonators. The Table lists the calculation data obtained from these formulas for uniform circuits with n = 1 (Nos.1, 8, and 15); for uniform circuits with n = 3 (Nos.2, 9, and 16); and for complex circuits with n = 3 (all other numbers).

For these calculations, the following values are accepted: $C_{in}$ = 5 μμf, λ = 20 cm, $r_n$ = 0.02 ohm. The concentric circuits are of copper, and the diameter of the inside conductor of every line is constant and equal to 20 mm.

STAT

Table

| № | $w_1$ ohm | $w_2$ ohm | $w_3$ ohm | $R_{exx}$ ohm | $Q_{xx}$ | $\Delta f$ mc |
|---|---|---|---|---|---|---|
| 1 | 15 | — | — | 5 640 | 400 | 7,05 |
| 2 | 15 | 15 | 15 | 3 650 | 835 | 2,18 |
| 3 | 15 | 15 | 60 | 9 700 | 1 640 | 2,95 |
| 4 | 15 | 15 | 90 | 10 300 | 1 670 | 3,07 |
| 5 | 15 | 60 | 60 | 3 980 | 2 780 | 0,71 |
| 6 | 15 | 60 | 90 | 6 460 | 3 880 | 0,83 |
| 7 | 15 | 90 | 90 | 4 100 | 4 180 | 0,49 |
| 8 | 60 | — | — | 18 200 | 882 | 10,3 |
| 9 | 60 | 60 | 60 | 12 300 | 3 450 | 1,78 |
| 10 | 60 | 60 | 90 | 21 500 | 5 180 | 2,07 |
| 11 | 60 | 90 | 90 | 12 700 | 5 020 | 1,76 |
| 12 | 60 | 90 | 60 | 720 | 346 | — |
| 13 | 60 | 15 | 60 | 36 500 | 3 100 | 5,9 |
| 14 | 60 | 15 | 90 | 39 700 | 3 270 | 6,05 |
| 15 | 90 | — | — | 20 000 | 957 | 10,45 |
| 16 | 90 | 90 | 90 | 13 700 | 5 170 | 1,32 |
| 17 | 90 | 60 | 60 | 13 200 | 3 530 | 1,87 |
| 18 | 90 | 60 | 90 | 23 700 | 5 450 | 2,16 |
| 19 | 90 | 15 | 90 | 46 000 | 3 690 | 6,25 |
| 20 | 90 | 15 | 60 | 41 800 | 3 440 | 6,08 |

The band of transmitted frequencies $\Delta f$ is determined at the level of half-power for a loaded resonator, whose equivalent resistance $R_{en}$, for all reviewed cases, is equal to 3000 ohms.

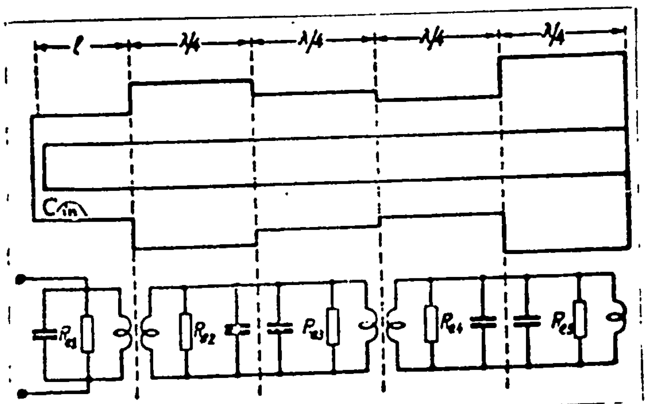

Fig.2

As it appears from the Table, the active resistance at the input of an unloaded complex resonator $R_{exx}$ for n = 3 can be greater than in a uniform resonator – even at n = 1 – which is due to transformation of the resistance $r_n$. (Compare No.1 with Nos.3 and 4, No.8 with Nos.10,13,14, etc.)

STAT



Declassified in Part - Sanitized Copy Approved for Release @ 50-Yr 2013/11/13 : CIA-RDP81-01043R002700130004-0

The frequency band $\Delta f$ of the complex resonators with $n = 3$ is smaller, than in a corresponding uniform resonator with $n = 1$, while it may be considerably larger for a uniform resonator with $n = 3$. (Compare Nos.3 and 4 with No.2, Nos.13 and 14 with No.9, Nos.19 and 20 with No.16, etc.)

These examples show the advisibility of using complex circuits in a number of cases.

Article received by the Editors 26 July 1956.

BIBLIOGRAPHY

1. Neyman,M.S. - Triode and Tetrode Generators for Superhigh Frequency. Published by "Sovetskoye Radio" (1950)
2. Zhivotovskiy,A.I. and Kraychik,A.B. - On the Calculation of Oscillatory Circuits in the Ultrashort-Wave Range. Radiotekhnika Vol.6, No.1 (1951)
3. Zhivotovskiy,A.I. and Kraychik,A.B. - Design Elements and Calculation of Superhigh-Frequency Generators and Amplifier. Izvest. LETI, Imeni Lenin, Vol.XXV (1953)
4. Grifone, Luigi - Dimensions of Cavity Resonators for Tubes with Plane Electrodes. Alta Frequenza, No.6 (1954)

STAT



Declassified in Part - Sanitized Copy Approved for Release @ 50-Yr 2013/11/13 : CIA-RDP81-01043R002700130004-0

# CALCULATION OF ABSORPTION LINE

by

V.S.Melnokov

Active Member of the Society

**This article presents an analysis of the absorption line designed in such a way, that energy absorption per unit length is constant all along the line.**

**Homogenous lines** used at present for power absorption are calculated for constant wave attenuation along the line. The power dissipated along each unit length of the circuit differs. At the beginning of the circuit, the dissipated power is high and decreases considerably at the end of the circuit. Consequently, the line is inefficiently utilized for the dissipation of energy.

It would be desirable to design an absorption line with an even power dissipation along its length.

When denoting by P (x) the power passing through the point at a distance x from the end of the circuit, the condition of continuously dissipated energy will be written as

$$\frac{dP(x)}{dx} = \text{const.} \tag{1}$$

Assuming that the total power put into the circuit is equal to P and the length of the circuit is $l$, we obtain, in accordance with eq.(1),

$$\left.\begin{aligned} \frac{dP(x)}{dx} &= -\frac{P}{l} \\ P(x) &= P\left(1-\frac{x}{l}\right) \end{aligned}\right\}. \tag{2}$$

The basic equations of a long circuit have the form

$$\left.\begin{aligned}\frac{dU}{dx} &= -z(x)I \\ \frac{dI}{dx} &= -y(x)U\end{aligned}\right\}. \qquad (3)$$

Solving these equations in accordance with our problem, it is advisable to introduce a new function ρ (x) which is the input resistance of a circuit whose length is (1 - x), at a point x distant from the end. Then eq.(3) can be written as*:

$$\frac{dU}{dx} + \frac{z(x)}{\rho(x)}U = 0; \qquad \frac{dI}{dx} + y(x)\rho(x)I = 0. \qquad (4)$$

A solution for eq.(4) can be sought in the form of:

$$\left.\begin{aligned}U &= U_0 e^{-\int_0^x \frac{z(x)}{\rho(x)}dx} \\ I &= I_0 e^{-\int_0^x y(x)\rho(x)dx}\end{aligned}\right\}. \qquad (5)$$

where $U_o$ and $I_o$ are arbitrary integrations.

According to the general theory of alternating current, we have

$$P(x) = \mathrm{Re}(U I^*), \qquad (6)$$

where I* is a current value at the point x, conjugate with I.

According to the conditions of the problem, the input resistance at the beginning of the circuit must be purely active at any frequency. Hence, to obtain a circuit with uniform structure along the entire line, it is sensible to request that ρ (x) should be a purely active value.

In the design in question, it is desirable that the conductance y (x) be purely reactive. Then,

$$I^* = I_0 e^{+\int_0^x y(x)\rho(x)dx}.$$

* Here the author uses a method borrowed from the work of V.A.Il'in.

STAT

Substituting U and I* into eq.(6) and taking into account the active character of $\rho(x)$, we obtain

$$P(x) = U_0 I_0 e^{\int_0^x \left\{ y(x)\rho(x) - \frac{z(x)}{\rho(x)} \right\} dx}. \qquad (7)$$

Hence

$$\frac{dP(x)}{dx} = P(x)\left\{ y(x)\rho(x) - \frac{z(x)}{\rho(x)} \right\}, \qquad (8)$$

but, since P(x) and $\frac{dP(x)}{dx}$ have been determined earlier [eq.(2)] , we have

$$\frac{z(x)}{\rho(x)} - y(x)\rho(x) = \frac{1}{l - x}. \qquad (9)$$

According to the preliminary conditions, y(x) must be purely reactive, while $\rho(x)$ must be active. Then we assume

$$\left.\begin{array}{r} z(x) = R_1 + i X_1 \\ y(x) = i b_1 \end{array}\right\}. \qquad (10)$$

After this substitution, eq.(9) is split into two equations

$$\left.\begin{array}{r} \frac{X_1}{\rho(x)} - b_1 \rho(x) = 0 \\ \frac{R_1}{\rho(x)} = \frac{1}{l - x} \end{array}\right\}. \qquad (11)$$

Based on design considerations, one can select a longitudinal active resistance of the circuit $R_1$ as being constant. Due to this fact, we will obtain from eq.(11):

$$\rho(x) = R_1 l\left(1 - \frac{x}{l}\right) = R\left(1 - \frac{x}{l}\right). \qquad (12)$$

Here R simultaneously becomes the input resistance of the circuit (when x = 0) and the total of the distributed active resistances.

From the first equation of the system (11) and from eq.(12), it is evident that

$$\sqrt{\frac{X_1}{b_1}} = R\left(1 - \frac{x}{l}\right). \qquad (13)$$

STAT



Declassified in Part - Sanitized Copy Approved for Release @ 50-Yr 2013/11/13 : CIA-RDP81-01043R002700130004-0

The value $\sqrt{\frac{X_1}{b_1}}$ is the characteristic impedance of the circuit under the assumption that the latter is free of losses. However, for a line without losses the condition $\sqrt{X_1 b_1} = \frac{2\pi}{\lambda}$ is valid. Then,

$$\left.\begin{aligned} L(x) &= L_0\left(1 - \frac{x}{l}\right) \\ C(x) &= \frac{C_0}{1 - \frac{x}{l}} \end{aligned}\right\}. \tag{14}$$

where L(x) and C(x) are the longitudinal induction and capacitance at the point x.

$L_0$ and $C_0$ are the longitudinal induction and capacitance at the beginning of the circuit.

From eqs.(13) and (14) it also follows that

$$W(x) = \sqrt{\frac{L(x)}{C(x)}} = R\left(1 - \frac{x}{l}\right). \tag{15}$$

It is apparent, that the characteristic impedance of a circuit free of losses W(x), is equal at the point x to the sum of the ohmic resistances from the point x to the end of the line.

If, in first approximation, it is assumed that the characteristic impedance of the described loss-free circuit, at any point, differs little from the characteristic impedance of a two-wire circuit, then

$$W(x) = R\left(1 - \frac{x}{l}\right) = 120 \ln\left[\frac{D}{d} + \sqrt{\left(\frac{D}{d}\right)^2 - 1}\right]. \tag{16}$$

Solving this equation with respect to D, we obtain a dependence of the distance between the two lines, the diameter of the conductor being constant

$$D = d \operatorname{sh}\left[\frac{R}{120}\left(1 - \frac{x}{l}\right)\right]. \tag{17}$$

Article received by the Editors 17 September 1956.

STAT

# DEVICE FOR VISUAL OBSERVATION AND MEASUREMENT OF FREQUENCY CHARACTERISTICS OF GROUP TIME OF PROPAGATION, PHASE SHIFT, AND MODULUS OF TRANSMISSION FACTOR

(Frequency Cathode-Ray Curve Tracer)

by

I.T.Turbovich

A.V.Knipper

V.G.Solomonov

Active Members of the Society

The article explains the principles of design for a device for rapid measurement of frequency characteristics, investigates the errors, and describes the basic diagram and some of its nodes.

## 1. Introduction

One of the basic parameters, determining the quality of the equipment and of the communication channels, are the frequency characteristics of the transmission factor modulus, of the phase shift and of the group propagation time. Especially high standards are placed on the frequency characteristics of equipment and channels in television.

The device measuring these characteristics must have an accuracy of not less than ± 0.02 μ sec when measuring the group propagation time and of ± 2% when measuring the transmission factor modulus (Bibl.1,2,3).

A substantial role is played by the time required for measuring the characteristics. Experience shows that measurement according to points of one frequency characteristic of the group propagation time in the television main line requires several hours. Moreover, when measuring according to points, certain overshoots in the characteristics may remain unnoticed.

A high degree of accuracy and of speed for measuring the frequency characteristics can be obtained by frequency modulation with the help of an oscillograph.

It has been stated that oscillographic methods for measuring characteristics are less accurate than methods for measuring by points. In our opinion, this is not so. Specific inaccuracies of oscillographic measurements of characteristics (on account of parallax, nonlinear dependence of the beam deflection on the voltage, etc.) can be eliminated by a direct comparison of the measurements of characteristic with the calibrated lines on the oscillograph screen, the distances between lines being set by the calibrating device.

High-speed measurements exclude errors due to unstable characteristics of the measured object. For instance, the characteristics of the group propagation time of television mains can be displaced parallel to themselves. This does not influence the quality of the television picture; however, if the characteristics change along the points, this may lead to considerable errors.

Further, in the case of high-speed measurements the requirements as to the stability of the equipment elements can be relaxed.

This article explains the principles of design for a high-speed measuring device of frequency characteristics, reviews errors, and gives the basic diagram of the schematics and of some nodes of the device, of independent importance. All this has been worked out in 1953-55 in the Research Laboratory for Scientific Problems of Communication, of the USSR Academy of Sciences (Bibl.4-5).

## 2. Errors in High-Speed Measurement of Frequency Characteristics

In measuring frequency characteristics by the method of frequency modulation, an error due to transient processes will arise. As a result of research on this error (Bibl.6) the following formula is obtained:

$$\Delta S(\omega) = \frac{1}{2} \frac{d^2 S(\omega)}{d\omega^2} \frac{d\omega}{dt}, \qquad (1)$$

where $\Delta S(\omega)$ is a complex error when measuring the transmission factor; $S(\omega)$ is the

STAT

transmission factor of the measured object; $\frac{d\omega}{dt}$ is the rate of frequency change during observation.

Calculations show that, for the vast majority of objects under study, operating at frequencies in the range of 6 mc per second, the error $\Delta S(\omega)$ is negligibly small. Therefore, when measuring a segment of the frequency characteristic whose width is in the range of 6–8 mc, the cycle of frequency modulation can be selected in the range of one second. Examples of calculation according to eq.(1) are elsewhere given (Bibl.7).

### 3. Methods for Measurement of Group Propagation Time

The measurement of group time is done by Nyquist's method (Bibl.1). This method is based on the fact that, during transmission of a modulated oscillation across a quadripole, the phase difference envelope at the input and output of the quadripole is approximately proportional to its group propagation time. This method has an inherent unavoidable error (Bibl.4). This error (see Appendix) can be expressed by the formula

$$\Delta\tau = -\frac{db(\omega)}{d\omega}\,\mathrm{tg}\left(\frac{\Omega^2}{2}\frac{d\tau}{d\omega}\right), \qquad (2)$$

where $\Delta\tau$ is the error of group time measurement, $\Omega$ is the amplitude of the frequency modulation (constant), $b(\omega)$ the attenuation of the measured object, $\tau$ the group propagation time, and $\omega$ the frequency at which the group time is measured.

Equations (1) and (2) show that, in the simultaneous presence (in the frequency characteristic of the object) of steep fronts of the transmission factor modulus and of group propagation time, it must be ascertained that both the error due to the high-speed measuring method [eq.(1)] and that due to the Nyquist formula [eq.(2)] do not exceed the prescribed value. For the majority of broad-band objects (with the exception of those with very steep fronts of characteristics) this error will be less than 0.02 $\mu$ sec.

## 4. Basic Diagram of the Device

The basic diagram of the device is shown in Fig.1. According to its purpose, it can be divided into two parts: the transmitting and the receiving portion.

### A. Transmitting Part

In the transmitting part a voltage of varying frequency is created, within the limits of the high-frequency band under study, and amplitude-modulated by a constant low frequency. This voltage is obtained as a result of pulses in the mixer (6) between the oscillation of a fixed-frequency oscillator (5) and the oscillation of the FM oscillator (3). Swinging of the FM generator is achieved by a sawtoothed oscillator (4). The amplitude modulation of the FM oscillator is caused by the modulator (2) which is fed with oscillations from the quartz oscillator (1). The frequency- and amplitude- modulated oscillations generated at the output of the mixer are amplified by a broad-band amplifier (8) and then by an output stage (10), and are fed to the input of the object under study (11). A constant amplitude of the output voltage envelope in the entire frequency band is required when measuring the transmission factor modulus and is achieved by using deep negative feedback at the frequency of amplitude modulation. This is done with the help of an automatic amplitude-envelope control (AAEC) (7).

The basic diagram of the transmitting part of the device remains unchanged when measuring all three characteristics.

### B. Receiving Part

The function of the receiving part is measurement of the amplitude of the envelope at the output of the object under study (when measuring the transmission factor modulus); comparison and measurement of the difference of the envelope phases at the input and output of the object under study (when measuring the group propagation time); integration of the group time as to frequency (when measuring the deviation of the phase shift characteristic from linear).

STAT

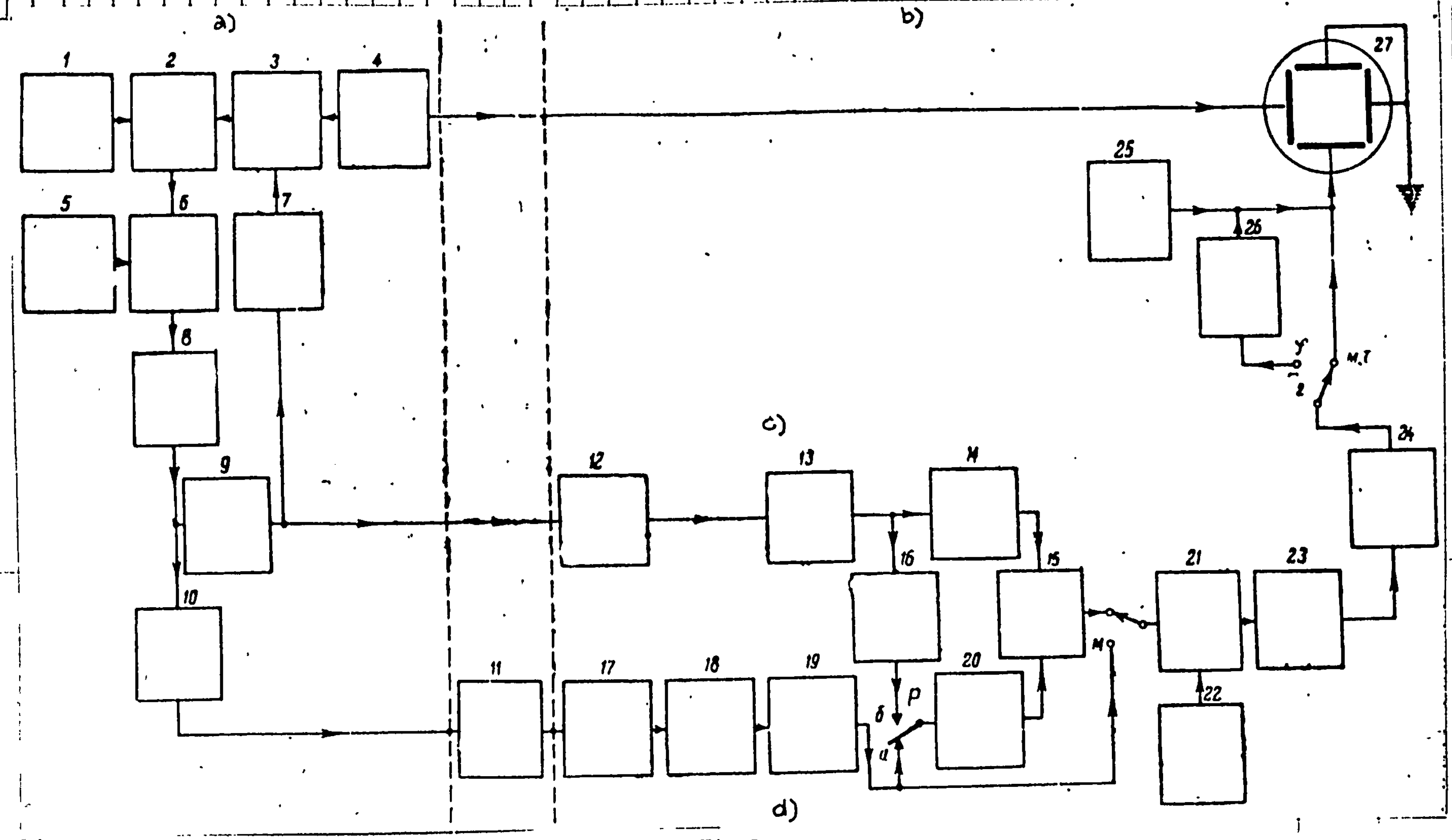


Fig.1

1 - Quartz oscillator, f = 10 kc; 2 - Modulator; 3 - FM oscillator, f = 40 - 48 mc; 4 - Sawtoothed oscillator, f = 1 cycle; 5 - Oscillator, f = 44 - 54 mc; 6 - Mixer; 7 - AAEC; 8 - Broad-band amplifier; 9 - Detector; 10 - Output stage; 11 - Object studied; 12 - Resonance amplifier, $f_o$ = 10 kc; 13 - Phase inverter for 360°; 14 - Limiter; 15 - Phase discriminator; 16 - Calibration phase inverter; 17 - Calibration modulator; 18 - Detector; 19 - Resonance amplifier, $f_o$ = 10 kc; 20 - Limiter; 21 - Mixer; 22 - Oscillator; 23 - IF amplifier, $f_o$ = 17 kc; 24 - Detector; 25 - Marker; 26 - Integrator; 27 - Oscilloscope

a) Transmitting part; b) Receiving part; c) Control channel; d) Measuring channel





Declassified in Part - Sanitized Copy Approved for Release @ 50-Yr 2013/11/13 : CIA-RDP81-01043R002700130004-0

The number of blocks utilized in the receiving part of the device varies, depending on the characteristic being measured.

Measurement of the transmission factor modulus consists in measuring the envelope amplitude at the output of the object under study. This is due to the fact that the envelope amplitude at the input is constant for the entire band of operating frequencies. For this measurement, only a part of the blocks in the described basic diagram is utilized.

The envelope (10 kc) is obtained through the detector action of the detector (18) of a high-frequency oscillation supplied from the output of the object under study (11). The obtained oscillation is amplified by the resonance amplifier (19) and is fed to the mixer (21) (switch $P_1$ in position "M"). In the mixer, the frequency of 10 kc is converted into a higher frequency by means of an auxiliary oscillator (22), is considerably amplified in the IF amplifier (23), is detected for the second time in (24) and, after filtration, is fed to the vertical deflecting plates of the oscillograph (27) (switch $P_2$ in position "M, $\tau$"). The horizontal deflecting plates of the tube are supplied with sawtooth voltage from the oscillator (4).

To eliminate errors, which might occur on account of the nonlinear character of detectors, amplifiers etc., as well as on account of parallax, a special calibrating device (17) provided in the equipment; its operating principle is given below.

The frequency is recorded by the marking device (25).

Measurement of Group Propagation Time

This is done according to Nyquist's method, i.e., by a comparison of the envelope phase at the input of the measured object with that at the output. Comparison of phases is done in the phase discriminator (15), which is supplied with two voltages of 10 kc frequency and equal in amplitude, from the test and control channels. The test channel includes the detector (18), the resonance amplifier (19), and the amplitude limiter (20) (Relay P in position a). The control channel includes the detector (9), the resonance amplifier (12), the adjusting phase inverter (13), and

STAT

the amplitude limiter (14).

The purpose of the amplitude limiters is to create substantially identical amplitudes at the discriminator input, independent of the amplitudes of the input voltages. The adjusting phase inverter (13) provides the initial phase setup for the test and control channels, to a value of about 180°.

The voltage at the input of the phase discriminator (15), is proportional (within certain limits) to the difference of the envelope phases at the input and at the output of the object, i.e., proportional to the group propagation time. This voltage, after its frequency has been changed (21 and 22) and amplified (23), is detected for a second time (24) and is sent to the vertical deflecting plates of the oscillograph tube (27). Recording of the group time is carried out by the calibrating device (16) (see below).

Measuring the Deviation of the Characteristic of Phase Shift from Linear. The deviation of the characteristic of phase shift from linear is obtained by integration of the frequency group time. If the frequency changes with time in a linear manner, the integration according to time can be substituted for integration according to frequency, which is done by the integrator (26).

## 5. Recording of Data from the Device

Recording of data from the device is done by means of comparison. The measuring process is divided into two cycles: measuring and calibrating. During the measuring cycle, the screen of the oscillograph tube shows the measured characteristic, while during the calibration cycle it shows two lines, the distance between which can be established by the calibrator. The tube used in the device has a considerable afterglow. For this reason, the measured characteristic and the calibrating lines are observed simultaneously and can be compared with each other.

### A. Recording of Transmission Factor Modulus

While recording the modulus of the transmission factor during the calibration cycle, frequency modulation ceases, and the input of the object under study is supplied with a constant frequency controlled by the operator. The calibrator (17) (Fig.1) is a potentiometer, whose transmission factor is being changed several times by a relay during the calibration cycle. This projects on the screen broken horizontal lines, whose position and spacing is determined by the attenuation of the potentiometer. Figure 2 shows an oscillogram of the frequency characteristic for the modulus of transmission factor from a double circuit, including calibration lines and marker spots.

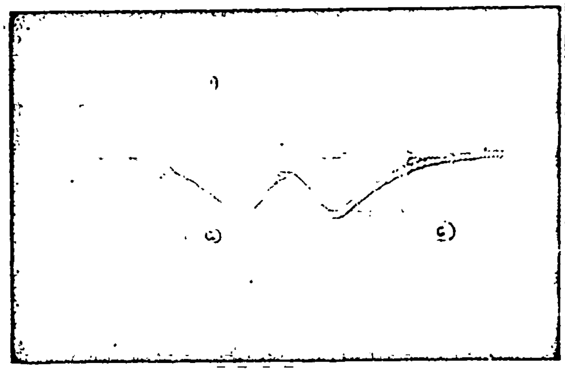

Fig.2

B. Recording of Group Propagation Time.

During the calibration cycle (Relay R in position b), one of the arms of the phase discriminator (15) (Fig.1) is supplied, instead of with test voltage, with voltage from the control channel across the calibrated phase inverter (16) and the limiter (20). During the calibration cycle, the phase shift created by the phase inverter is changed several times in jumps, creating calibrated lines on the screen, whose spacing can be read from the scale of the phase inverter. The phase inverter is graduated in microseconds.

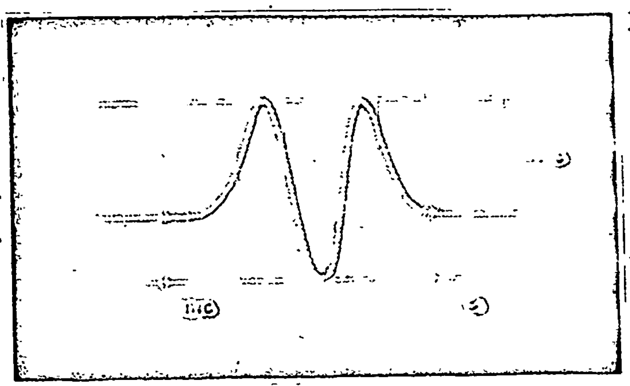

Fig.3

Figure 3 shows the oscillogram of a frequency characteristic for group propagation time of the same object, together with calibration lines.

STAT

C. Recording Deviation of the Phase Shift Characteristic from Linear

When recording the deviation of the phase shift characteristic from linear, the device operates in the same way as in recording group time. The only difference consists in the following: the voltage from the detector output (24) in this case goes through the integrator (26), which results in a calibration curve in the shape of triangles instead of rectangles. The oscillogram of the deviation of the phase shift characteristic from linear and the calibration lines are shown in Fig.4.

6. Phase Discriminator

The phase discriminator (15) represents a summator which is fed, in antiphase, by two low-frequency oscillations of approximately the same amplitude. This brings the output voltage to a value in proportion with the phase difference of these oscillations.

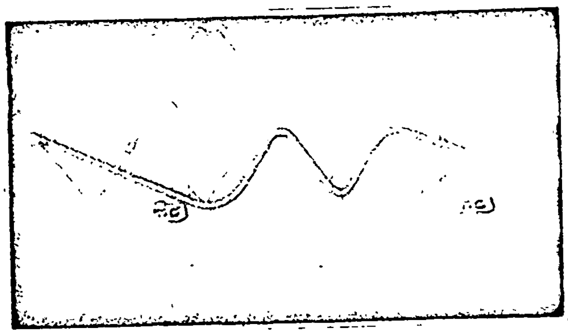

Fig.4

Deviation from the correct proportion (error of discriminator) is caused by: a) nonlinear characteristic of the discriminator when the phase greatly differs at the input, b) difference of amplitudes of the input voltages.

If the phase discriminator input is fed with voltages $u_1 = U_1 \sin(\Omega\tau + \frac{\varphi}{2})$ and $u_2 = -U_2 \sin(\Omega t - \frac{\varphi}{2})$, whose phase difference is $\varphi + \pi$, and if we designate the relative amplitude difference by $\delta = \frac{U_1 - U_2}{\frac{1}{2}(U_1 + U_2)}$, then the voltage at the discriminator output can be written as

$$u = \frac{U_1 + U_2}{2}\left\{\left[1 + \frac{\delta}{2}\right]\sin\left(\Omega t + \frac{\varphi}{2}\right) - \left[1 - \frac{\delta}{2}\right]\sin\left(\Omega t - \frac{\varphi}{2}\right)\right\} = \frac{U_1 + U_2}{2}\left(2\cos\Omega t \sin\frac{\varphi}{2} + \delta \sin\Omega t \cos\frac{\varphi}{2}\right).$$

The amplitude of this voltage will be determined as

$$U=\frac{U_1+U_2}{2}\,2\sqrt{\sin^2\frac{\varphi}{2}+\frac{\delta^2}{4}\cos^2\frac{\varphi}{2}}\,, \tag{3}$$

from which, as the discriminator error $\Delta\varphi$, we obtain the expression

$$\Delta\varphi=2\sqrt{\sin^2\frac{\varphi}{2}+\frac{\delta^2}{4}\cos^2\frac{\varphi}{2}}-\varphi. \tag{4}$$

Figure 5 shows the curves for the dependence of the error $\Delta\varphi$ on the phase difference $\varphi$, caused by the amplitude difference $\delta$.

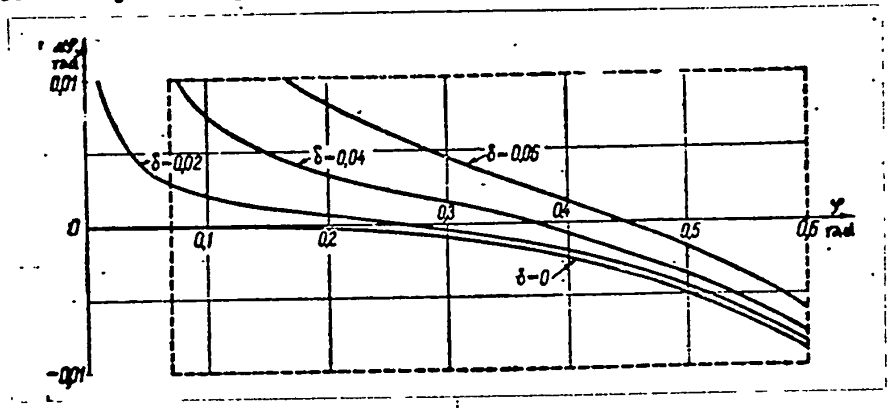


Fig.5

The diagram indicates that the error accrues rapidly in the area of small angles. The operating band of the discriminator should be selected, for practical reasons, within the limits of 0.07 to 0.6 radians. Moreover, if the relative amplitude difference does not exceed 2-3% the error of the discriminator will not exceed 1%.

If the error of the discriminator in the area of non-zero phase difference drops abruptly, the requirements for stable voltage at the output of the limiter also decrease. This is an advantageous feature of this method, as compared with measurements according to points, where the recording is done at zero phase difference.

## 7. Limiter

The limiter block consists of a resonance amplifier stage, a cathode repeater, and the limiter proper whose diagram is shown in Fig.6. The presence of stray coupling between input and output of the limiter creates a spurious amplitude and a phase modulation at its output. To compensate this stray coupling, an additional coupling (a small capacitance C and a large resistance R) is established between the input and output of the limiter, to compensate for the stray coupling.

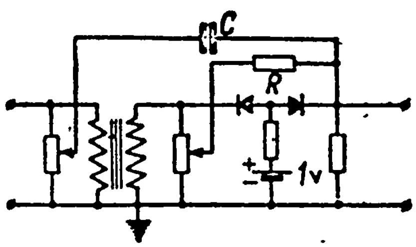

Fig.6

Besides its direct purpose (to obtain the same amplitudes at the input of the phase discriminator) the limiter is also used to obtain harmonics of the fundamental frequency. If the phases of the harmonics in the phase discriminator are compared, the sensitivity of the discriminator will increase in proportion with the number of the harmonic. For this purpose, the device uses the ninth harmonic.

Connecting in series two limiter blocks, a change of voltage in the input of the first one by about five times will yield, at the output of the second one, rectangular pulses whose harmonics amplitudes (up to the ninth inclusive) are constant with an accuracy of 1%. In this case, a phase shift between input and output of the limiters (for the fundamental harmonic) does not exceed $10^{-3}$ radian, while the value for the ninth harmonic is $10^{-2}$ radian.

Since the accuracy of the device is defined by the basic error introduced into the limiter, the phase difference between the HF voltage envelope at the input and output of the test object can be measured with an accuracy to within $10^{-3}$ radian.

## 8. Integrator

A most practical layout for integration is one with a capacitance feedback, as shown in Fig.7a. Here R and C are the integrating resistance and capacitance. $R_n$ is the load resistance, $C_c$ and $R_y$ are the stray capacitance and leakage resistance, respectively.

An expression for the transmission factor of this hookup has a rather complex

STAT



Declassified in Part - Sanitized Copy Approved for Release @ 50-Yr 2013/11/13 : CIA-RDP81-01043R002700130004-0

aspect (Bibl.5). However, if the real values of the circuit parameters are taken into consideration and if, in this expression, terms higher than the second order of smallness, i.e., terms whose value is smaller than $10^{-2}$, are taken into consideration, an expression for the transmission factor k is obtained, determined by the ratio of the output to the input voltage, as follows:

$$K = \frac{u_{out}}{u_{in}} = -\left[\frac{1-\frac{1}{\mu}}{RpC} - \frac{\frac{1}{\mu}+\frac{R}{R_y}}{(RpC)^2}\right], \qquad (5)$$

where p is the Laplacian operator.

The first term of eq.(5) is proportional to $\frac{1}{p}$ (the operator $\frac{1}{p}$ means integration) and is a useful value, while the second is proportional to $\frac{1}{p^2}$, i.e., to the double integral and represents an integration error. This error is caused by the finiteness of the tube amplification factor ( $\frac{1}{\mu} \neq 0$) and by the presence of leakage $\frac{1}{R_y}$ from the integrating capacitor.

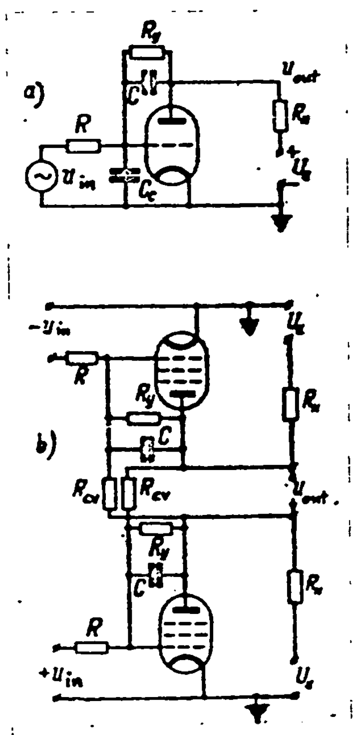

Fig.7

From eq.(5) it is apparent that the value of the stray capacitance $C_c$ does not enter into the expression for the transmission factor, i.e., the error caused by this fact is small compared with errors caused by other parameters.

To compensate the integration error, the circuit must be complicated in such a manner that an additional term would appear in the transmission factor. This term would be proportional to $\frac{1}{p^2}$ but with a sign opposite to that of the error.

In the case of a symmetric circuit, such compensation is very simple and consists in sending a voltage from the output of one integrator across the resistance $R_{cv}$ to the input of the other one or vice versa (Fig.7b). Having written an expression for the transmission factor of this diagram we obtain the condition for compensating the integration error, as follows

$$\frac{1}{R_{cv}} = \frac{1}{\mu R} + \frac{1}{R_y}. \qquad (6)$$

This defines the value of the compensating resistance $R_{cv}$. In actual circuits, the value $R_{cv}$ is in the range of 200 megohms.

When compensation is available, it becomes possible to obtain in the diagram of Fig.7b (with tubes of type 6Zh8) an integration with an accuracy to within 1%, with the full swing of the output voltage in the range of 600–700 v.

## 9. Input Detector

To decrease the dependence of the phase shift in a detected low-frequency oscillation on the high-frequency amplitude, a circuit of consecutive detection without capacitance is used.

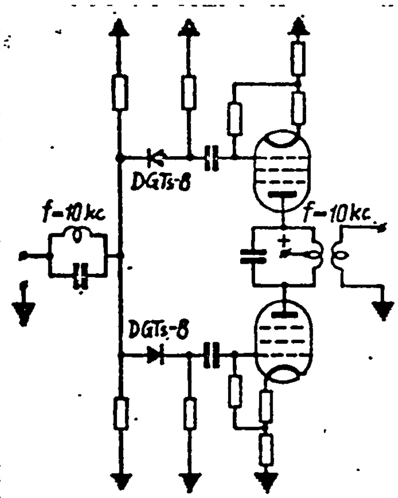

Fig.8

When a modulated signal passes through the measured object having a nonlinear character, the voltage sent to the detector may have a low-frequency component producing large errors. To eliminate a voltage of this frequency, a rejection filter and a symmetric detection system (Fig.8) are used. To eliminate the tube input capacitance, deep negative feedback is applied.

Such a diagram ensures the independence of the amplitude on the detected voltage, with an accuracy to within 1% and of the phase to $10^{-3}$ radian – when the carrier frequency changes from 0.2 to 10 mc. Moreover, the phase of the detected oscillation does not depend (with an approximation as mentioned above) upon the amplitude of the input voltage, if this latter is changed by 5 times.

## 10. Experimental Testing of the Accuracy of the Device

Testing of the device is carried out as follows:

a) The input of the device is shorted to the output; then the transmission factor modulus is equal to 1, while the group time is equal to 0 in the entire frequency band. A comparison of the resultant characteristics with the calibration lines shows that the errors do not exceed the permissible values;

b) The errors of the device are measured in the same manner by coupling it with voltage divider which does not cause phase distortions and is used as reference;

c) The characteristics of a series of uncomplicated objects, as measured by the device, are compared with the theoretical calculations.

## 11. Technical Data of the Device

Frequency band: 0.2 - 10 mc;

Test band of group propagation time: up to 10 $\mu$sec;

Measuring accuracy of group time: 2% $\pm$ 0.02$\mu$ sec, with attenuation drop to 1.5 neper;

Measuring accuracy of the modulus of transmission factor: $\pm$ 0.02 neper in the band to 0.5 neper; and $\pm$ 0.05 in the band to 1.5 neper;

Output resistance: 75 ohms;

Input, high-ohmic or 75 ohms.

## Appendix

The input of the measured object is supplied with a modulated voltage

$$u_1 = U\cos\omega t(1+m\cos\Omega t) = U\left[\cos\omega t+\frac{m}{2}\cos(\omega+\Omega)t+\frac{m}{2}\cos(\omega-\Omega)t\right]. \tag{7}$$

If $F(\omega)$ is used for denoting the transmission factor modulus of the studied object, and $\varphi(\omega)$ for the phase shift, then the output voltage of the object under test can be expressed by

$$u_2 = F(\omega)U\left\{\cos[\omega t+\varphi(\omega)]+\frac{mF(\omega+\Omega)}{2F(\omega)}\cos[\omega t+\varphi(\omega+\Omega)]+\frac{mF(\omega-\Omega)}{2F(\omega)}\cos[\omega t+\varphi(\omega-\Omega)]\right\}. \tag{8}$$

STAT

Let us expand $F(\omega \pm \Omega)$ and $\varphi(\omega \pm \Omega)$ into a Taylors series, limiting the first expansion to two and the second - to three terms.

Then,

$$F(\omega \pm \Omega) = F(\omega) \pm \Omega \frac{dF(\omega)}{d\omega} + \dots \qquad (9)$$

$$\varphi(\omega \pm \Omega) = \varphi(\omega) \pm \Omega \frac{d\varphi(\omega)}{d\omega} + \frac{\Omega^2}{2} \frac{d^2\varphi(\omega)}{d\omega^2} + \dots =$$

$$= \varphi(\omega) \pm \Omega\tau + \frac{\Omega^2}{2} \frac{d\tau}{d\omega} + \dots, \qquad (10)$$

where $\tau = \frac{d\,\varphi(\omega)}{d\omega}$ is the group propagation time.

Substituting eqs.(9) and (10) into eq.(8) and making transformations we obtain

$$u_2 = UF(\omega)\left\{\cos\omega(t+\tau)\left[1 + m\cos\Omega(t+\tau)\cos\frac{\Omega^2}{2}\frac{d\tau}{d\omega} + \frac{m\Omega\,db(\omega)}{d\omega}\sin\Omega(t+\tau)\times\right.\right.$$

$$\left.\times\sin\frac{\Omega^2}{2}\frac{d\tau}{d\omega}\right] + \sin\omega(t+\tau)\left[m\cos\Omega(t+\tau)\sin\frac{\Omega^2 d\tau}{2d\omega} - \frac{m\Omega\,db(\omega)}{d\omega}\times\right.$$

$$\left.\left.\times\sin\Omega(t+\tau)\cos\frac{\Omega^2}{2}\frac{d\tau}{d\omega}\right]\right\}. \qquad (11)$$

where $b(\omega) = -\ln F(\omega)$ - is the attenuation of the test object.

The amplitude of the high-frequency voltage A is equal to the square root from the sum of the squares of the factors with orthogonal components i.e.,

$$A = UF(\omega)\left\{1 + \frac{m^2}{2} + \frac{1}{2}\left[\frac{m\Omega\,db(\omega)}{d\omega}\right]^2 + 2m\cos\Omega(t+\tau)\cos\frac{\Omega^2}{2}\frac{d\tau}{d\omega} -\right.$$

$$- \frac{2m\Omega\,db(\omega)}{d\omega}\sin\Omega(t+\tau)\sin\frac{\Omega^2 d\tau}{2d\omega} +$$

$$\left. + \frac{1}{2}m^2\left[1 + \frac{\Omega\,db(\omega)}{d\omega}\right]^2\cos 2\Omega(t+\tau)\right\}^{\frac{1}{2}}. \qquad (12)$$

Expanding eq.(12) into a Fourier series and neglecting the small terms, we find that the first harmonic of the envelope at the output of the object is shifted, relative to the input envelope, through an angle of

$$\psi = \Omega\tau - \mathrm{arctg}\left[\frac{\Omega\,db(\omega)}{d\omega}\,\mathrm{tg}\,\frac{\Omega^2 d\tau}{2d\omega}\right]. \qquad (13)$$

If, according to Nyquist, the group time $\tau^*$ given by the device, is determined

STAT

as

$$\tau^* = \frac{\psi}{\Omega}, \tag{14}$$

then as the error of method $\Delta\tau = \tau^* - \tau$, the following is obtained

$$\Delta\tau = -\frac{1}{\Omega}\,\mathrm{arc\,tg}\left[\frac{\Omega\, db(\omega)}{d\omega}\,\mathrm{tg}\left(\frac{\Omega^2}{2}\frac{d\tau}{d\omega}\right)\right]. \tag{15}$$

Considering that the value contained in the brackets is small compared with unity and assuming $\tan^{-1} Z \approx Z$ we obtain eq.(2).

The authors thank V.P.Savel'yev and A.A.Koloskov for their help in carrying out the experiments.

Article received by the Editors 28 July 1956.

BIBLIOGRAPHY

1. Nyquist,H. and Brand,S. - Measuring of Phase Distortions. BSTJ, Vol.9 (1930), p.522

2. Hunt,L.E. and Albersheim,W.J. - Device for Rapid Measurement of Distortions of the Characteristics of Group Time. PIRE, Vol.4 (1952), pp 454 - 459

3. Alsberg,D.A. - Accurate Measurement of the Vectors of the Total Resistance by the Method of Frequency Modulation. PIRE. (1951), XI, 39, 11, p.1393

4. - Device for Measuring the Distortions of the Phase-Shift Characteristic in Broad-Band Communication Channels. Research Laboratory for Scientific Work on Communication Problems, Acad.Sci. USSR (1952)

5. - Device for Visual Observation and Measurement of Frequency Characteristics. Research Laboratory for Scientific Work on Communication Problems, Acad.Sci. USSR (1954-55)

6. Turbovich,I.T. - Progress in Measuring Frequency Characteristics by the Method of Frequency Modulation. Radiotekhnika, Vol.9, No.4 (1954)

STAT

7. Turbovich, I.T. and Solomonov, V.G. - Progress in Accurate Measurement of Frequency Characteristics of Telephone Channels. Collection of Scientific Papers on Wire Communications. Izd.AN SSSR, No.4 (1955)

# THE PROBLEM OF INTERMEDIATE PROCESSES IN PULSE SCHEMATICS WITH CRYSTAL POINT-CONTACT TRIODES.

by

O.G.Yagodin

The article reviews a method of analysis for intermediate processes with crystal point triodes, based on a substitution of the dynamic properties of a triode by an approximate equivalent circuit and by aligning of the nonlinear triode characteristics. Intermediate processes are studied in a diagram of a single-cycle relaxator and in a trigger device with a triode working without saturation.

Calculation methods for pulse schematics with point-contact triodes have been worked out with sufficient details in application to slow processes. In this case the calculation of the basic parameters for pulse oscillations and operating conditions of the circuit is, in fact, reduced to a determination of the input characteristic of the circuit, for instance, $u_e = f(i_2)$ with $E_k$ = const, $R_b$ = const and $R_k$ = const (Fig.1) and to its analysis. The input characteristic can be obtained from known statistics of characteristics for a triode, either by graphic methods (Bibl.1) or analytically (Bibl.2). In the latter case, the real characteristics of a triode is aligned within the area of cutoff (I) of the active section (II) and of the saturation areas (III). For each of these areas the values of a triode parameter are determined and linear equivalent circuits, usually T-networks, are composed. With the help of such a model of a crystal triode, the characteristics of pulse oscillations can be calculated, under the assumption that jumps in the circuits are momentary (Bibl.3,4), that the influence on such jumps by the parameters of the triode and the circuit have been considered, and that useful operating conditions for the circuit have been determined, etc. However, for an analysis of intermediate pro-





Declassified in Part - Sanitized Copy Approved for Release @ 50-Yr 2013/11/13 : CIA-RDP81-01043R002700130004-0

cesses in the circuit, the dynamic properties of crystal triodes must be known.

It has been experimentally proved that the dynamic properties of point-contact triodes, notwithstanding a sufficiently pronounced field effect and surface phenomena in the area near the limit frequencies or exceeding it, are determined by the diffusional character of the movement of the charge carriers. Thus, in first approximation, both for point-contact and planar triodes the one-dimensional diffusion equation obtained by V.Shokli (Bibl.5) can be applied. However, the solutions of this equation for intermediate operation (Bibl.6, 7,8) cannot be used for practical calculations, in view of their complexity.

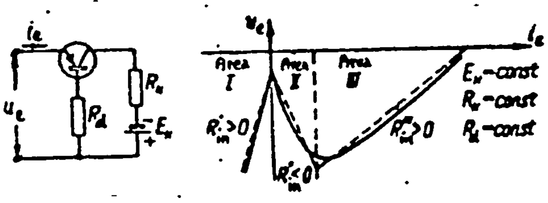

Fig.1

To investigate processes in circuits with planar triodes, the approximate expression for an intermediate characteristic, as offered by E.I.Adirovich and V.G.Kolotilova (Bibl.9), can be used. However, for engineering calculations, with the aim of simplification, it is more practical to represent crystal triodes by equivalent circuits reflecting their dynamic properties and assuring the requested accuracy of calculation. The necessary elements of such circuits are elements taking into consideration a weakening and a phase shift of high-frequency signal components and reflecting a delay in the reaction of the system to the input disturbance, caused by the tail portion of the diffusion. In point-contact triodes practically no diffusion delay appeared, so that the equivalent circuit becomes much simpler for these triodes.

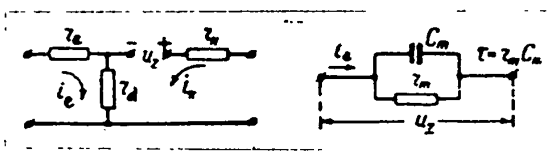

Fig.2

It is known that, in a broad frequency band (up to critical frequencies) a point-contact triode can be represented by a low-signal equivalent circuit (Fig.2) for which

$$U_z(p) = \frac{r_m I_e(p) + \tau U_{z_0}}{1 + p\tau}, \qquad (1)$$

or by a circuit as per Fig.3 in which, for dynamic operating conditions, the current in an oscillator $i_g$ and in the circuit of the emitter $i_e$ are connected by the relation

$$I_g(p) = \frac{I_e(p)}{1+p\tau}, \tag{2}$$

$$\tau = \frac{1}{2\pi f_0}, \tag{3}$$

where $f_0$ is the limit frequency of the triode, at which the current amplification factor drops to 0.7 of its value at low frequencies.

For large signals it is necessary to take into consideration the nonlinear character of a triode. If the triode does not reach the saturation point, its properties can be duplicated by an equivalent circuit as shown in Fig.4. Within the limits of the active area, the time constant of the equivalent current generator, in the schematics in Fig.3 and 4, is equal to

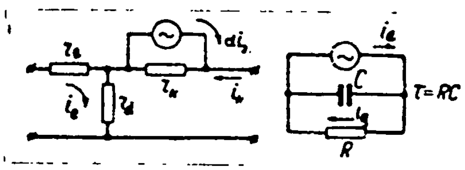


Fig.3

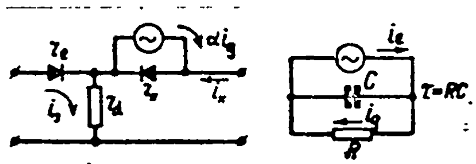


Fig.4

$$\tau = RC. \tag{4}$$

Under the operating conditions of a saturated triode, i.e., under a changed status of an equivalent diode in a collector circuit, which corresponds to the condition

$$\alpha i_g > -i_k, \tag{5}$$

the phenomenon of accumulation of nonbasic carriers occurs; in first approximation, this can be taken into consideration by introducing a new discrete value for the time constant of the current generator

$$\tau_s > \tau. \tag{6}$$

In this case, the use of point-contact triodes may become limited. The latter condition, in particular, limits the maximum speed of count in discriminator circuits.

The existence of approximate linear equivalent circuits of crystal point-contact triodes permits a calculation of both rapid and slow processes in the circuits with the help of a device based on the classical theory of circuits.

Thus, the approximate solution of the problem of intermediate processes in a nonlinear system is reduced to consecutive linear solutions obtained for a series of areas and to their subsequent reconciliation at the boundaries of these areas.

As concrete examples, let us consider intermediate processes in the circuit of a single-cycle relaxator and in a trigger device with a point-contact triode, working without saturation.

In the general case, the circuit of a single-cycle relaxator, started by a positive pulse, sent to the circuit of the emitter, can be designed as per Fig.5*.

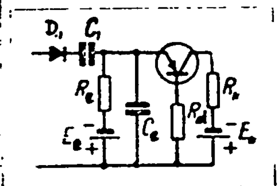

Fig.5

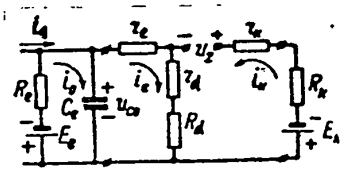

Fig.6

Let us consider intermediate processes in this circuit under the assumption that triggering is accomplished by the action of a current gap, received from an oscillator with an infinite internal resistance; the transition of the circuit from the state of stable equilibrium to an active state occurs instantly; the load resistance in the collector circuit $R_k$ is not great. Under these assumptions, the movement of the systems in the active area can be represented by the equivalent circuit shown in Fig.6.

The initial condition for this movement can be written as

$$\boxed{i_e(0) \approx 0.} \tag{7}$$

With an input disturbance of

$$\left.\begin{aligned} i_g(t) &= 0 \text{ for } t<0 \\ i_g(t) &= I_e \text{ for } t>0 \end{aligned}\right\} \tag{8}$$

* The simplest schematic of a trigger device is reduced to the same configuration, when taking into consideration the influence of input stray capacitance.

we have

$$i_0(t) = \frac{N}{K}\left[\frac{S}{M} + \frac{\alpha^2 + Q\alpha + S}{\alpha(\alpha-\beta)} e^{\alpha t} + \frac{\beta^2 + Q\beta + S}{\beta(\beta-\alpha)} e^{\beta t}\right], \tag{9a}$$

$$i_e(t) = \frac{U}{K}\left[\frac{W}{M} + \frac{\alpha^2 + V\alpha + W}{\alpha(\alpha-\beta)} e^{\alpha t} + \frac{\beta^2 + V\beta + W}{\beta(\beta-\alpha)} e^{\beta t}\right], \tag{9b}$$

$$i_\kappa(t) = -\frac{X}{K}\left[\frac{Z}{M} + \frac{\alpha^2 + Y\alpha + Z}{\alpha(\alpha-\beta)} e^{\alpha t} + \frac{\beta^2 + Y\beta + Z}{\beta(\beta-\alpha)} e^{\beta t}\right], \tag{9c}$$

where

$$\left.\begin{aligned}
&\alpha = -\frac{1}{2}\left(L - \sqrt{L^2 - 4M}\right); \quad \beta = -\frac{1}{2}\left(L + \sqrt{L^2 - 4M}\right)\\
&K = \tau T_e (T_{11} R_\Sigma - T_{12} R_{12})\\
&L = \frac{R_\Sigma(\tau T_e + \tau T_{11} + T_e T_{11}) - T_{12}(\tau R_{12} + T_e R_{21})}{K}\\
&M = \frac{R_\Sigma(T_e + T_{11}) - T_{12} R_{21}}{K}; \quad N = \tau F (T_{11} R_\Sigma - T_{12} R_{12})\\
&Q = \frac{\tau R_\Sigma F + T_{11} R_\Sigma F + \tau T_{12} E - T_{12} R_{21} F + \tau R_\Sigma D}{N}\\
&S = \frac{R_\Sigma F + T_{12} E_\kappa + R_\Sigma D}{N}\\
&U = \tau T_e (R_\Sigma D + T_{12} E)\\
&V = \frac{\tau R_\Sigma D + T_e R_\Sigma D + \tau T_{12} E + T_e T_{12} E_\kappa + \tau R_\Sigma F}{U}\\
&W = \frac{R_\Sigma F + T_{12} E_\kappa + R_\Sigma D}{U}; \quad X = \tau T_e (T_{11} E + R_{12} D)\\
&Y = \frac{\tau T_e E + \tau T_{11} E + \tau R_{12} D + \tau_e R_{12} F + T_e R_{21} D + T_e T_{11} E_\kappa}{X}\\
&Z = \frac{T_e E_\kappa + T_{11} E_\kappa + R_{21} D + R_{21} F}{X}; \quad R_\Sigma = R_{22} + R_\kappa\\
&T_e = R_e C_e; \quad T_{11} = R_{11} C_e; \quad T_{12} = R_{12} C_e\\
&D = C_e U_{c_0}; \quad E = E_\kappa + U_{g_0}; \quad F = I_e T_e - C_e(E_e + U_{c_0})\\
&U_{g_0} = -E_\kappa - (U_{c_0} - i_{e_0} R_{11}) \frac{R_{22} + R_\kappa}{R_{12}} - i_{e_0} R_{12}; \quad R_{ij} = r_{ij} + R_d
\end{aligned}\right\} \tag{10}$$

($r_{ij}$ is the small signal parameter of a triode in the active area).

Superimposing on eq.(9) the initial eq.(7) we will obtain equations, describing movement of the system in the active area, i.e.,

$$0 < i_e < I_{es}, \tag{11}$$

STAT

Where $I_{e_s}$ is the value of emitter current at the instant $t_s$, when saturation of the triode is achieved, i.e., when eq.(5) is satisfied. The method for determining $I_{e_s}$ and the time $t_s$ has been described before (Bibl.10).

The movements of the system in the saturation area are reviewed analogously, for when

$$I_{e_s} < i_e < I_{e_{max}}, \qquad (12)$$

for which case, the initial conditions are as follows:

$$\left.\begin{aligned} i_e(t-t_s)\big|_{t=t_s} &= I_{e_s} \\ U_e(t-t_s)\big|_{t=t_s} &= R_{11}I_{e_s} + R_{12}I_{K_s} \end{aligned}\right\}, \qquad (13)$$

The value $I_{e_{max}}$ in a circuit of a single-cycle relaxator can be determined with sufficient accuracy from a study of the input characteristic.

Having equations for the system displacement in the active area and in the saturation area and knowing the limits of the current changes of the emitter from eqs.(11) and (12), one can calculate the duration of the leading edge of the pulse emitted by the system. The duration of the pulse proper is determined according to known formulas (Bibl.3,4).

Notwithstanding the fact that in a single-cycle relaxator the process of reverse tilting happens without outside influence, the speed of this process depends on $\tau_2$, on account of the effect of accumulating holes. The accumulation of holes limits the minimum duration of the pulse, obtainable from a single-cycle relaxator.

Simultaneous use in the pulse circuits of crystal diodes and triodes improves - sometimes very substantially - the operating quality of the circuit. For instance, with the help of a diode, the limit frequency of repeated pulses in a single-cycle relaxator can be increased.

The use of a crystal diode in conjunction with a source of constant Q shift of the load element in the emitting circuit yields a broken characteristic of the load, which gives the possibility, at our choice, to secure the points of intersection of

STAT

the load with the input characteristics. In particular, all three points of intersection may be outside the saturation zone (Fig.7). It is evident that, if in this case the stability of two equilibrium states can be assured, then such a circuit can be used as a trigger device with a diminished time count since the operation of the triode itself in this circuit is characterized by the absence of saturation.

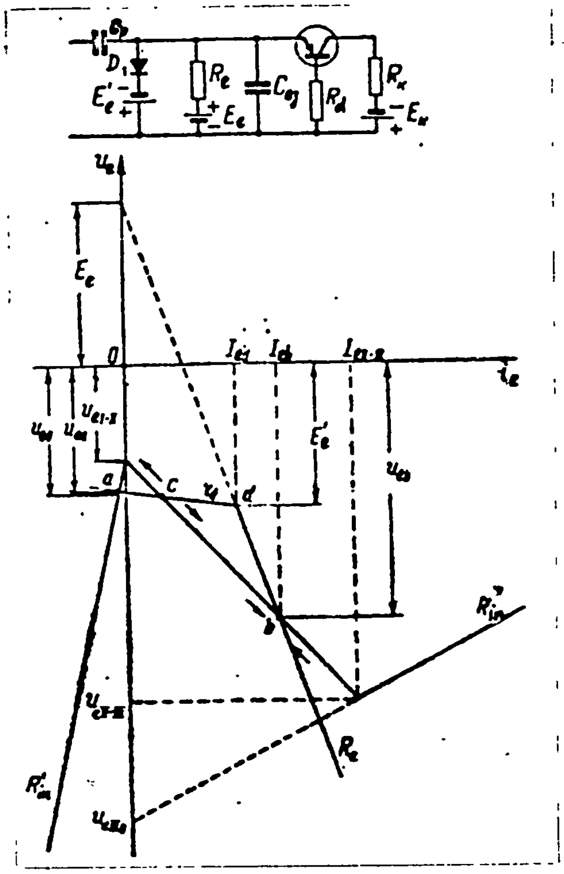

Fig.7

As shown by the author (Bibl.11), if the collector-to-ground capacitance is neglected, which is permissible for a great number of schematics with point-contact triodes, the conditions for a stable equilibrium in the descending branch of the input characteristic, in the general case, have the form

$$C_{e_1} < \frac{\tau}{R_N R_e}(R_e + r_1), \qquad (14a)$$

$$R_e > R_N, \qquad (14b)$$

where $R_N$ is the steepness of the descending branch in the aligned input characteristic, equal to

$$\left.\begin{aligned} R_N &= \frac{R_{12}R_{21}}{R_{22}+R_k} - R_{11} \\ r_1 &= R_{11} - \frac{R_{12}^2}{R_{22}+R_k} \end{aligned}\right\}. \qquad (15)$$

From here it is immediately apparent that, if the condition (14a) is satisfied, the point b will correspond to a state of stable equilibrium in the system, while

STAT

the point c will represent the unstable one.

The trigger device shown in Fig.7 (Bibl.12) – after taking the influence of the emitter-ground capacitance $C_{e_z}$ into account – represents a system with two degrees of freedom, analogous to the reviewed schematic of a single-cycle relaxator. The basic difference between these schematics, when reviewing the intermediate processes, is this: for the schematic as per Fig.7 the equations deducted for the active zone remain valid during the entire process. However, the inclusion into the circuit of the emitting diode $D_1$ and the source of the shift $E_e'$, causes the parameters entering into these equations to have two series of discrete values corresponding to the value of the emitter current. If $I_{e_{com}}$ denotes the value of the emitter current which produces a commutation of the load resistance in the emitter circuit, this resistance can be expressed by

$$R_н \approx r_d \text{ for } 0 < i_e < I_{e_{com}}, \tag{16}$$

$$R_н \approx R_e \text{ for } i_e > I_{e_{com}} \tag{17}$$

assuming that

$$r_d \ll R_e \ll r_{d\,rev}, \tag{18}$$

where $r_d$ and $r_{d_{rev}}$ are, respectively, the resistances of diode $D_1$ in the forward and reverse directions.

It is obvious that, within the limits of the active area at $i_e = I_{e_{com}}$, the boundary conditions must be satisfied. In conformity with eqs.(16) and (17) let us agree to call "first subarea" of the active area that part of the latter within which the current of the emitter changes within the limits $0 \le i_e \le I_{e_{com}}$, while the other part of the active area, determined by the condition $I_{e_{com}} \le i_e \le I_{es}$, – will be called: "second subarea".

Let us review the process of direct reversal in the circuit (transition from state a to state b) under the influence of a current gap. Suppose that the circuit with a terminal input capacitance $C_{e_s}$ is under the influence of a current gap (8) size $I_z$ is sufficient to bring the system out of the state a.

The first commutation of parameters in the circuit takes place at the transition from the cutoff area into the active area, i.e., when the equivalent diode: emitter-base (Fig.4) opens, which happens when $i_e = 0$. The instants of subsequent parameter commutations are determined from the condition $i_d = 0$, where $i_d$ is the current flowing through the diode $D_1$ (Fig.7). Considering, as before, that under the influence of the gap, the transition of the circuit into the active area happens instantly and that eq.(18) is satisfied, we find for the first subarea an equivalent circuit as shown in Fig.8. The initial condition for moving the system is eq.(7). For the schematic in Fig.8, which is analogous to the one shown in Fig.6, a solution of general aspect has been obtained in eq.(9). In the present specific case, the current $i_o$ corresponds to the current $i_d$

$$\left.\begin{aligned} T_e &= C_{e_3} r_d \\ F &= T_e I_3 - C_{e_3}\left(E'_e + u_{e_3}\right) \\ u_{z_0} &= -E_k - \left(u_{r_0} - R_{11} i_{e_0}\right)\frac{R_{22}+R_k}{R_{12}} - R_{12} i_{e_0} \end{aligned}\right\} \qquad (19)$$

while the balance of the symbols corresponds to eq.(10).

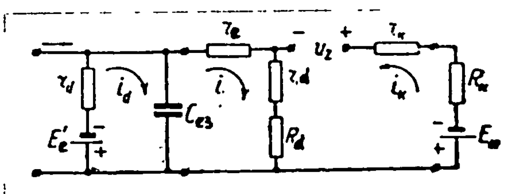

Fig.8

After substituting eq.(7) in eqs.(10) and (19), and further in eq.(9), we obtain the final expressions for the currents $i_d$, $i_e$, and $i_k$ taking into account the initial conditions in the circuit.

A solution of the equation (9a) of the type

$$\lambda + \mu e^{\alpha t} - \nu e^{\beta t} = 0$$

permits determining the instant $t_{com}$ at which a new commutation of parameters takes place, and also permits determining, from eq.(9a), the value $I_{e\ com}$.

The equivalent circuit for the second subarea [satisfying eq.(18)] corresponds to the time interval $t_{com} \le t \le t_{stab}$ where $t_{stab}$ is the time during which the transition of the circuit into a new state of equilibrium, as shown in Fig.9, takes place. The application limits of this equivalent circuit can be determined in the following manner:

$$I_{e\,com} \leqslant i_e \leqslant I_{e_b} + I_z, \tag{20}$$

where $I_{e_b}$ is the value of the emitter current, corresponding to the point b on the input static characteristic. It is obvious that, for operation of the crystal triode without saturation, the following condition must be satisfied:

$$I_{eb} + I_z < I_{e_s}. \tag{21}$$

The initial conditions in the second subarea can be written as

$$\left.\begin{array}{l} i_e(t_{com}) = I_{e\,com} \\ u_c(t_{com}) = U_{e\,com} \end{array}\right\}. \tag{22}$$

The voltage at the capacitance $C_{ez}$, at the instant of commutation, reads as follows

$$u_c(t_{com}) = U_{e\,com} = R_{11} I_{e\,com} + R_{12} I_{\kappa\,com} = -E'_e, \tag{23}$$

while the voltage of the equivalent emitter is

$$u_z(t_{com}) = -E_\kappa + (E'_e + R_{11} I_{e\,com}) \frac{R_{22} + R_\kappa}{R_{12}} - R_{12} I_{e\,com} \tag{24}$$

The solution of a system of equations describing the schematic of the Fig.9 results in

$$i_R(t - t_{com}) = \frac{N'}{K'} \left[ \frac{S'}{M'} + \frac{\alpha'^2 + Q'\alpha' + S'}{\alpha'(\alpha' - \beta')} e^{\alpha'(t - t_{com})} - \frac{\beta'^2 + Q'\beta' + S'}{\beta'(\alpha' - \beta')} e^{\beta'(t - t_{com})} \right], \tag{25a}$$

$$i_e(t - t_{com}) = \frac{U'}{K'} \left[ \frac{W'}{M'} + \frac{\alpha'^2 + V'\alpha' + W'}{\alpha'(\alpha' - \beta')} e^{\alpha'(t - t_{com})} - \frac{\beta'^2 + V'\beta' + W'}{\beta'(\alpha' + \beta')} e^{\beta'(t - t_{com})} \right], \tag{25b}$$

STAT

$$i_\kappa(t - t_{com}) = -\frac{X'}{K'}\left[\frac{Z'}{M'} + \frac{\alpha'^2 + Y'\alpha' + Z'}{\alpha'(\alpha' - \beta')} e^{\alpha'(t - t_{com})} - \frac{\beta'^2 + Y'\beta' + Z'}{\beta'(\alpha' - \beta')} e^{\beta'(t - t_{com})}\right]. \qquad (25c)$$

In eqs.(25), the values of the factors differ from those obtained before, for the first subarea. This depends both on the changed value of the load in the emitter circuit, and on the change of the initial movement conditions during the second commutation of the parameters in the system. These factors can be determined in the following way:

$$\left.\begin{aligned}
&D' = -C_{e_2}E'; \quad E' = E_\kappa + U_{z\,com}; \quad F' = C_{e_2}(E_e + E_e') \\
&T_e' = C_{e_2}R_e; \quad T_{11}' = T_{11} = C_{e_2}R_{11}; \quad T_{12}' = T_{12} = C_{e_2}R_{12}. \\
&\alpha' = -\frac{1}{2}\left(L' - \sqrt{L'^2 + 4M'}\right); \quad \beta' = -\frac{1}{2}\left(L' + \sqrt{L'^2 - 4M'}\right) \\
&K' = \tau T_e'(T_{11}R_\Sigma - T_{12}R_{12}); \\
&L' = \frac{R_\Sigma(\tau T_e' + \tau T_{11} + T_e'T_{11}) - T_{12}(\tau R_{12} + T_e'R_{21})}{K'} \\
&M' = \frac{R_\Sigma(T_e' + T_{11}) - T_{12}R_{21}}{K'}; \quad N' = \tau F'(T_{11}R_\Sigma - T_{12}R_{12}) \\
&Q = \frac{R_\Sigma(\tau F' + T_{11}F' + \tau D') + T_{12}(\tau E' - R_{21}F')}{N'} \\
&S' = \frac{R_\Sigma(D' + F') + T_{12}E_\kappa}{N'} \\
&U' = \tau T_e'(R_\Sigma D' + T_{12}E') \\
&V = \frac{R_\Sigma(\tau D' + T_e'D' + \tau F') + T_{12}(\tau E' + T_e'E_\kappa)}{U'} \\
&W' = \frac{R_\Sigma(D' + F') + T_{12}E_\kappa}{U'}; \quad X' = \tau T_e'(T_{11}E' + R_{12}D') \\
&Y' = \frac{\tau E'(T_e' + T_{11}) + \tau R_{12}(D' + F') + T_e'(R_{21}D' + T_{11}E_\kappa)}{X'} \\
&Z' = \frac{E_\kappa(T_e' + T_{11}) + R_{21}(D' + F')}{X'}
\end{aligned}\right\} \qquad (26)$$

The transit time of the system in the second subarea is determined from eq.(25b), if it is assumed that

$$i_e(t_{stab} - t_{com}) = I_{eb} + I_s. \qquad (27)$$

STAT

It is obvious that eq.(27) is true only when the trigger device trips under the influence of a current gap or of a current pulse whose duration $T_z$ is greater than the action time of the circuit $t_{stab}$ while the duration of the leading edge is considerably less than $t_{stab}$ and eq.(21) is satisfied.

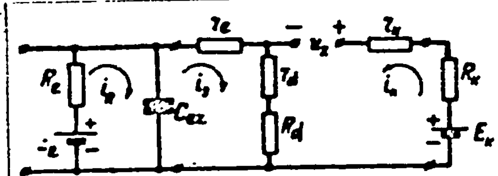

Fig.9

The complete action time of the trigger circuit is determined as the sum of time intervals required for carrying out the transition of the system over both subareas.

A review of the process of reverse tipping in the trigger device under the influence of a negative current gap will be made under the assumption that, at the instant of an input disturbance, all intermediate processes in the circuit have been completed and the system is in a state, corresponding to the point b at the input static characteristic. Such an assumption is true when the negative drop is applied to the circuit at the instant $t_1$, while $t_1 \gg T_z > t_{stab}$, where $T_z$ is the duration of the starting pulse, causing a straight tipping of the system, while $t_{stab}$ is the total time of action of the system during straight tipping.

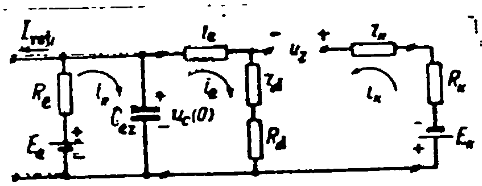

Fig.10

The equivalent circuit for the second subarea will have the same aspect as the circuit in Fig.9, with the only difference that its input is connected to a negative current drop (Fig.10).

The initial condition is determined by the initial state of stable equilibrium

$$i_e(0) = I_{eq}. \tag{28}$$

The limit condition for the second subarea is the commutation condition

$$u_{c\,com} = -E_e'. \tag{29}$$

Let us remark that, to achieve a reverse tipping, the value of the drop $I_{z1}$ must be sufficient to cause opening of the diode $D_1$ in the emitter circuit, in view of the fact that, without complying with this condition, the circuit cannot be brought out of its state of equilibrium.

Having determined the value of the emitter current in the commutation moment $I_{e_{com1}}$, we find the initial conditions of the system movement within the first subarea

$$\left.\begin{aligned} i_e(t_{com1}) &= I_{e\,com1} \\ u_c(t_{com1}) &= -E'_e \end{aligned}\right\}. \qquad (30)$$

For the first subarea at reverse tipping, we obtain the equivalent circuit shown in Fig.11, which is valid when

$$0 \leqslant i_e \leqslant I_{e\,com1}, \; i_d > 0. \qquad (31)$$

The transit time through the second subarea at reverse tipping can be found on the basis of the known boundary equation

$$i_e(t_{stab1} - t_{com1}) = 0. \qquad (32)$$

For the case of excitation of the trigger device shown in Fig.7 by the current drop the above expressions for currents in circuits, permit determining the reaction of the system to the input disturbance which, in principle, has any complex form.

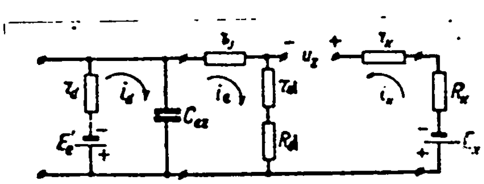

Fig.11

However, the presence of a very complex dependence of the factors on the parameters of the circuit and on the initial conditions, leads to cumbersome results.

A considerable simplification of the process analysis for a schematic, yielding understandable conclusions, is achieved for such parameters of the triode and of the trigger circuit, at which the influence of the capacitance $S_{e_z}$ in the emitter circuit can be neglected. Obviously, this can be done only when one of the roots of the characteristic equations for a system with two degrees of freedom is considerably smaller than the other (in the general case, taking into consideration the output resistance in the generator of starting pulses).

STAT

It is easy to show (Bibl.11) that the influence of the capacitance $S_{e_z}$ does not have to be taken into consideration if the following condition is satisfied:

$$C_{e_z}R_N \ll \tau. \tag{33}$$

In actual cases, due to the high action speed of trigger circuits with point-contact triodes, it frequently happens that the rate of build-up of the starting signal is equivalent to or even less than the tripping speed. Therefore, it is interesting to review the influence of the final speed of build-up of the starting signal on the intermediate processes in the trigger circuit.

Assume that starting of the circuit is done by a rather large separating capacitance from the emitter by a linearly varying voltage whose internal resistance is equal to $r_g$ and that the influence of the capacitances emitter-ground and collector-ground can be neglected.

Considering that, in the active area, $r_d \ll R_N$ and that $r_b \ll R_b$, the first sub-area can be represented by the equivalent circuit of Fig.12*.

Let us assume that the starting voltage changes according to the law

$$u_g(t) = at. \tag{34}$$

If the rate of change of the starting voltage is small as compared to the speed of action in the trigger device, then it is assumed that the starting voltage remains within the circuit during the entire tipping process.

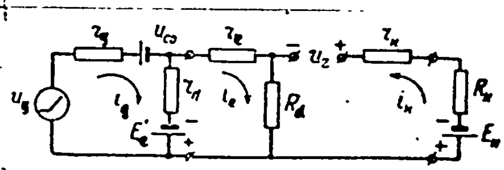

Fig.12

For the circuit in Fig.12, the initial and boundary conditions for a forward tipping are known

$$i_e(0) \approx 0, \tag{35}$$

$$u_e(t_{com}) = -E_e. \tag{36}$$

*Movement of the system in the current cutoff area is not considered here.

STAT

Solving a system of equations for this circuit and taking into consideration that usually $r_d \ll R_N$ and $r_d \ll r_1$ we will obtain, after superimposition of eq.(35):

$$
\left.
\begin{aligned}
i_g(t) &= \frac{1}{r_g + r_d}\Big\{E'_e - U_{c0} - \frac{r_d}{R_N}\Big(E_k\frac{R_{12}}{R_\Sigma} - U_{c0}\Big) + at + \\
&\quad + \Big[\frac{r_d^2}{r_1(r_g - r_d)}(U_{c0} - E'_e) + \frac{r_d}{R_N}\Big(E_k\frac{R_{12}}{R_\Sigma} - U_{c0}\Big)\Big]\,e^{\frac{R_N}{r_1}\frac{t}{\tau}}\Big\} \\
i_e(t) &= \frac{1}{R_N(r_g + r_d)}\Big\{-\Big[\Big(E_k\frac{R_{12}}{R_\Sigma} - E'_e\Big)(r_g + r_d) + \\
&\quad + (E'_e - U_{c0})\,r_d + \Big(1 + \frac{r_1}{R_N}\Big)a\tau r_d\Big] - a r_d t + \\
&\quad + \Big[\Big(E_k\frac{R_{12}}{R_\Sigma} - E'_e\Big)(r_g + r_d) + (E'_e - U_{c0})\,r_d + \\
&\quad + \Big(1 + \frac{r_1}{R_N}\Big)a\tau r_d\Big]\,e^{\frac{R_N}{r_1}\frac{t}{\tau}}\Big\} \\
i_k(t) &= \frac{1}{R_N R_\Sigma (r_g + r_d)}\Big\{r_g(E_k R_{11} - E'_e R_{21}) + \\
&\quad + r_d(E_k R_{11} - U_{c0}R_{21}) + a\tau r_d\frac{R_{11}}{R_N}(R_{21} - R_{12}) + a r_d R_{21} t - \\
&\quad - \Big[\frac{R_N R_\Sigma}{R_{12}}(E'_e r_g + U_{c0} r_d) + r_g(E_k R_{11} - E'_e R_{21}) + \\
&\quad + r_d(E_k R_{11} - U_{c0}R_{21}) + a\tau r_d\frac{R_{11}}{R_N}(R_{21} - R_{12})\Big]\,e^{\frac{R_N}{r_1}\frac{t}{\tau}}\Big\}
\end{aligned}
\right\} \qquad (37)
$$

The instant of time, corresponding to the commutation of the parameters in the schematic, is determined by the solution of eq.(36).

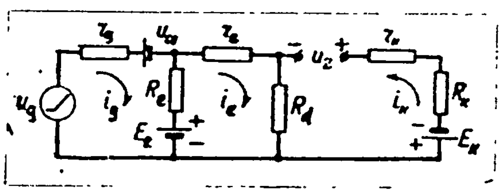

Fig.13

For the second subarea, complying with the condition $R_e \ll r_{d\,rev}$ the equivalent circuit takes the aspect shown in Fig.13. The initial conditions for movement in this subarea are:

$$
\left.
\begin{aligned}
i_e(t_{com}) &= I_{e\,com} \\
u_g(t_{com}) &= a t_{com}
\end{aligned}
\right\}. \qquad (38)
$$

In the case when $r_g \ll R_e$ – which might happen frequently – and after superimposing the initial eqs.(38) on the solution of the equation system, we have:

$$\left.\begin{aligned}
i_g(t-t_{com}) &= -\frac{1}{R_N}\left[a\tau\left(1+\frac{r_1}{R_N}\right)-\left(1-\frac{R_N}{R_e}\right)(E_e+E_e')+\right.\\
&\quad\left.+\frac{R_{12}}{R_\Sigma}E_\kappa+E_e\right]-\frac{a}{R_N}\left(1-\frac{R_N}{R_e}\right)(t-t_{com})+\\
&\quad+\left\{I_{e\,com}-\frac{E_e+E_e'}{R_e}+\frac{1}{R_N}\left[a\tau\left(1+\frac{r_1}{R_N}\right)-\right.\right.\\
&\quad\left.\left.-\left(1-\frac{R_N}{R_e}\right)(E_e+E_e')+\frac{R_{12}}{R_\Sigma}E_\kappa+E_e\right]\right\}e^{\frac{R_N}{r_1}\frac{t-t_{com}}{\tau}}\\
i_e(t-t_{com}) &= \frac{1}{R_N}\left\{-\left[\frac{R_{12}}{R_\Sigma}E_\kappa-E_e'+a\tau\left(1+\frac{r_1}{R_N}\right)\right]-\right.\\
&\quad-a(t-t_{com})+\left[I_{e\,com}R_N+\frac{R_{12}}{R_\Sigma}E_\kappa-E_e'+\right.\\
&\quad\left.\left.+a\tau\left(1+\frac{r_1}{R_N}\right)\right]e^{\frac{R_N}{r_1}\frac{t-t_{com}}{\tau}}\right\}\\
i_\kappa(t-t_{com}) &= -\frac{1}{R_NR_\Sigma}\left\{R_{11}E_\kappa-R_{21}E_e'+a\tau\left(R_{12}+\right.\right.\\
&\quad\left.+R_{21}\frac{r_1}{R_N}\right)+aR_{21}(t_1-t_{com})+\left[I_{e\,com}R_{11}\frac{R_NR_\Sigma}{R_{12}}+\left(\frac{R_vR_\Sigma}{R_{12}}+\right.\right.\\
&\quad\left.\left.\left.+R_{21}\right)E_e'-R_{11}E_\kappa-a\tau\left(R_{12}+R_{21}\frac{r_1}{R_N}\right)\right]e^{\frac{R_v}{r_1}\frac{t-t_{com}}{\tau}}\right\}
\end{aligned}\right\} \qquad (39)$$

The boundary condition for the second subarea

$$\boxed{i_e(t_{stab}-t_{com})=I_{e_b}} \qquad (40)$$

in connection with eq.(36) gives a possibility of determining the total time of tipping the schema $t_{stab}$ when started by a linearly increasing voltage.

It is not difficult to demonstrate by a direct calculation that the period of action of the trigger device with a triode working without saturation, with a forward tipping is basically determined by the time required for transition into the first subarea, i.e., by the time required for changing the status of the diode in the emitter circuit.

In considering the process of reverse tipping the transit time of the system

STAT

in the area of cutoff can be neglected. Then, let us assume that, at the moment of the starting action by the voltage at the separating capacitance, a voltage $U_{C1}$ has been established, under the initial condition of

$$i_{e1}(0) = I_{eb} \tag{41}$$

and

$$u_{q1} = -a_1 t, \tag{42}$$

For the second subarea, we will obtain

$$\left.\begin{aligned} i_{e1}(t) &= \frac{1}{R_N}\left\{-\left[\frac{R_{12}}{R_\Sigma}E_\kappa + U_{eb} - a_1\tau\left(1+\frac{r_1}{R_N}\right)\right] + a_1 t + \right.\\ &\left. + \left[R_N I_{eb} + \frac{R_{12}}{R_\Sigma}E_\kappa + U_{eb} - a_1\tau\left(1+\frac{r_1}{R_N}\right)\right] e^{\frac{R_N}{r_1}\frac{t}{\tau}}\right\} \\ i_{\kappa 1}(t) &= -\frac{1}{R_N R_\Sigma}\left\{R_{11}E_\kappa + R_{21}U_{eb} - a_1\tau\left(R_{12} + \frac{r_1}{R_N}R_{21}\right) - \right.\\ &- a_1 R_{21} t + \left[\frac{R_N R_\Sigma}{R_{12}}(R_{11}I_{eb} - U_{eb}) - R_{11}E_\kappa - R_{21}U_{eb} + \right.\\ &\left.\left. + a_1\tau\left(R_{12} + \frac{r_1}{R_N}R_{21}\right)\right] e^{\frac{R_N}{r_1}\frac{t}{\tau}}\right\} \end{aligned}\right\} \tag{43}$$

where $U_{eb}$ is the voltage at the emitter, corresponding to equilibrium at the point b.

Having determined the commutation moment of the parameters $t_{com_1}$ from the equation

$$u_e(t_{com_1}) = R_{11} i_{e1}(t_{com_1}) + R_{12} i_{\kappa 1}(t_{com_1}) = -E_e', \tag{44}$$

we will find the initial conditions for the first subarea:

$$\left.\begin{aligned} i_{e1}(t_{com_1}) &= I_{e\,com_1} \\ u_{q1}(t_{com_1}) &= -a_1 t_{com_1} \end{aligned}\right\}. \tag{45}$$

Then the solution for the first subarea can be presented in the form of

$$i_{q1}(t - t_{com_1}) = -\frac{1}{r_q + r_d}\left\{\frac{r_d}{R_N}\left(E_\kappa \frac{R_{12}}{R_\Sigma} - E_e\right) + \right. \tag{46}$$

$$+ a_1 (t - t_{com_1}) - \Big[ r_d I_{e\,com_1} +$$

$$+ \frac{r_d}{R_N}\Big(E_\kappa \frac{R_{12}}{R_\Sigma} - E'_e\Big)\Big] e^{\frac{R_N}{r_1}\frac{t - t_{com_1}}{\tau}} \Big\}$$

$$i_{e1}(t - t_{com_1}) = \frac{1}{R_N (r_q + r_d)} \Big\{ - \Big[ \Big( E_\kappa \frac{R_{12}}{R_\Sigma} - E'_e \Big)(r_q + r_d) -$$

$$- a_1 \tau r_d \Big(1 + \frac{r_1}{R_N}\Big)\Big] + a_1 r_d (t - t_{com_1}) + \Big[ R_N (r_q + r_d) I_{e\,com_1} +$$

$$+ \Big(E_\kappa \frac{R_{12}}{R_\Sigma} - E'_e\Big)(r_q + r_d) - a_1 \tau r_d \Big(1 + \frac{r_1}{R_N}\Big)\Big] e^{\frac{R_N}{r_1}\frac{t - t_{com_1}}{\tau}} \Big\} \qquad (46)$$

$$i_{\kappa_1}(t - t_{com_1}) = \frac{1}{R_N R_\Sigma (r_q + r_d)} \Big\{ (E_\kappa R_{11} - E'_e R_{21})(r_q + r_d) -$$

$$- a_1 \tau r_d \frac{R_{11}}{R_N}(R_{21} - R_{12}) - a_1 r_d R_{21} (t - t_{com_1}) -$$

$$- \Big[ \frac{R_N R_\Sigma R_{11}}{R_{12}} (r_s + r_d) I_{e\,com_1} + \frac{R_N R_\Sigma}{R_{12}} (r_q + r_d) E'_e + (E_\kappa R_{11} -$$

$$- E'_e R_{21})(r_q + r_d) - a_1 \tau r_d \frac{R_{11}}{R_N}(R_{21} - R_{12}) \Big] e^{\frac{R_N}{r_1}\frac{t - t_{com_1}}{\tau}} \Big\}$$

The action time of the trigger device in reverse tipping $t_{stab_1}$ is determined from eq.(44) and from the condition

$$i_{e1}(t_{stab_1} - t_{com_1}) = 0. \qquad (47)$$

As indicated in eqs.(37), (39), (43), and (46), the rate of the process - both forward and reverse tipping in the discussed trigger circuit is determined by a factor of the exponential term, which is the same for all cases and is equal to

$$\frac{R_N}{r_1}\frac{t}{\tau} \approx \Bigg( \frac{\alpha}{1 + \frac{R_\kappa}{r_\kappa}} - 1 \Bigg) \frac{t}{\tau}. \qquad (48)$$

As it appears from eq.(48), the action time of the trigger device, other conditions being equal, will be as much shorter as the current amplification factor of the triode $\alpha$ and the resistance $r_k$ of the potential barrier of the collector become greater or as the critical frequency of the triode $f_o$ becomes higher and the load resistance in the collector circuit $R_k$ becomes smaller.

Thus, from the point of view of reducing the duration of intermediate processes in pulse circuits, it is preferable to use crystal triodes with a high resistance $r_k$, having at the same time a high $\alpha$ and a high critical frequency $f_o$. Usually, when having point-contact triodes with high values of $\alpha$ and $f_o$, the circuit in Fig.7 must be inspected whether the condition a stable equilibrium in the active area has been satisfied.

Article received by the Editors 6 February 1956.

BIBLIOGRAPHY

1. Hunter,L.P. and Fleisher,H. - PIRE Vol.40, No.11 (1952)
2. Anderson,A.E. - PIRE Vol.40, No.11 (1952)
3. Lo,A.W. - PIRE Vol.40, No.11 (1952)
4. McDuffie,G.E. - PIRE Vol.40, No.11 (1952)
5. Shokli,V. - Theory of Electronic Transistors. Part 12, IL (1953)
6. Shea,R.F. - Principles of Transistor Circuits. Ch.17, New York (1953)
7. Schaffner,J.S. and Suran,J.J. - Journ. Appl. Physics. Vol.24, No.11 (1953)
8. Adirovich,E.I. and Kolotilova,V.G. - Zhurn. Elek. Tekh. Fiz. Vol.29, No.6 (12) (1955)
9. Adirovich,E.I. and Kolotilova,V.G. - Dokl. AN, Vol.105, No.4 (1955)
10. Yagodin,O.G. - Trudy VKIAS imeni S.M.Budenni, No.51 (1956)
11. Yagodin,O.G. - Thesis, VKIAS (1955)
12. Baker,R.H., Lebow,I.L. and McMahon,R.E. - PIRE Vol.42, No.7 (1954)

STAT

# FREQUENCY FEEDBACK IN RECEIVERS OF SIGNALS WITH FREQUENCY MODULATION

by

D.Ya. Kantor

The necessity to maintain a limiter in a FM receiver with frequency feedback is discussed. A transmission band is determined for an IF amplifier in such a receiver, this band being essential for stability and for nonlinear distortions. The concept of optimum depth of frequency feedback is introduced.

1. A principal schematic for a FM receiver with frequency feedback (FF) is shown in Fig.1. The voltage from a frequency detector (4) is sent through a correcting circuit (6) and a frequency modulator (7) to the heterodyne (8), creating frequency modulation of the latter.

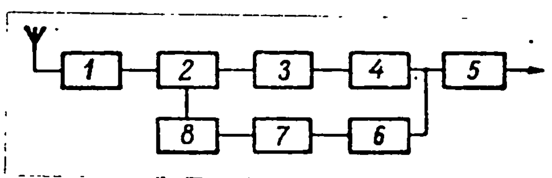


Fig.1

Here (1) denotes an HF amplifier, (2) a frequency converter, (3) an IF amplifier, (5) a LF amplifier. In case of negative feedback, the frequency modulation of the local heterodyne coincides with the phase of the frequency modulation of the received signal. Thus, the IF signal has a diminished frequency deviation.

The voltage at the output of the frequency detector is determined by the expression

$$\dot{E}_2 = \frac{\dot{\kappa}}{1+\dot{\beta}\dot{\kappa}}(\Delta\dot{\omega}), \qquad (1)$$

where $\dot{k} = \dot{E}_c\dot{D}$,

$\dot{E}_c$ is the voltage amplitude of the signal at the converter output,

$\dot{D}$ is the steepness of the frequency detector characteristic taken at the converter input at unit signal voltage;

$\dot{\beta}$ is a constant of frequency modulation of the heterodyne, taking the transmission factor of the correcting circuit into consideration.

2. Equation (1) indicates that the frequency feedback reduces the influence of amplitude modulation on the output voltage. For instance, if $E_c \dot{D}\beta \gg 1$, then $E_2 = \frac{(\Delta\omega)}{\beta}$, which means that it does not depend on the voltage amplitude at the receiver input.

Introduction of frequency feedback leads also to a voltage drop of the frequency-modulated signal at the output. This drop can be compensated by a corresponding increase of the frequency deviation in the receiver or by increasing the steepness of the frequency characteristic of the detector. In the first case, the advantages presented by FM are increased. Only the second case is of practical importance, when the frequency deviation of the received signal remains constant. Under this condition, a system with deep frequency feedback for damping of noises is practically equivalent to a system with a limiter (Bibl.1).

However, eq.(1) shows that the depth of feedback is proportional to the amplitude of the input signal. If a certain signal voltage is sufficient to obtain the required depth of feedback, then the amplitude reserve for stability will be exceeded at a higher signal and self-excitation will occur. Therefore, a limiter must be used in a receiver with frequency feedback. A fractional detector cannot replace a limiter, since it does not eliminate the dependence of the output voltage on the average level of the input signal.

A limiter is also required in view of the fact that a shortening of the linear section of the detector, which is necessary to damp the amplitude modulation, leads to a lowered selectivity in the adjacent channel (Bibl.2).

In the presence of a limiter, we have

$$\dot{\kappa} = \dot{D},$$

where D is the steepness of the frequency characteristic of the detector, taken at the converter input, when the signal exceeds the threshold of the limit.

3. Frequency feedback greatly diminishes nonlinear distortions in the IF ampli-

STAT

fier and in the frequency detector. Besides the usual decrease by $(1 + \beta k)$ times, for systems with feedback, it must be taken into consideration that the signal at the output of the converter has a lowered frequency deviation. Using the results obtained by I.S.Gonorovskiy (Bibl.3), it can be shown that the factor of nonlinear distortions in the third harmonic in the IF amplifier, for the same single circuits, proportionally decreases $(1 + \beta k)^3$ times. This expression does not take into account phase shifts in the loop; it is assumed that a quasi-stationary solution is permissible.

4. The introduction of frequency feedback, in itself, does not change the signal-to-noise ratio, since the frequency modulation, carrying both the useful communication and the interference, decreases in the same proportion. However, in view of the statements in Section 3, the band of the frequency amplifier can be narrowed and the selectivity in the adjacent channel can be raised. On the basis of the condition that the factor of nonlinear distortions of the third harmonic, after introduction of frequency feedback, remains the same as without it, the band can be narrowed by $(1 + \beta k)$ times. This corresponds to curve 1 in Fig.2 and to the equation

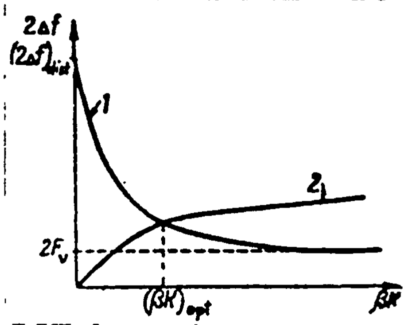


Fig.2

$$(2\Delta f) = \frac{(2\Delta f)_{dist}}{1+\beta k}, \qquad (2)$$

where $(2\Delta f)_{dist}$ is the transmission band of the IF amplifier without frequency feedback, a band which is necessary for the prescribed nonlinear distortions.

The narrowing of the transmission band of the IF amplifier is limited to a value of $2F_v$, where $F_v$ is the highest modulation frequency (Bibl.4).

5. It is known that on introduction of feedback, into a system with minimum phase shift, it is necessary (to avoid self-excitation) that the steepness of the descending branch of the amplitude-frequency characteristic of the open loop should

STAT

not exceed a certain value (12 decibels per octave) until the transmission factor modulus in the loop does not reach unity. The necessary slope of the frequency characteristic is ensured by the correcting circuit in the feedback channel, but the transmission band of the IF amplifier should not be below a certain value $(2\Delta f)_{min}$.

Let us represent the frequency characteristic of the IF amplifier as a broken line OAB (Fig.3), where the straight line AB represents the asymptote of the real characteristic OCB*. The steepness of the straight line AB is 6n decibels/octave, where n is the number of circuits in the IF amplifier (the frequency is plotted on a logarithmic scale). The general characteristic of the loop (without the correcting circuit) represents the total of the frequency characteristics of the IF amplifier and of the section between the frequency detector and the heterodyne frequency modulator. Let us assume that the transmission band of this section is much broader than the band of the IF amplifier, so that the general frequency characteristic repeats the characteristic of the frequency amplifier. This simplification is not only practical, but also basically permissible. A broadening of the transmission band from the detector to the FM heterodyne, in principle, presents no difficulties, since the IF amplifier must ensure selectivity in the adjacent channel.

The transmission factor modulus in the open feedback loop in the transmission band of the IF amplifier can be determined as the ratio of the voltage $E_\Omega$ (at the output of the frequency detector) to the voltage $E_M$ (at the input of the frequency modulator).

In the presence of a limiter, this factor is equal to

$$|K_1| = S_{FMH}|D|, \qquad (3)$$

where $S_{FMH}$ is the steepness of the modulation characteristic $[\Delta f = \psi(E_M)]$ of the

---

* The stability of the system is studied at small frequency deviations. In this case, half of the symmetric characteristic of the HF amplifier corresponds exactly to the characteristic of the LF amplifier.

FM heterodyne.

The maximum possible depth of feedback for optimum correction is determined according to the formula (Bibl.5)

$$(\beta\kappa)_{mdb} = 40\lg\frac{4f_a}{nF_v}, \qquad (4)$$

where $f_a$ is the frequency at which the transmission factor for the loop becomes unity.

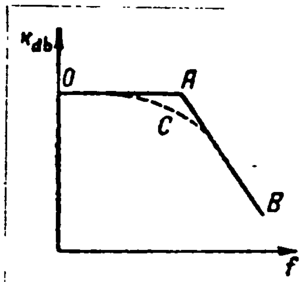

Fig.3

After simple transformations, we obtain

$$(\beta\kappa)_{mdb} = 40\lg\frac{4\Delta f'}{nF_v} + 2\frac{\kappa_{1db}}{n}, \qquad (5)$$

where $\Delta f'$ is half of the transmission band of an idealized characteristic of the IF amplifier (segment OA, Fig.3).

Solving eq.(5) for $\Delta f'$, we have

$$(2\Delta f)_{min} = \frac{nF_v}{2}\,\frac{\sqrt[n]{(\beta\kappa)_m}}{\sqrt[n]{\kappa_1}}. \qquad (6)$$

To change to the transmission band of the real characteristic of the IF amplifier at the level of 0.7, it is sufficient to multiply the result obtained by a certain factor b, depending on the circuit of the interstage connection and the number of stages

$$(2\Delta f)_{min} = \frac{bnF_v}{2}\cdot\frac{\sqrt[n]{(\beta\kappa)_m}}{\sqrt[n]{\kappa_1}}. \qquad (7)$$

It can be demonstrated that, for an amplifier with identical single circuits, the value of b is determined according to the formula

$$b = \sqrt{2^{\frac{1}{n}} - 1}. \qquad (8)$$

Equation (7) is illustrated by curve 2 in Fig.2.

6. From Fig.2 it is evident that, at optimum depth of feedback $(\beta k)_{opt}$ the narrowest transmission band for the IF amplifier is obtained. At lesser depth of

STAT

frequency feedback, the band must be broader to ensure sufficiently small nonlinear distortions, whereas at greater depth, considerations of stability are involved.

Optimum depth of feedback can be determined by solving eqs.(2) and (7) jointly. The resulting formula will have the aspect

$$(\beta\kappa)_{opt} = \left[\sqrt[3]{\frac{C}{2}+\sqrt{\frac{C^2}{4}+\frac{1}{27}}} - \frac{1}{3\sqrt[3]{\frac{C}{2}+\sqrt{\frac{C^2}{4}+\frac{1}{27}}}}\right]^2, \qquad (9)$$

where

$$C = \frac{4\Delta f_{dist}\cdot\sqrt[n]{\kappa_1}}{bnF_v}.$$

The corresponding band of the IF amplifier can be determined according to eq.(2).

For instance, for a radio transmitter with a three-stage IF amplifier on single circuits ($n = 3$) in the presence of nonlinear 0.5% distortions, the IF amplifier requires a band of $(2\Delta f)_{dist} = 220$ kc; $b = 0.51$; $F_v = 15$ kc.

Calculations and practical experience have shown that, without special difficulties, a value of $k_1 = 100$ can be obtained (the nonlinear distortions in the discriminator being 0.5%). Then $C = 90$.

With such a high value for C, eq.(9) can be simplified, to read

$$(\beta\kappa)_{opt} = C^{\frac{2}{3}} = \left(\frac{4\Delta f_{dist}\sqrt[n]{\kappa_1}}{bF_v n}\right)^{\frac{2}{3}}. \qquad (10)$$

For our particular data, we have $(\beta k)_{opt} = 20$.

Equations (9) and (10) must be considered as only theoretical limits. Actually, one has to use considerably less deep feedback because of additional phase shifts in the frequency detector and the heterodyne frequency modulator. An especially important point is the fact that it is difficult to produce and maintain in operation an ideal frequency characteristic of the loop, which needs a stability reserve. The

STAT

magnitude of the stability reserve is determined in the design stage, according to the schematic and the design of the receiver, the Q-factor of the limiter, and the operating conditions.

If it is assumed, for instance, that the stability reserve of the phase is 30° and of the amplitude 6 decibels*, then eq.(7) takes the form

$$2\Delta f_{min} = 0{,}9 n F_v b \frac{(\beta \kappa)_m^{0,6}}{\sqrt{2\kappa_1}}. \qquad (7')$$

Having simultaneously solved eqs.(7') and (2), a curve of the type shown in Fig.4 can be plotted. From this diagram, the optimum feedback for the discussed example can be found, being approximately 12.

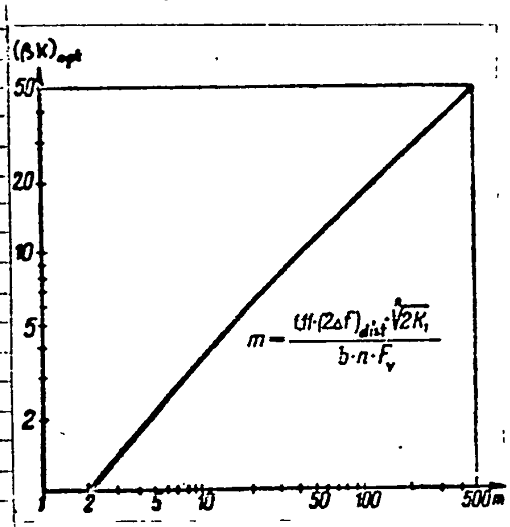


Fig.4

7. By introducing frequency feedback, the transconductance of the discriminator and, consequently, the factor $k_1$, can be increased proportionally. In this case, a considerable narrowing of the amplifier band is possible. However, it has been mentioned before that a decrease of the linear segment in the discriminator band is undesirable.

Article received by the Editors 5 November 1955 and, after revision, 29 August 1956.

BIBLIOGRAPHY

1. Chaffee - The Application of Negative Feedback to FM Receivers. PIRE May 1939
2. Plusg - Investigation of FM Signal Interference. PIRE November 1947

* These are minimum figures; actually one frequently needs a greater reserve, especially for the phase.

3. Gonorovskiy, I.S. - Radio Signals and Intermediate Effects in Radio Circuits. Svyaz'izdat (1955)

4. Bell - Reduction of Bandwidth in FM Receivers. The Wireless Eng. November (1942)

5. Bode, G. - Circuit Theory and Designing of Amplifiers with Feedback. Publ. House of Foreign Literature (1948)

STAT

# SELF-OSCILLATOR WITH EXTENSIVE CIRCUIT DAMPING

by

A.Z.Khaikov

The question is reviewed of the dependence of the form of self-oscillation and energy ratios in a self-oscillator on attenuation in its circuit: The optimum operating conditions are investigated from the viewpoint of power transmitted to load and of efficiency.

## 1. Introduction

With the help of a quasi-linear theory one can calculate a self-oscillator, provided the Q-factor of the circuit is sufficiently high. Then the voltage in the circuit is basically created by the first harmonic of the plate current, for which the circuit is equivalent to an active resistance. In this case, the operating conditions for the oscillator under which maximum oscillating power $P_\sim$ is emitted by the circuit, are determined.

The power $P_{\sim n}$ emitted in the load depends on the efficiency of the circuit

$$\eta_k = \frac{P_{\sim n}}{P_\sim} = 1 - \frac{\delta}{\delta'},$$

where $\delta$ is the natural damping of the circuit, $\delta'$ the total damping (reduced) of the circuit, the load being taken into consideration. To maintain the efficiency of the circuit near unity, the total attenuation must exceed the natural attenuation by many times, the natural damping being normally in the range of a few thousandth or hundredth. However, the operation of a self-oscillator cannot be described by the quasi-linear theory if this theory is applied to high values of circuit attenuation. Operation at high attenuation leads to a change in the voltage shape in the circuit and to a change in the self-oscillation frequency. This does not in principle meet with objections for an oscillator made for industrial purposes. However, an increase in $\delta'$, besides leading to an increase in circuit efficiency, may result in a change in oscillating power and efficiency of the self-oscillator.

The purpose of this article is an investigation of the effect of total attenuation of the circuit on the frequency and the shape of self-oscillations and on the energy ratios of the self-oscillator.

## 2. Equation of Self-Oscillations

Let us limit the scope to a review of a single-circuit self-oscillator with inductive backfeed. The equivalent circuit for such a high-frequency self-oscillator is shown in Fig.1, representing the load by a resistance $R_e$. The resistance connected in parallel with the circuit corresponds to the case of an oscillator for dielectric heating. In investigating only the boundary operating condition, we assume that the current in the circuit of the first grid is equal to zero. Taking into account the plate reactance, we can construct a system of differential equations:

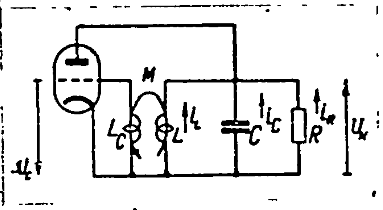


Fig.1

$$i_a = i_L + i_C + i_R, \tag{1}$$

$$i_a = f(u_y), \tag{2}$$

where the control voltage is $u_y = u_c - Du_k$, with D being the grid through of the tube

$$u_k = L\frac{di_L}{dt}, \tag{3}$$

$$i_C = C\frac{du_k}{dt}, \tag{4}$$

$$i_R = \frac{u_k}{R_e}, \tag{5}$$

$$u_c = M\frac{di_L}{dt}. \tag{6}$$

In the resultant system of equations appear only alternating voltages at the grid and at plate of the tube; the influence of direct voltages at the plate and grid and thus of the cutoff angle of the plate current is fully taken into account by the assignment of the function $i_a = f(u_y)$.

For analytical calculations, let us substitute the real characteristic of the plate current by a broken line. Then the function $f(u_y)$ will be represented by three segments: In the first segment whose right-hand boundary is determined by the angle of cutoff of the plate current $\frac{\partial f}{\partial u_y} = 0$; in the second segment $\frac{\partial f}{\partial u_y} = S$; in the third segment whose left-hand boundary is determined by the appearance of grid current, $\frac{\partial f}{\partial u_y} < 0$; while S is the static transconductance. Since the alternating voltage on the grid is proportional to the direct voltage, let us introduce a new function $f_1(u_c) = \frac{\partial f(u_y)}{\partial u_c}$. It is evident that

$$f_1(u_c) = 0 \quad \text{for} \quad u_c < U_{c0},$$

$$f_1(u_c) = S\left(1 - \frac{D}{n}\right) \quad \text{for} \quad U_{c0} < u_c < U_{c\,lim},$$

$$f_1(u_c) < 0 \quad \text{for} \quad u_c > U_{c\,lim}.$$

Here $U_{c}o$ and $U_{c\ lim}$ are constant values depending upon the grid voltage at the tube anode, determining the moments when plate and grid currents appear; $n = \frac{u_c}{u_k} = \frac{M}{L}$ is the feedback coefficient.

The system of differential equations (1)-(6) is reduced to one equation

$$LC\frac{d^2u_c}{dt^2} + \left[\frac{L}{R_s} - Lnf_1(u_c)\right]\frac{du_c}{dt} + u_c = 0. \tag{7}$$

To generalize the conclusions, it is advantageous to operate with relative and dimensionless quantities. For this purpose, let us introduce the following denotations:

$\omega_o = \frac{1}{\sqrt{LC}}$ is the angular frequency of the circuit;

$\rho = \omega_o L$ is the characteristic resistance of the circuit;

$\delta' = \frac{\rho}{R_e}$ is the total attenuation of the circuit;

$\tau = \omega_o t$ is the natural time of the system;

$x = \frac{u_c}{}$ is the wanted time function;

$\alpha = \frac{U_{co}}{U_{cgp}}$ is the parameter determining the angle of the plate-current cutoff.

Then, in its final form the equation for the described oscillator will take the following form:

$$\frac{d^2y}{d\tau^2} + [\delta' - \delta' R_e S(n-D)\psi(y)]\frac{dy}{d\tau} + y = 0, \qquad (8)$$

where

$$\psi(y) = 0 \quad \text{for} \quad y < \alpha,$$
$$\psi(y) = 1 \quad \text{for} \quad \alpha < y < 1,$$
$$\psi(y) < 0 \quad \text{for} \quad y > 1.$$

Since the coefficient before the first derivative in the equation is a function of y, while the value of total attenuation of the circuit $\delta'$ in the case of high circuit efficiency is in the range of unity or more, eq.(8) has an essentially nonlinear character.

In studying the energy dependence in a self-oscillator, an idea as to the form of self-oscillations is required. Methods which only permit determination of the amplitude of the first harmonic of stablized self-oscillations, cannot be used. Nearest to the solution of eq.(8) is the method of small parameters, by Poincaré, modified by A.A.Andronov, and the method of graphic plotting of curves on a phase plane by Lenard. However, in the case of strongly nonlinear equations, the method of Poincaré can only give a qualitatively correct solution. The Lenard method can be used for investigating the shape of self-oscillations for any value of $\delta'$. With the help of a graphic plotting, an accurate phase portrait on a plane $(y, y')$ can be obtained. The phase portrait, with help of graphic plotting is followed by a preliminary determination of the function. For example, by plate characteristic by a broken line and studying the lower segment of the characteristic, G.S.Ramm in his article "Application Limits for Quasi-linear Methods" (Radiotekhnika Vol.9, No.1, 1954) obtained the proportion of self-oscillations. However, the Lenard method is unsuitable for energy calculations, since they are inaccurate and complex.

When representing the plate-current by a broken line, the nonlinear term of eq.(8) remains constant when the function varies within the limits of a given area, but changes in a jump when crossing from one area to another. Thus in each of the regions, the equation has the form of a linear differential equation whose solution is extremely simple. Difficulties arise when combining solutions corresponding to different regions. By superimposing conditions for the transit from one area to another, a complicated system of transcendental equations is obtained. However, by investigating the operations of a self-oscillator under boundary conditions with an angle of plate-current cutoff of $0 = 90^{\circ}$ (which is of practical interest), the solution is obtained in a simple analytical form. Then all power calculations can be made with the above assumptions, with the desired degree of accuracy.

3. Form of Self-Oscillations

Let us prove that the grid voltage and its first derivative in time and, consequently, y and $\frac{dy}{d\tau}$ during a transit from one area into the other change continuously with time. Let us base the calculation on the fact that, for the schematic in Fig.1, the inductive current $i_L$ and the voltage at the capacitor $u_k$, cannot contain any jumps. Then, on the basis of eqs.(1)-(5) $i_R = \frac{u_k}{R_e}$, $i_a = f[(1 - \frac{D}{n}) u_c]$, $i_C = i_a - i_L - i_R$, $\frac{du_k}{dt} = \frac{1}{C} i_C$, $u_c = nu_k$, $\frac{du_c}{dt} = n \frac{du_k}{dt}$ are continuous functions of time. Therefore, $y = \frac{u_c}{U_{co}}$ and $\frac{dy}{d\tau} = \frac{1}{\omega_o U_{c_{lim}}} \cdot \frac{d_{uc}}{dt}$ cannot change in jumps.

If we limit ourselves to a review of the boundary conditions at $0 = 90^{\circ}$, we obtain $\alpha = 0$, since in this case $U_{co} = 0$. Equation (8) can be represented by two equations corresponding to the first and second areas:

$$\boxed{\frac{d^2y_1}{d\tau^2} + \delta' \frac{dy_1}{d\tau} + y_1 = 0, \quad y = y_1 \quad \text{at} \quad y_1 < 0.} \qquad (9)$$

$$\boxed{\frac{d^2y_2}{d\tau^2} + [\delta' - \delta' R_e S(n - D)] \frac{dy_2}{d\tau} + y_2 = 0, \; y = y_2 \quad \text{at} \quad y_2 > 0.} \qquad (10)$$

The beginning of the $\tau$ count can be selected arbitrarily. To simplify the corresponding equations it is advantageous to count $\tau$ from the instant of transition by $y$ from the first area into the second and, in addition, to introduce an independent variable $\tau_1 = -\tau$ with the beginning of the count coinciding with the beginning of the count for $\tau$; then $\frac{dy}{d\tau_1} = -\frac{dy}{d\tau}$ and $\frac{d^2y}{d\tau_1^2} = \frac{d^2y}{d\tau^2}$. Equations (9) and (10) will then take the following form:

$$\frac{d^2y_1}{d\tau_1^2} - 2h_1\frac{dy_1}{d\tau_1} + y_1 = 0, \tag{11}$$

$$\frac{d^2y_2}{d\tau^2} - 2h_2\frac{dy_2}{d\tau} + y_2 = 0, \tag{12}$$

where

$$2h_1 = \delta', \tag{13}$$

$$2h_2 = \delta' K_e S(n - D) - \delta'. \tag{14}$$

The solutions of eqs.(11) and (12) will be

$$y_1 = C_1 e^{h_1\tau_1} \sin(\omega_1\tau_1 + \varphi_1)$$

and

$$y_2 = C_2 e^{h_2\tau} \sin(\omega_2\tau + \varphi_2),$$

so that

$$\omega_1 = \sqrt{1 - h_1^2}, \quad \omega_2 = \sqrt{1 - h_2^2}.$$

At $\tau = \tau_1 = 0$, the condition of continuous function and its derivative must be satisfied:

$$y_1(0) = y_2(0) = 0,$$

$$\left.\frac{dy_1}{d\tau_1}\right|_{\tau_1=0} = -\left.\frac{dy_2}{d\tau}\right|_{\tau=0}.$$

This corresponds to the equalities

$$C_1 \sin\varphi_1 = 0,$$

$$C_2 \sin\varphi_2 = 0,$$

$$C_1h_1 \sin\varphi_1 + C_1\omega_1 \cos\varphi_1 = -C_2h_2 \sin\varphi_2 - C_2\omega_2 \cos\varphi_2.$$

From the latter equalities it follows that $\varphi_1 = \varphi_2 = 0$ since we are seeking a solution at $C_1 \neq 0$ and $C_2 \neq 0$, and that $C_1\omega_1 = -C_2\omega_2$.

At certain $\tau_1 = \tau'_1$ and $\tau = \tau'$, the functions $y_1$ and $y_2$ will again pass through zero. Therefore, the following conditions must be satisfied:

$$y_1(\tau'_1) = y_2(\tau') = 0$$

and

$$\left.\frac{dy_1}{d\tau_1}\right|_{\tau_1=\tau'_1} = -\left.\frac{dy_2}{d\tau}\right|_{\tau=\tau'}.$$

Therefore,

$$C_1 e^{h_1\tau'_1}\sin\omega_1\tau'_1 = 0, \quad \text{where} \quad \tau'_1 = \frac{\pi}{\omega_1},$$

$$C_2 e^{h_2\tau'}\sin\omega_2\tau' = 0, \quad \text{where} \quad \tau' = \frac{\pi}{\omega_2},$$

$$C_1\omega_1 e^{h_1\tau'_1} = -C_2\omega_2 e^{h_2\tau'}.$$

Taking into account that $C_1\omega_1 = -C_2\omega_2$, we obtain

$$e^{h_1\frac{\pi}{\omega_1}} = e^{h_2\frac{\pi}{\omega_2}},$$

from which it follows that

$$h_1 = h_2. \tag{15}$$

Equation (15) is a condition for self-excitation of the self-oscillator. Taking into consideration eqs.(13) and (14), we transform the latter equation

$$R_e S(n - D) = 2.$$

This condition fully coincides with the condition of self-excitation according to the quasi-linear theory for $\theta = 90^\circ$.

From eq.(15) it also follows that $\omega_1 = \omega_2$ and $C_1 = -C_2$.

From the conditions of transit of the function from one area to another we have determined the amplitude of the self-oscillations $C_2$, since for all $y \leq 1 (u_c \leq U_{c_{lim}})$ and for $h_1 = h_2$, the self-oscillations are stable. However, actually eq.(15) cannot be exactly satisfied. At $h_2 < h_1$, the oscillations will decay and, at $h_2$ somewhat greater than $h_1$, the amplitude will be limited by the build-up of grid currents.

STAT

With sufficient accuracy, it can be assumed that

$$y_{max} = 1, \tag{16}$$

which corresponds to boundary conditions. Let us introduce the denotations: $h = h_1 = h_2$ and $\omega = \omega_1 = \omega_2$ and let us designate the maximum function $e^{h\tau}\sin\omega\tau$ by $\varphi(h)$. At a certain $\tau = \tau_m < \frac{\pi}{\omega}$

$$\frac{d}{d\tau}\left(e^{h\tau}\sin\omega\tau\right)_{\tau=\tau_m} = 0.$$

Hence $\tau_m = \frac{\arcsin\omega}{\omega}$, and $\omega\tau_m > \frac{\pi}{2}$, since $\tan\alpha\tau_m = -\frac{\omega}{h} < 0$. This gives a possibility to calculate $\varphi(h) = e^{h\tau_m}\sin\omega\tau_m$ for different h.

Taking eq.(16) into consideration, we will obtain for y, in final form,

$$\left.\begin{aligned} y_1 &= \frac{1}{\varphi(h)}e^{-h\tau}\sin\omega\tau, \quad y = y_1 \qquad \text{at} \quad -\frac{\pi}{\omega} < \tau \leqslant 0 \\ y_2 &= \frac{1}{\varphi(h)}e^{h\tau}\sin\omega\tau, \quad y = y_2 \qquad \text{at} \quad 0 \leqslant \tau < \frac{\pi}{\omega} \end{aligned}\right\}. \tag{17}$$

Let us find the value of harmonics for different $\delta'$. For this, we expand the function y into a Fourier series. Since the function is odd, it will contain only sinusoidal harmonics; their coefficients are found according to the formula

$$a_k = \frac{2\omega}{\pi\varphi(h)}\int_0^{\frac{\pi}{\omega}} e^{h\tau}\sin\omega\tau\cdot\sin k\omega\tau\, d\tau,$$

where k is the number of the harmonic. According to the last formula we obtain:

$$a_1 = \frac{4\omega^3\left(e^{\frac{h\pi}{\omega}} - 1\right)}{\pi\varphi(h)\,h\,(4 - 3h^2)},$$

$$a_2 = \frac{-8\omega^3 h\left(e^{\frac{h\pi}{\omega}} + 1\right)}{\pi\varphi(h)(9 - 8h^2)},$$

$$a_3 = \frac{12\omega^3 h\left(e^{\frac{h\pi}{\omega}} - 1\right)}{\pi\varphi(h)(4 - 3h^2)(16 - 15h^2)}\ldots$$

STAT

At maximum attenuation $\delta' = 2$,

$$\lim_{h\to 1}\frac{a_2}{a_1} = -2, \quad \lim_{h\to 1}\frac{a_3}{a_1} = 3.$$

The Table gives values for $\varphi$ (h) depending on $\delta'$.

Table

| $\delta'$ | $h$ | $\varphi(h)$ |
|---|---|---|
| 0,02 | 0,01 | 1,016 |
| 0,04 | 0,02 | 1,032 |
| 0,1 | 0,05 | 1,084 |
| 0,2 | 0,1 | 1,18 |
| 0,4 | 0,2 | 1,41 |
| 0,6 | 0,3 | 1,72 |
| 0,8 | 0,4 | 2,17 |
| 1,0 | 0,5 | 2,90 |
| 1,2 | 0,6 | 4,21 |
| 1,4 | 0,7 | 7,20 |
| 1,6 | 0,8 | 16,95 |
| 1,8 | 0,9 | 112,7 |
| 1,9 | 0,95 | 1695 |
| 2,0 | 1,0 | $\infty$ |

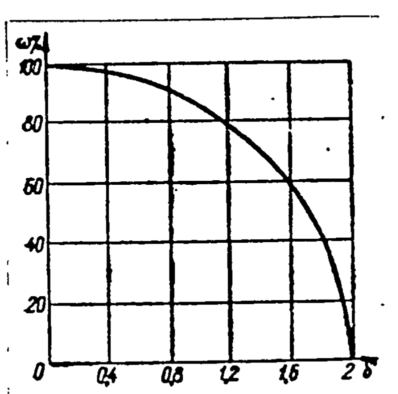


Fig.2

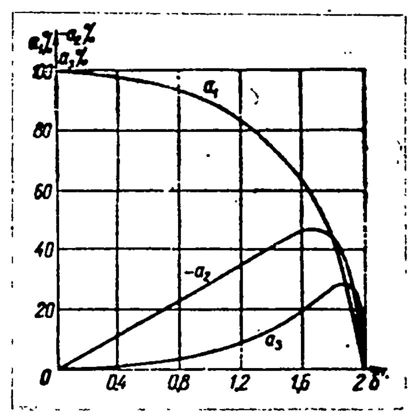


Fig.3

Figure 2 represents a diagram $\omega = \omega(\delta')$ which shows the decrease in the fre-

STAT

quency of self-oscillations at an increase in the total attenuation of the circuit. At $\delta' \geq 2$, the oscillations decay. A diagram for $a_1$, $a_2$, and $a_3$ as a function of the value $\delta$ is shown in Fig.3.

From eq.(17) the form of the grid voltage for different values of $\delta'$ can be directly determined. It is sufficient to make the calculation for y when $0 \leq \tau \leq \frac{\pi}{\omega}$, since y is an odd function.

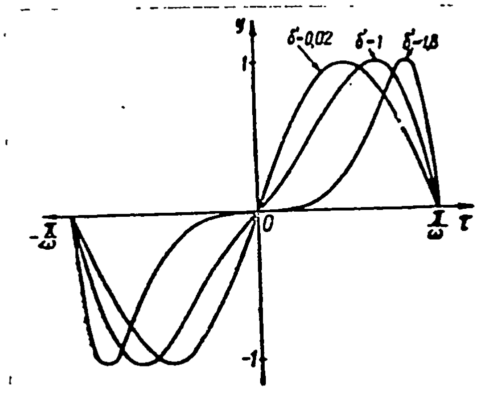


Fig.4

Figure 4 gives the aspect of the function y for different $\delta'$. The function y is nothing but grid voltage in relative units. The voltage of of the circuit, the control voltage, and the current flowing through the load are correlated to the grid voltage by proportional factors and therefore have the same aspect as y. The plate current is equal to zero at $y = 0$ and is proportional to y at $y > 0$.

## 4. Power Ratios

According to definition, the oscillatory power of a vacuum-tube generator is

$$P_\sim = \frac{1}{T}\int_0^T \frac{u_r^2}{R_e}\,dt.$$

The voltage of the circuit, as a value proportional to the grid voltage, is an odd function. Therefore,

$$P_\sim = \frac{\omega}{\pi}\int_0^{\frac{\pi}{\omega}} \frac{u_r^2}{n^2 R_e}\,d\tau = \frac{\omega U_{c\,1im}^2}{\pi n^2 R_e}\int_0^{\frac{\pi}{\omega}} y^2\,d\tau$$

where $\delta' \to 0$, $y \to \sin\tau$ and $P_\sim \to P_{\sim 0} = \frac{U_{c\,1im}^2}{2n^2 R_e}$

The value $\frac{P_\sim}{P_{\sim 0}}$ characterizes a change in the oscillating power at a change in $\delta'$

$$\frac{P_\sim}{P_{\sim 0}} = \frac{2\omega}{\pi}\int_0^{\frac{\pi}{\omega}} y^2\,d\tau = \frac{2\omega}{\pi\gamma^2(h)}\int_0^{\frac{\pi}{\omega}} (e^{h\tau}\sin\omega\tau)^2\,d\tau.$$

STAT

After integration, we obtain

$$\frac{P_\sim}{P_{\sim 0}} = \frac{\omega^2}{2\pi\varphi^2(h)\,h}\left(e^{\frac{2h\pi}{\omega}} - 1\right), \qquad (18)$$

$$\lim_{h\to 1}\frac{P_\sim}{P_{\sim 0}} = 0.$$

The power input is

$$P_- = \frac{1}{T}\int_0^T E_a i_a\,dt = \frac{\omega}{2\pi}\int_0^{\frac{\pi}{\omega}} E_a S\left(1 - \frac{D}{n}\right)U_{c_{lim}}\,y\,d\tau.$$

At $\delta' \to 0$,

$$P_{-0} = \frac{E_a S\left(1 - \frac{D}{n}\right)}{\pi}U_{c_{lim}}.$$

Then,

$$\frac{P_-}{P_{-0}} = \frac{\omega}{2\varphi(h)}\int_0^{\frac{\pi}{\omega}} e^{h\tau}\sin\omega\tau\,d\tau,$$

$$\frac{P_-}{P_{-0}} = \frac{\omega^2}{2\varphi(h)}\left(e^{\frac{h\pi}{\omega}} + 1\right), \qquad (19)$$

$$\lim_{h\to 1}\frac{P_-}{P_{-0}} = 0.$$

A change in the efficiency of the self-oscillator will be characterized by the value

$$\frac{\eta}{\eta_0} = \frac{P_\sim}{P_-} : \frac{P_{\sim 0}}{P_{-0}} = \frac{P_\sim}{P_{\sim 0}} : \frac{P_-}{P_{-0}}.$$

According to eqs.(18) and (19)

$$\frac{\eta}{\eta_0} = \frac{\omega}{\pi h\varphi(h)}\left(e^{\frac{h\pi}{\omega}} - 1\right). \qquad (20)$$

The graphs for the values $\frac{P_\sim}{P_{\sim 0}}$, $\frac{P_=}{P_{=0}}$ and $\frac{\eta}{\eta_0}$ are shown in Fig.5.

From this, it is possible to find the dependence of the power $P_{\sim n}$ transmitted to the load and of the oscillator efficiency $\eta_\Sigma$ on the magnitude of total attenuation of the circuit. Let us characterize these dependences as

$$\frac{P_{\sim n}}{P_{\sim 0}} = \frac{P_{\sim}}{P_{\sim 0}} \eta_k$$

and

$$\frac{\eta_{\Sigma}}{\eta_0} = \frac{\eta}{\eta_0} \eta_k .$$

The results of calculations, for a characteristic Q-factor of the circuit of $Q = \frac{1}{\delta} = 100$, are shown in Fig.6.

## 5. Conclusions

An exact solution for the equation of the self-oscillator according to areas, shows that the frequency and shape of the self-oscillations depend on the total attenuation of the circuit. The frequency decreases with increasing $\delta'$. When the damping values approach 2, the oscillations are distinctly different from sinusoidal.

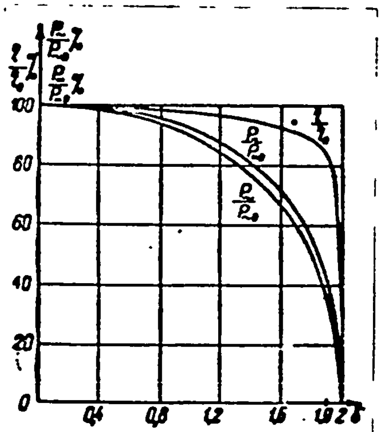

Fig.5

With an increasing $\delta'$, the amplitude decreases for the first harmonic and increases for higher harmonics. This leads to a decreased efficiency of the oscillator and of the oscillatory power, when $\delta'$ increases. The diagrams of power delivered to the load and of the overall efficiency of the oscillator have their maximums at certain values of $\delta'$. Their location depends on the natural Q-factor of the circuit: the higher the value of Q, the smaller are the values of $\delta'$ corresponding to the maximum of the curve.

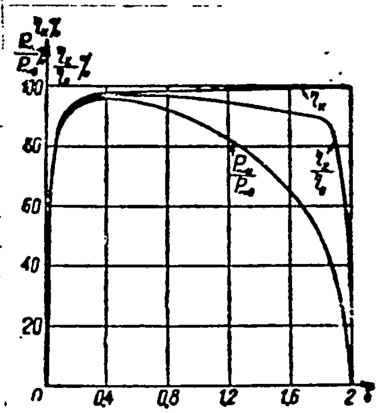

Fig.6

Only at $\delta' \to 0$ does the self-oscillator reach the values $P_{\sim 0}$ and $\eta_0$, as given by a calculation according to the quasi-linear theory. The power transmitted to the load is less than $P_{\sim 0}$ at any value of circuit efficiency.

An optimum operating condition with respect to the selection of $\delta'$, will occur when $P_{\sim n}$ and $\eta_{\Sigma}$ are at their maximum. This operating condition depends on the inherent Q-factor of the circuit. However, the above-mentioned calculations show that operation at $Q' = 5 - 2$ is most advantageous. Solving eq.(8) by the Poincaré method for different $\alpha$ values, one can evaluate the influence of the cutoff angle of the plate current on the extent to which the oscillating power decreases at increasing attenuation. Such an evaluation has shown that, at $\theta < 90^\circ$, the power drops more rapidly than at $\theta = 90^\circ$ and less rapidly at $\theta > 90^\circ$.

In conclusion, I express my thanks to G.S.Ramm for his help in preparing this work.

Article received by the Editors 24 September 1956.

STAT

# PROBLEM OF GENERATING BELL-SHAPED PULSES

by

L.I.Kastal'skiy

The article describes a schematic for the generation of bell-shaped pulses and gives the results of an experimental verification of the schematic.

It is essential, in transmitting pulses, to know how stable is the system to interference. In view of the fact that the signal-to-noise ratio depends on the shape and the duration of the pulse, the problem of the pulse shape requires first consideration in many cases.

**This article contains the description of one system for generating bell-shaped pulses.**

## 1. Optimum Pulse Shape for Pulse Systems in Multichannel Communications

A bell-shaped pulse, described by the equation

$$f(t) = Ae^{-at^2} \tag{1}$$

is the best solution, compared with other pulse shapes, from the point of view of obtaining a small product*

$$\Delta f \cdot \Delta t,$$

where $\Delta f$ characterizes the concentration of the frequency spectrum of a pulse, while $\Delta t$ characterizes the pulse concentration in time.

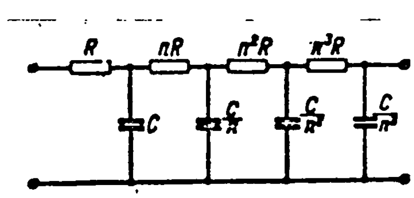


Fig.1

From eq.(1) it appears that the bell-shaped pulse is well concentrated in time. At the same time, the spectral concentration of a bell-shaped pulse also changes according to the bell law

* See, for instance, A.A.Kharkevich: Spectra and Analysis (1953)

$$C_{(\omega)} = 2A\sqrt{\frac{\pi}{a}}\,e^{-\frac{\omega^2}{4a}}, \tag{2}$$

i.e., the frequency spectrum of such a pulse is compactly concentrated.

These features of the bell-shaped pulse are especially important when using it as a working pulse in multichannel systems of radio communications, which require a minimum of cross distortions, combined with a maximum reduction of mutual interference by radio stations.

When the energies of a rectangular and of a bell-shaped pulse as well as their duration are equal, the signal-to-noise ratio will be greater for the bell-shaped pulse: Its frequency band will be smaller in this case and, consequently, at the same signal-to-noise ratio a greater quantity of channels can be placed in a multichannel system when using the bell-shaped pulse. Moreover, a bell-shaped pulse, compared with a rectangular pulse, has a better resolving power*.

It is also known that the limit resonance curve of a multistage amplifier has the form of a Gaussian distribution curve, i.e., is bell-shaped. The same shape is exhibited by the limit curves of the output voltage envelopes, from different-type packets (rectangular, bell-shaped, exponential, and others).

From this point of view, the use of a rectangular packet cannot be justified.

Bell-shaped pulses can be obtained by the method of filtering the lower frequencies and also by the method of deforming a rectangular pulse.

Let us consider a practical schematic for obtaining bell-shaped pulses by the first method, since the second method is nothing but the method of a band filter, where the bell-shaped curve is obtained as a limit curve of a multistage resonance amplifier.

For different values of a bell curve $f(t) = A \cdot e^{-at^2}$ a series of calculation

* Here, resolving power is to mean a minimal shift in time between input pulses, while the output pulses can still be received separately.

STAT

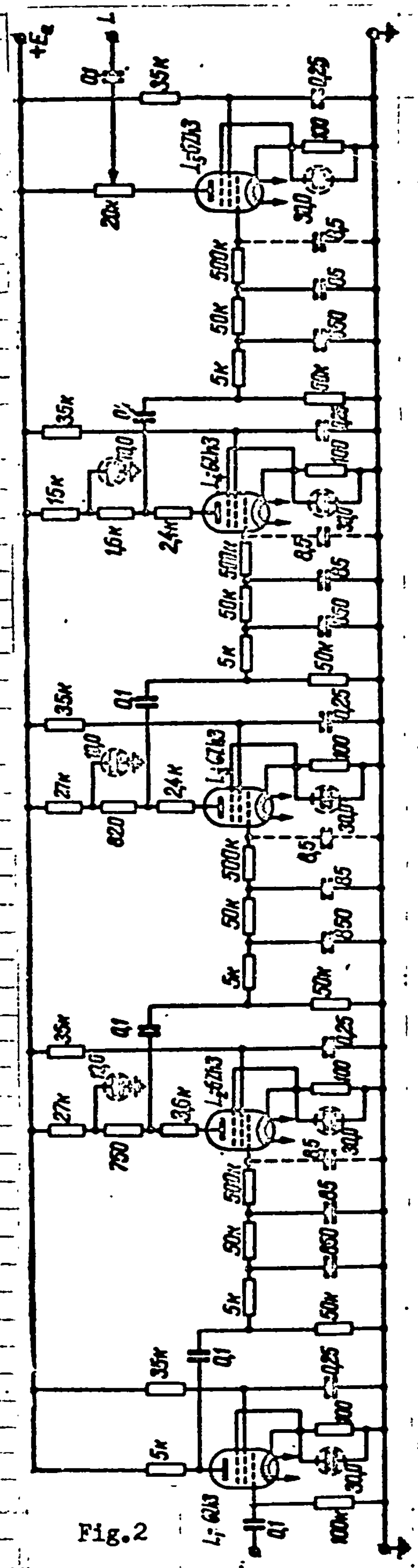

Fig.2

curves (Fig.3) were plotted and compared with experimentally obtained curves.

## 2. Method of Low-Pass Filter

Although the continuity of the function $e^{-t^2}$ does not assure an accurate reproduction of a bell curve when a limited number of filter sections is available, already 10 sections are amply sufficient to obtain actually pulses nearly coinciding with the calculated bell curves.

In the present case, bell curves are obtained by using a filter of a type shown in Fig.1, in which impedances are connected in sequence of their increasing magnitude.

Figure 2 shows a tested practical schematic, consisting of a four-stage filter with three sections in each stage. Experiments showed that a further increase of stages and sections is of small practical influence on the final result.

Considering that the factor n has a value in the range of ten, filter attenuation is compensated by inserting over each three sections, pulse separator tubes of the type 6Zh3 which have an input capacitance in the range of 8 μμf.

The testing of the schematic was done under the following conditions: duration of input pulses $\delta_{in}$ = 2 - 7 sec; duration of output pulses $\delta_{out}$ = 2.5 - 8 μ sec; frequency of pulse sequence F = 25 kc.

As variable parameter of the schematic, the duration of input and output pulses was used. The duration of pulses was counted on the level of 0.67 from the maximum amplitude.

At output, an emitter of rectangular pulses of the conventional type was used.

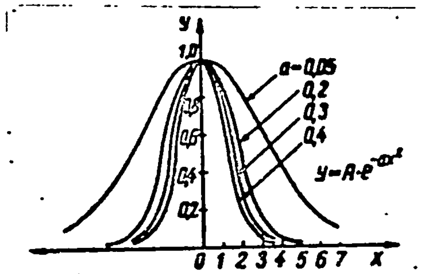


Fig.3

Fig.4

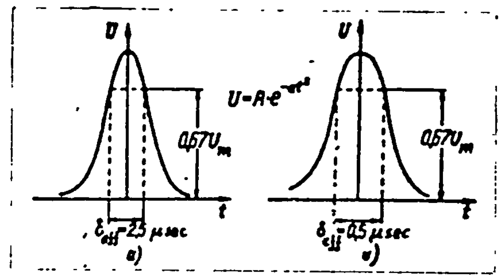


In the schematic, pulses with a duration of 3 - 10 μsec were obtained.

Such a schematic gives a sufficiently good approximation of the experimental curve as compared to the calculated one (Figs.3 and 4).

Article received by the Editors 30 March 1956.

STAT

tion of input and output pulses was used. The duration of pulses was counted on the level of 0.67 from the maximum amplitude.

At output, an emitter of rectangular pulses of the conventional type was used.

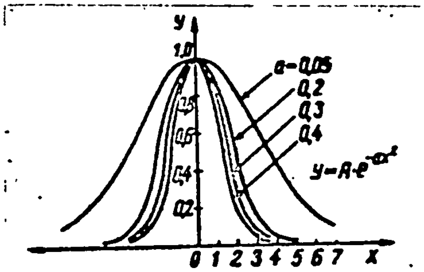


Fig.3

Fig.4

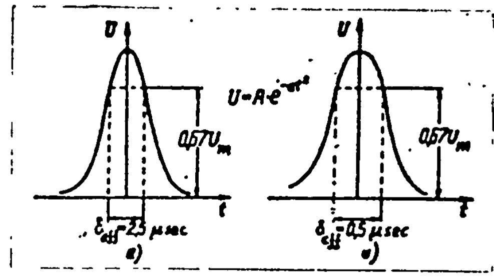


In the schematic, pulses with a duration of 3 - 10 μsec were obtained.

Such a schematic gives a sufficiently good approximation of the experimental curve as compared to the calculated one (Figs.3 and 4).

Article received by the Editors 30 March 1956.

# LETTER TO THE EDITOR

by

V.S.Voyutskiy

In an article by A.Ye.Basharinov "Noiseproof Features of a Correlation Method of Reception" (Radiotekhnika No.5, 1956) treating the possibilities of correlation reception, the author arrives at a conclusion based on the submitted calculations, that "special attention to correlation methods is scarcely justified", since the noiseproof features of a correlation receiver are not much superior to the noiseproof features of the widely used and well-known receiver with a square-law detector.

I consider this conclusion incorrect and believe that it puts the readers of the magazine on a wrong track with respect to the possibilities of reception by a two-channel correlation or autocorrelation receiver.

The author assumes that the value of the signal-to-noise ratio at the output $(\frac{N}{S})_{out}$ characterizes the noiseproof feature of reception. This ratio is determined by the relation of the rms value of a fluctuating component $\sigma_z$ to the variation in the average value of the output voltage, in the presence of a signal $\Delta Z_T$

$$\left(\frac{N}{C}\right)_{out} = \frac{\sigma_z}{\Delta Z_T}.$$

Comparing the ratio $(\frac{N}{S})_{out}$ expressed by the ratio $(\frac{N}{S})_{in}$ of various correlation receivers with a receiver with a square-law detector, the author finds that an improvement of the noiseproof feature in reception by a correlation receiver, as compared with a square-law one (in the noncoherent case) does not exceed $\sqrt{2}$, which is certainly not sufficient and does not prove a tangible advantage of correlation reception.

However, the noiseproof feature characteristic, as accepted by the author is not sufficient to judge the comparative advantages of correlation reception over a

STAT



Declassified in Part - Sanitized Copy Approved for Release @ 50-Yr 2013/11/13 : CIA-RDP81-01043R002700130004-0

square-law reception, since it does not take into consideration an unstable level of the noises and of the amplification factor of the device, which is unavoidable under actual conditions of reception. Exactly in this lies the error of the author.

Actually, the mean voltage $Z_T$ at the output of the correlation element, during a sufficiently long observation time, does not depend upon the noise intensity, while for a square-law detector we have

$$Z_T = \frac{1}{2} A^2 + \sigma_u^2,$$

where $\sigma_u^2$ is the dispersion of the noise voltage at the input. This constitutes an enormous advantage of correlation receivers over receivers with square-law detectors.

In case of reception under the condition $(\frac{S}{N})_{in} \ll 1$, even small changes in the noise level at the detector input may lead to very substantial changes in the direct component of the output voltage $Z_T$. These changes are not only comparable but exceed, in their value, by far the changes in the direct component $\Delta Z_T$ caused by the presence of the signal. Thus, these changes are the reason for distorted reception or make the latter impossible.

For instance, when $(\frac{S}{N})_{in} = 10^{-3}$* any change in noise level or in the amplification factor of the device, even of a negligible magnitude of the order of 0.1%, will cause a change in measurement at the output, corresponding to the limit values of the received signals, which will render reception impossible.

As a substantiation of the above statement, I am enclosing an oscillogram containing comparative recordings of a receiver with a square-law detector and of a receiver equivalent to a correlation receiver under equal reception conditions at their input, same signals, and same noises. The oscillogram in Fig.1 shows I - Recording for marking the instant of appearance of the signal with a continuous background of noises (inherent noise of the device). This instant is marked by an arrow.

* Such small ratios $(\frac{S}{N})_{in}$ usually are found in receivers with square-law detectors, used, for instance, in radio astronomy.

II - Recording of receiver with a square-law detector. III - Recording of receiver with asynchronous storage, equivalent in its noiseproof features to a two-channel correlation receiver, IV - Recording of time marks.

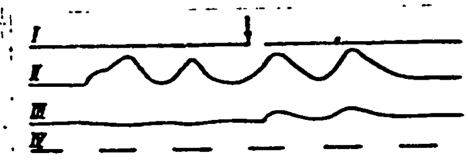

Fig.1

The advantages of a receiver equivalent to a correlation receiver are evident, since the latter almost does not react to noise (see left side of the oscillogram until the instant of the signal) while at the output of the receiver with a square-law detector, the noise is very intense and a dependable detection of the signal from the background is impossible.

According to Basharinov, the noiseproof features of both receivers are approximately equal; actually, the noiseproof features of the receiver with a square-law detector are near zero.

REPLY TO THE REMARKS BY V.S.VOYUTSKIY

The letter by V.S.Voyutskiy contests the deductions of the article and contains considerations indicating the necessity of taking into account an unstable level of noise and of the amplification factor, when determining the noiseproof features. It is admitted that the material contained in the article with respect to noiseproof features, does not permit final conclusions as to the relative value of correlation reception because of the assumed idealized conditions (the signal is represented by a harmonic function, the noise by a fluctuating stationary process, and parameters of the receiver are stable during the reception).

No doubt, the conditions may change during actual reception. However, it must be supposed that, in a series of cases, the deductions concerning comparative noiseproof features of correlation detectors will be qualitatively maintained.

The necessity to discount the unstable amplification factor for a raised sensitivity is well known from radio astronomic experience. In this connection, compensating and modulating methods of reception were elaborated. The example mentioned by

STAT



Declassified in Part - Sanitized Copy Approved for Release @ 50-Yr 2013/11/13 : CIA-RDP81-01043R002700130004-0

V.S.Voyutskiy confirms this situation but does not give direct proof of a superiority of correlation reception over square-law receivers since it does not discount the effect achieved by using compensating or modulating devices.

A detailed discussion of the mentioned problems goes beyond the scope of this article.

A.Ye.Basharinov

STAT

## S.A.VEKSHINSKIY

### On his 60th Anniversary

Sixty years elapsed since the birth and 35 years of scientific and technical activities of one of the most famous of Soviet scientists, academician Sergey Arkad'yevich Vekshinskiy.

S.A.Vekshinskiy started his career in 1920 in the laboratory of Prof. M.M.Bogoslovskiy at the Petrograd Polytechnic Institute, where on orders of the Peoples Commissariat of Post and Telegraph amplifying and transmitting electron triodes of original design with tungsten cathodes.

In 1922 in Petrograd, under the direction of M.M.Bogoslovskiy and S.A.Vekshinskiy, the Electrovacuum Plant was organized. In this plant, S.A.Vekshinskiy worked until 1928 as chief engineer. Under his direction, the technology of thoriated tungsten cathodes was worked out and the production of the then popular thoriated cathode tubes (Micro, MDS, UT, and others) was begun.

In 1925, S.A.Vekshinskiy organized at the plant a vacuum-chemical research laboratory and, in 1926, designed low-voltage cathode oscillographs with fluorescent screens for three colors.

In 1928 the Electrovacuum Plant merged with the electric bulb plant "Svetlana". S.A.Vekshinskiy became the head of the consolidated research laboratory and carried out considerable work on organizing pilot workshops and new production lines.

From 1928 to 1933, S.A.Vekshinskiy, with Prof. P.I.Lukirskiy as consultant, directed scientific research on the basic problems in electro-vacuum physics and technique and published a series of important basic articles, both in Soviet and foreign scientific journals. At the same time, he played a leading role in the setup and development of electro-vacuum devices in the "Svetlana" plant.

In the years 1929-32, under the immediate supervision of S.A.Vekshinskiy, the technology of manufacturing barium cathodes was developed. This permitted the Sov

STAT

Union to avoid acquiring a license for manufacturing barium cathodes from the Philipps Company. At the plant, the development and production of the economical and reliable barium receiving and amplifying tubes: UB-107, UB-110, UB-132 etc. was started.

In 1934, the laboratory of the "Svetlana" plant supervised by S.A.Vekshinskiy was reorganized into the Vacuum Specialty Laboratory, which, while a part of the plant, was basically a scientific and technical center of Soviet electronics.

From 1934 to 1937, S.A.Vekshinskiy directly supervised the V.S.L. and, at the same time, did personal research on secondary emission tubes and antimony-cesium photocathodes. At the same time, he worked out and introduced the production of secondary electron multiplier with electrodes in the shape of louvres. Simultaneously he directed the work of creating powerful oscillators, cathode-ray tubes, gas-discharge rectifiers, and other electro-vacuum devices.

From 1937 to 1938, S.A.Vekshinskiy was chief engineer of the "Svetlana" plant.

While he worked on the physical chemistry of photocathodes, S.A.Vekshinskiy discovered in 1939 a new method of alloy study by simultaneous vacuum-deposition of various metals and by a subsequent metallographic study of the physical and chemical properties of the prepared systems.

In the last prewar years, S.A.Vekshinskiy created a new laboratory which, during the Great Fatherland War, had been transferred to Novosibirsk. There he was highly active in the organization of electro-vacuum production under difficult wartime conditions. At the same time, he continued his research on physical-chemical systems and, in 1944, published a monograph: "A new Method of Metallographic Study of Alloys".

In 1945, he was awarded the scientific title of doctor of physical and mathematical sciences. In 1946, he was elected member-correspondent and, in 1953, active member of the Academy of Sciences USSR.

In 1946, by order of the government, S.A.Vekshinskiy organized the Central Vacuum Laboratory; this was the beginning of the Scientific Research Vacuum Institute in which S.A.Vekshinskiy worked as director since its inception in 1947 up to the

STAT

present date.

S.A.Vekshinskiy created a school of Soviet electro-vacuum specialists for industrial and of laboratory use.

In consideration of the services of S.A.Vekshinskiy in science and vacuum technology and on the occasion of his 60th anniversary, the Presidium of the Supreme Soviet of USSR granted him the title of Hero of Socialistic Labor and awarded him the order of Lenin and the gold medal: "Hammer and Sickle".

The Soviet radiotechnical community, marking the anniversary of S.A.Vekshinskiy wishes him good health and a fruitful activity for the best of our country.

## A.A.PISTOL'KORS

### At his 60th Anniversary

The scientific and technical community marked the 60th anniversary and 30 years of scientific activity of the Gold medal imeni A.S.Popov, laureate member-correspondent of the Academy of Sciences USSR, Aleksandr Aleksandrovich Pistol'kors, one of the great specialists in radiation, receiving and channeling of electromagnetic oscillations.

The scientific activity of Aleksandr Aleksandrovich began at the time of broad dissemination of radio communications and radiophone on short and medium waves. His books and papers devoted to calculating methods for the mutual interference of oscillators, complex short-wave and medium wave antennas, and antennas composed of linear oscillators for other bands became widely known and helped to create a comprehensive method of analysis and engineering calculations for multiple unit antennas.

The work by A.A.Pistol'kors on the theory of receiving leads had great theoretical and practical importance. His work on the theory of coupled assymmetric circuits permitted determination of the current distribution at the input resistance of assymmetric circuits, and creation of engineering methods for calculating assymmetric antennas - loop vibrators, antennas with upper and with shunted feed, etc.

A.A.Pistol'kors and his students elaborated design problems of antennas with a prescribed radiation pattern.

Beginning in 1944, Aleksandr Aleksandrovich published a series of works on the theory of slot antennas.

In recent years, under the direction of Aleksandr Aleksandrovich a series of important projects were successfully launched for creating rectifier devices with ferrite inserts.

The above-mentioned work does not cover the entire volume of theoretical studies by Aleksandr Aleksandrovich. Special mention must be made of his very important work

STAT

devoted to the determination of parameters of horizontal leads, located near the surface of the earth.

A.A.Pistol'kors is not only a theoretician of high calibre but also a talented inventor. He proposed widely used antennas and measuring devices: the loop vibrator; the horizontal V-antenna; measuring devices for the traveling-wave ratio, reflectometer, developed together with M.S.Neyman, and others.

During the period 1930-50, A.A.Pistol'kors carried out extensive pedagogical work at the Leningrad Electrotechnical Institute, Leningrad and Moscow Electrotechnical Institutes for Communications. Aleksandr Aleksandrovich has written several books on the theory and technique of antenna arrays, including the textbook "Antennas" which is widely used in electrotechnical colleges.

A.A.Pistol'kors is carrying out considerable and fruitful work, coordinating scientific studies covering antenna designs and lines for transmitting high frequency power.

The editorial staff of the journel "Radiotekhnika" wishes Aleksandr Aleksandrovich Pistol'kors good health and further success in his fruitful work.

## NEW BOOKS

M.I.Vitenb rg. Calculation of Electromagnetic Relays for Automation Devices and for Communications. Gosenergoizdat, Moscow-Leningrad 1956, 464 pages, price 14 r 50 k

The book is devoted to theoretical questions and to the calculation of electromagnetic relays for DC and AC in automation devices and communications. Analytical and graphic-analytical methods for calculation of electromagnetic relays are reviewed, their construction is described, and experimental data are given on basic types of relays for automation and communication. The book is intended for engineers and technicians making calculations and designing relays and electromagnetic mechanisms, as well as for students of electrotechnical colleges and corresponding departments.

M.P.Kaplanov and V.A.Levin. Automatic Frequency Control. Second Edition, revised, Gosenergoizdat, Moscow-Leningrad 1956, 200 pages, price 11 r 50 k

Various types of automatic frequency control systems as used in radio technical devices are described and classified. The calculation formulas given in the book can be used for designing devices with automatic frequency regulation. The book is intended for radio specialists and for students of higher courses in universities.

Developments in Electro-Vacuum Technique. Edited by Prof. G.A.Tyagunov. Gosenergoizdat, Moscow-Leningrad, 1956, 256 pages, price 10 r 25 k

A collection of articles dedicated to a description of types, calculation methods, properties and physical effects in certain new types of electro-vacuum devices (stabilitrons, gas-discharge tubes for ultrahigh frequencies, electron-beam devices, etc.).

The collection is for students and teachers in universities, training specialists in electro-vacuum physics and technique, and for scientific workers of the electro-vacuum industry.

STAT

F.V.Mayorov. Electronic Regulators. Gosenergoizdat, Moscow, 1956, 492 pages price 14 r 20 k.

Elements and assemblies of electronic regulators for continuous and intermittent action are reviewed, including practical schematics for electronic regulators.

The book is intended for engineers and technical workers whose specialty is automatic regulation.

P.V.Sakharov. Technology of Designing Electric Equipment. Part I: Features of Designing Electric Equipment. Technology of Conductor Parts and of Magnetic Circuits. Moscow-Leningrad, Gosenergoizdat, 1956, 315 pages, price 7 r 85 k.

Special features of building electric equipment, problems of design, and technology are reviewed.

The book can serve as an aid for students at colleges and technical schools, also for instructors, engineers and technicians specializing in building electric equipment.